THE Journal OF THE AMERICAN LEATHER CHEMISTS ASSOCIATION

October 2023 Vol. CXVIII, No.10 *JALCA* 118(10), 401–452, 2023

118th Annual Convention

May 21–23, 2024
Hershey Lodge
325 University Drive
Hershey, PA 17033

For more information go to:
leatherchemists.org/
annual_convention.asp

Contents

Distributed by
University of CINCINNATI
LIBRARY PUBLISHING SERVICES

An imprint of the University of Cincinnati Press

ISSN: 0002-9726

Communications for Journal Publication

Manuscripts, Technical Notes and Trade News Releases should contact:
Mr. Steven D. Lange, Journal Editor, c/o University of Cincinnati, 5997 Center Hill Ave., Bldg. C, Cincinnati, OH 45224, USA
E-mail: jalcaeditor@gmail.com Mobile phone: (814) 414-5689

Contributors should consult the Journal Publication Policy at:
http://www.leatherchemists.org/journal_publication_policy.asp

SPONSORS FOR THE 117th ANNUAL MEETING

ADMIRAL —$4,500

North American Minerals Corporation

ELITE —$4,000

TFL USA/Canada, Inc.

PLATINUM — $3,500

Erretre SpA
Stahl USA

DIAMOND —$2,500

Buckman
Pangea Made, Inc.

GOLD LEVEL — $1,750

American Chrome & Chemicals LTP Inc.
Dow Coating Materials
Tannin Corporation

SILVER LEVEL — $1500

Atlas Refinery Inc.
D. R. Diedrich and Co.
Hermann Oak Leather Co.
JBS USA
NTE Company (Pty) Ltd
Quaker Color
Tyson Foods, Inc.

BRONZE LEVEL — $1000

Chemtan Company
Cromogenia Units
Curfimex SA de CV
Leather Miracles
SB Foot Co./Red Wing Shoe Co.
Twin City Hides
Union Specialties Inc.
Wickett & Craig of America

JOURNAL OF THE
AMERICAN LEATHER CHEMISTS ASSOCIATION

Proceedings, Reports, Notices, and News
of the
AMERICAN LEATHER CHEMISTS ASSOCIATION

THE JOURNAL OF THE AMERICAN LEATHER CHEMISTS ASSOCIATION (USPS #019-334) is published monthly by The American Leather Chemists Association, c/o University of Cincinnati, 5997 Center Hill Ave., Bldg. C, Cincinnati, Ohio 45224. Telephone (513) 290-2505. Single copy price: $10.00 members, $20.00 non-member plus shipping and handling. Subscriptions: $185 for hard copy plus postage and handling of $60 for domestic subscribers and $70 for foreign subscribers; $220 for ezine only; and $240 for hard copy and ezine plus postage and handling of $60 for domestic subscribers and $70 for foreign subscribers.

Periodical Postage paid at Cincinnati, Ohio and additional mailing offices. Postmaster send change of addresses to The American Leather Chemists Association, c/o University of Cincinnati, 5997 Center Hill Ave., Bldg. C, Cincinnati, Ohio 45224.

Website: www.leatherchemists.org E-mail: hallks@ucmail.uc.edu

COLD
Milling

Smooth Leather Milling

Erretre
Tannery Innovations

Erretre s.p.a. | Via Ferraretta,1 | Arzignano (VI) 36071 | tel. +39 0444 478312 | info@erretre.com

Interaction between Amphoteric Polymer and Silicic Acid Tanned Leather: Ingenious Regulation of pH based on Isoelectric Point

by

Ze Liang,[1,2] Zetian Zhang,[1,2] Yang Liu[1,2] and Zhengjun Li[1*1,2]

[1]*National Engineering Research Center of Clean Technology in Leather Industry, Sichuan University*, Chengdu, 610065, China

[2]*Key Laboratory of Leather Chemistry and Engineering of Ministry of Education, Sichuan University,* Chengdu, 610065, China

Abstract

Silicic acid-based tanning system is an effective and promising chrome-free tanning technology, and it is urgent to develop compatible post-tanning processes. Fatliquoring is one of the key procedures to determine the quality of resulted leather and fatliquoring agents mainly play the role of an effective softer/plasticizer in leather production. However, there is a mismatch between most commercial fatliquoring agents (mainly compatible with chrome tanned leather) and silicic acid tanned leather (named SATL). Herein, an amphoteric polymer emulsion (APE) was prepared by free radical polymerization using methacryloxyethyl trimethyl ammonium chloride (DMC), 2-acrylamido-2-methylpropanesulfonate (AMPS), lauryl methacrylate (LMA), dimethylaminoethyl methacrylate (DMAEMA) as monomers. And in order to improve the lubricating property, APE was further compounded with castor oil to obtain an amphoteric fatliquoring agent (named COAPE). Comprehensive characterization showed that the amphoteric (pI=8.22) and amphiphilic APE could reduce the surface tension of water to 38.6 mN/m. The fatliquoring process was controlled by ingenious regulation of pH based on isoelectric points (pIs) of APE and SATL. In the initial stage, the pH of the bath was adjusted to be lower than the pIs of APE and SATL, amphoteric polymer molecules could easily penetrate into SATL leather as they are all positively charged. While during the fixing stage, the pH of the bath was adjusted between the pIs of APE and SATL, so the electrostatic interaction between amphoteric polymer molecules and SATL leather, as well as the aggregation of amphoteric polymers can promote their combination synergistically. As a fatliquoring agent, the application of COAPE demonstrated that its absorpotion rate (90.5%) was much higher than anionic commercial fatliquoring agent (63.2%), thus imparting SATL leather better softness (6.5 mm), elongation at break (95.5%) and tensile strength (11.6 N/mm^2). These findings therefore provided scientific basis and technical support for the application of amphoteric materials to silicic acid-modified collagen matrix and would promote the practical application of silicic acid-based chrome-free tanning technology.

1. Introduction

Currently, chrome tanning still occupies the dominant position in leather industry as it can endow leather with excellent thermal stability and organoleptic properties.[1] However, chrome tanning process is facing severe restrictions due to the pressure of environmental protection and resource conservation.[2] Therefore, in recent years, people have devoted themselves to the research of chrome-free tanning systems, and some of them have achieved satisfactory results in practical application, including a muti-metal complex tanning system,[3] Tanfor T™ tanning system,[4] TWT/TWS tanning system,[5] F-90 tanning system[6] and so on. Our team also developed a silicic acid-based chrome-free tanning system, which can obviously improve shrinking temperature and the porous structure of leather.[7] The analysis of tanning mechanism revealed that the intermolecular co-condensation of Si-OH groups of silicic acid as well as hydrogen bonds between silicon hydroxyl groups and collagen amino groups played major roles in the tanning process.[8] Moreover, this silcic acid-based tanning process can be further improved by adding pretreatment additives or combination tanning methods.[7,9] However, the comprehensive properties of silicic acid tanned leather (SATL), such as lack of sufficient softness and flexibility, need to be improved through subsequent post-tanning processes. Therefore, it is an impending requirement for its practical application to develop matchable post-tanning processes.

Among post-tanning processes, fatliquoring is one of the key operations since it gives leather softness, fullness and elasticity.[10] During the fatliquoring process, the fatliquoring agent can penetrate into collagen fibers, and play a role in lubrication and plasticization by reducing friction in woven fiber network, preventing the collagen fibers from adhesion to each other during drying, thus providing pleasant softness and flexibility for leather.[11] However, at present, the fatliquoring agents used in leather production are mainly those with anionic charges that are compatible with chrome tanned leather. Unfortunately, similar to most organic tanning processes, in the silicic acid tanning process, amino groups of collagen fibers are mainly consumed which makes tanned leather have a lower isoelectric point, thus leading to poor absorption of anionic

*Corresponding author email address: lizhengjun@scu.edu.cn

Manuscript received March 193, 2023, accepted for publication May 7, 2023.

fatliquoring agent.[8,12,13] Hence, it is necessary to develop novel fatliquoring agents matching well with SATL leather.

Fortunately, the amphoteric polymeric fatliquoring agent contains both anionic and cationic groups with pH-responsive function, exhibiting positive or negative charges at different pH.[14,15] By changing the pH of bath liquid, the charge state of amphoteric fatliquoring agent can be adjusted to adapt to the surface charge state of chrome-free tanned leather, allowing them to carry the same or opposite charge, thus effectively overcoming the problem of absorption caused by weak electrostatic interaction, which has been confirmed by recent reports.[16,17] Hao et al. synthesized an imidazole ionic liquid-based amphoteric polymer as fatliquoring agent for F-90 tanned leather, which has higher absorption rate than a commercial anionic fatliquoring agent.[18] Sun et al. obtained an amphoteric peptide-based fatliquoring agent, which has good compatibility with F-90 organic chrome-free tanning system.[19] Liu et al. designed a amphoteric polymer P(AA-AM-C12DM) with retanning and fatliquoring dual functions, which endows the organic chrome-free TWS tanned leather with excellent softness, thickening rate and mechanical properties, and has greater absorption rate (96%) than that of an anionic commercial fatliquoring agent (75.8%).[20] However, a systematic analysis of the penetration and combination of amphoteric fatliquoring agents in leather from the perspective of their surface charge states, and especially the application of amphoteric polymers to silicic acid tanned leather or silica-modified collagen materials has not been reported yet.

On the other hand, leather made from animal skin or hide is rich natural biomass polymer matrix, which is mainly composed of collagen.[21] Collagen is a typical amphoteric polyelectrolyte since it contains basic amino acid residues (lysine, arginine and histidine) and acidic amino acid residues (glutamic acid and aspartic acid), which also confer amphoteric character to leather.[22] During the process of leather manufacture, the variation of pH of bath liquid can directly affect the surface charge state of leather.[16] Additionally, the electrostatic interaction between the chemicals (including fatliquoring agents) and leather is the decisive factors of their mass transfer and combination in leather.[23] Therefore, based on their pIs, the surface charge states of amphoteric fatliquoring agent and leather can be changed by ingeniously regulating the pH value of bath liquid, so as to accurately control the penetration, distribution and fixation of amphoteric fatliquoring agents in the leather matrix. What's more, the combination mechanism between amphoteric fatliquoring agents and leather can be easily explored from the perspective of their surface charge states.

Herein, in this work a novel amphoteric polymer emulsion (APE) was synthesized by free radical polymerization with methacryloxyethyl trimethyl ammonium chloride (DMC), 2-acrylamido-2-methylpropanesulfonate (AMPS), lauryl methacrylate (LMA) and dimethylaminoethyl methacrylate (DMAEMA) as monomers, and it was compounded with castor oil to prepare amphoteric fatliquoring agent (COAPE). Both of them were applied to the fatliquoring process of SATL leather for comparison. Meanwhile, a commercial anionic polymer fatliquoring agent was adopted as a contrast. From the point of view of surface charge states, the interaction mechanism between the amphoteric polymer and SATL leather as well as the function of amphoteric characteristics were systematically studied. The research results can provide technical support for the application of amphoteric polymers in silicic acid tanned leather, which is of great significance for the improvement of silicic acid-based tanning system. It can also provide reference for the development of other chrome-free technologies.

2. Experimental

2.1 Materials

Silicic acid tanned goatskins were prepared in our laboratory according to our previous work.[7] DMC (75%) was purchased from Macklin Biochemical Co., Ltd. (Shanghai, China). AMPS (98%), LMA (96%) and DMAEMA (99%) were purchased from Aladdin Reagent Co., Ltd. (Shanghai, China). Sodium dodecyl sulfonate (SDS, AR), Aliphatic alcohol polyoxyethylene ether (AEO-9, AR), potassium persulfate (KPS, AR), and sodium hydroxide (NaOH, AR) were purchased from Chengdu Kelong Chemical Reagent Co., Ltd. (Sichuan, China). Commercial fatliquoring agent (copolymer of modified natural/synthetic oil and acrylic acid, anionic) and other chemicals used for leather manufacturing were of industrial grade. All reagents were used directly without any further purification.

2.2 Synthesis of amphoteric polymer emulsion (APE) and amphoteric fatliquoring agent (COAPE)

APE was synthesized by free-radical emulsion polymerization. Firstly, the required amount of water-soluble monomers AMPS (anionic), DMC (cationic), DMAEMA (cationic) and deionized water were uniformly mixed in a beaker, and the pH value was adjusted to 5.0 with 10wt% sodium hydroxide to prepare a water-soluble monomer mixture. Then, emulsifier AEO-9 and SDS were added into a four-neck round-bottom flask equipped with a reflux condenser, a mechanical stirrer, a thermometer and additional funnels together with appropriate water, and stirred at 75°C for 30 min in nitrogen atmosphere. After that, the water-soluble monomer mixture, LMA (oil-soluble monomer) and the pre-prepared initiator solution were respectively dropped into the flask simultaneously within 2 h. The reaction continued at 80°C for 2 h, and then the reaction was kept at 85°C for another 2 h in order to complete the conversion. Finally, the milky white emulsion APE with a solids content of about 33% was obtained by naturally cooling to ambient temperature and filtering through a 200-mesh nylon net. In addition, the APE sample was precipitated and washed with anhydrous ethanol to remove residual monomers, and then the precipitate was dried in a vacuum oven at 40 °C for 24 h to obtain pure amphoteric polymer poly(AMPS-DMC-DMAEMA-LMA). The synthetic route of APE is shown in Figure 1a.

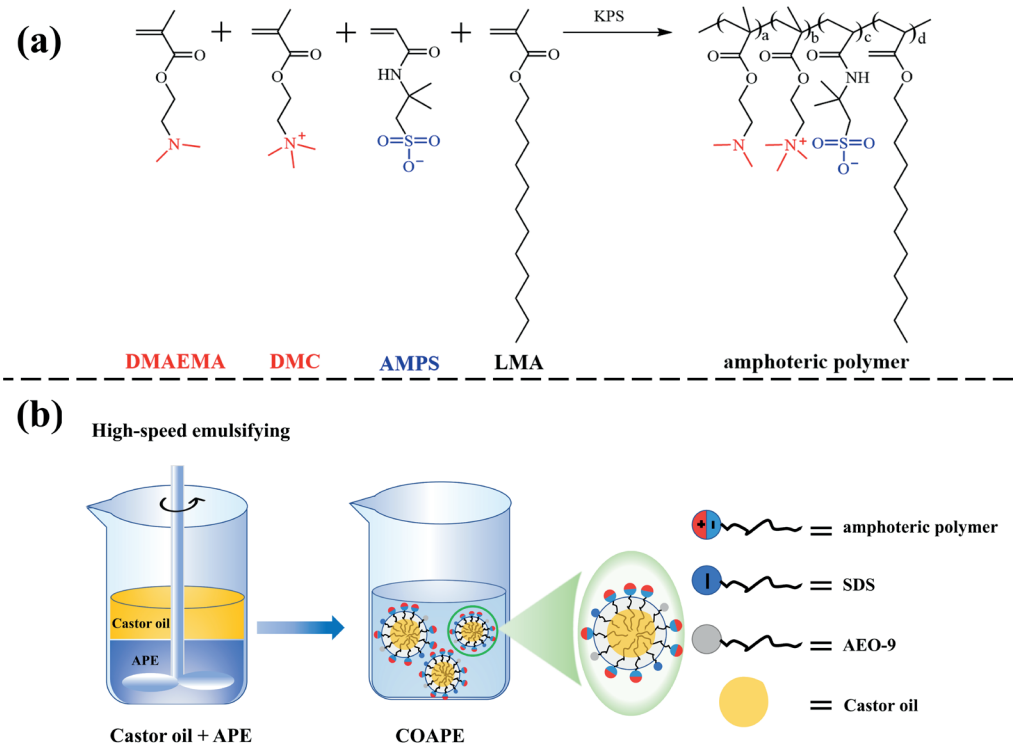

Figure 1. Synthetic route of **(a)** APE and **(b)** COAPE

Furthermore, castor oil was emulsified by APE at about 1:1 mass ratio to prepare COAPE. In brief, 30.0 g of APE, 9.9 g of castor oil and 9.6 g of deionized water were mixed at 3500 rpm for 20 min by a high-speed dispersion homogenizer (XHF-DY, SCIENTZ, China). The solid content of COAPE was maintained at 40 % (Figure1b).

2.3 Characterization and properties of APE and the amphoteric polymer

2.3.1 Fourier transform infrared (FTIR) spectrometry

FTIR spectra was collected at ambient temperature using a Nicolet iS10 FTIR spectrometer (Thermo Scientific, USA). The samples were prepared by KBr tablet method, which was measured in the range of 400 - 4000 cm^{-1}.

2.3.2 X-ray Photoelectron Spectroscopy (XPS)

X-ray photoelectron spectroscopy spectra were conducted using the Escalab-220i XPS (Kratos, Japan) with a monochromated Al Kα (hυ =1100 eV) X-ray source of 250 W at 15 kV. Particularly, the high-resolution XPS spectra of the N1s and O1s was measured respectively at energy 20 eV.

2.3.3 Determination of surface tension

The surface tension of APE and the corresponding amphoteric polymer aqueous solution were respectively measured by Wilhelmy plate method on an automatic surface tensiometer (BZY-1, Shanghai Hengping Instrument and Meter Co., ltd., China).[24] Thus, various concentrations of APE were prepared for measurement, and each test was conducted in triplicate at ambient temperature.

2.3.4 Average particle size, particle size distribution and zeta potential

Average particle size, particle size distribution and zeta potential of APE were determined using a dynamic light scattering particle size analyzer (Zetasizer nano zsp, Malvern, England). The pH of APE with a mass fraction of 0.2% was adjusted to 3.0 - 10.0 by 0.1 mol/L HCl or NaOH solution before test.

2.4 Application of APE and COAPE in leather fatliquoring process

2.4.1 The pI of SATL leather

The pI of SATL leather was represented approximately by the pI of silicic acid treated gelatin solution, which was prepared according to the literature.[8] Then the zeta potential of silicic acid treated gelatin solution (0.2 wt.%) under different pH conditions were recorded, and its pI was calculated.

2.4.2 Fatliquoring process

The detailed fatliquoring process is shown in Table I. In order to better promote the penetration and absorption of APE in SATL leather and further explore the binding mechanism between amphoteric copolymer and SATL leather, we preset different initial pH values of fatliquoring and fixing pH values at the end of fatliquoring to control the surface charge states of amphoteric copolymer and SATL leather during fatliquoring. The corresponding preset initial pH value and fixing pH value are shown in Table II. In schemes 1, 2 and 3, sufficient penetration of fatliquoring agent was expected at the initial stage (setting the initial pH value below the pI of APE and

Table I

Fatliquoring process

Process	Chemicals	Dosage[a] (%)	Temperature(°C)	Time(min)	Remarks
Washing	Water	200×2	25	15×2	Drain
Adjusting pH value	Water	100	25		
	Sodium bicarbonate or formic acid	0.5×n		30	Achieving the initial pH, drain
Fatliquoring	Water	150	50		
	Fatliquoring agent	5		90	
Fixing	Sodium bicarbonate or formic acid	0.5×n		30	Achieving the fixing pH, drain
Washing	Water	200×2	25	10×2	Drain
Hang drying					

[a] The dosage of chemicals was calculated based on the weight of SATL leather.

SATL to 4.0) aiming at obtaining optimal fixing pH value that can achieve the best combination effect. Then, on this basis, in schemes 4, 5 and 6, the optimal fixing pH was kept constant to explore the optimal initial pH that can achieve the best penetration effect. Finally, in schemes 7, 8 and 9, under the above-obtained optimal initial pH and fixing pH conditions, SATL leather was fatliquored with APE, COAPE, and a commercial fatliquoring agent, so as to investigate whether the amphoteric fatliquoring agent COAPE matched with the silicic acid-based tanning system. Notably, the silicic acid tanned goatskin leather was cut symmetrically into small samples (20 cm × 20 cm) along the back ridge line to keep the starting states roughly identical.

2.4.3 Absorption of fatliquoring agent

The total organic carbon concentration (TOC) of bath liquid samples at the beginning and the end of fatliquoring were measured using a TOC analyzer (Vario TOC, Elementar, Germany). Then the absorptivity of fatliquoring agent was calculated by the following formula (1):

$$Absorptivity\ (\%) = \frac{(T_0 - T_1)}{T_0} \times 100\% \quad (1)$$

where T_0 is the TOC of bath liquid sample at the beginning fatliquoring, and the T_1 is the TOC of bath liquid sample at the end fatliquoring.

2.4.4 Shrinkage temperature (T_s)

Shrinkage temperatures of leather samples treated with different schemes were tested on a digital shrinkage thermometer (MSW-YD4, Sunshine Electronic Research Institute of Shaanxi University of Science and Technology, China). Each sample was tested three times and the average value of these tests was calculated.

Table II

Fatliquoring agent and pH value of bath liquid used in different fatliquoring schemes

Schemes	Fatliquoring agent	Initial pH	Fixing pH
Scheme 1	APE	4.0	6.0
Scheme 2	APE	4.0	7.5
Scheme 3	APE	4.0	8.0
Scheme 4	APE	4.0	7.5
Scheme 5	APE	5.0	7.5
Scheme 6	APE	6.0	7.5
Scheme 7	APE	4.0	7.5
Scheme 8	COAPE	4.0	7.5
Scheme 9	Commercial polymer fatliquoring agent	4.0	7.5

2.4.5 Thickening rate

The thicknesses of leather before and after fatliquoring were measured with a thickness gauge. The thickness of untreated leather was marked as d_0(mm), while the thickness of fatliquored leather was recorded as d_1 (mm). Subsequently, the thickening rate (*Tr*) was calculated according to the following formula (2):

$$Tr\ (\%) = \frac{(d_1 - d_0)}{d_0} \times 100\% \quad (2)$$

2.4.6 Physical and mechanical properties

The tensile strength and elongation at break were measured by a tensile tester (AI-7000S, GotechTesting Machines Inc., China) according to ISO 3376-2020. According to the principle of symmetrical position sampling, two horizontal and two vertical samples were taken from the corresponding positions of leathers treated with different schemes, then these samples were conditioned according to ISO 2419-2012 before test.

The softness of leather samples before and after fatliquoring was measured by a leather softness tester (GT-303, Gotech Testing Machines Inc., China) referring to the standard of ISO 17235-2015. Each sample was tested at least three times at different parts of leather, the average value of these tests was calculated.

2.4.7 Scanning electron microscope (SEM)

The cross-sections of leather samples treated with different fatliquoring agents were observed using field emission scanning electron microscopy (SEM, JSM-7500F, JEOL, Japan) at 3.0 kV with different magnifications. The specimens with uniform size were coated with gold before testing. Finally, the pore size distribution and the average pore diameter were calculated by software Nano-Measurer according to these SEM images.

2.4.8 Light fastness

A discoloration meter (GX-503-A, Gaoxin Testing Machines Inc., China) was applied to measure the light fastness of leather samples under simulated sunlight. Specifically, the leather samples with the size of 120 mm×40 mm were placed on the tray of discoloration meter and aged by at 50°C for 12h with a 300 W bulb constituted the simulated sunlight source. The grain of leather faced the bulb and was 250 mm apart. Then the color of the leathers was measured according to the Commission Internationale de l'Eclairage (CIE) 1976 L*a*b* color spaces.[25] The L* (lightness-darkness), a* (redness-greenness), b* (yellowness-blueness) values were measured by Chromaticity analyzer (CM3700A, Konica Minolta Inc., Japan), and the color difference between unaged and aged leather was calculated by the following formula (3):

$$\Delta E = \sqrt{(\Delta L^*)^2 + (\Delta a^*)^2 + (\Delta b^*)^2} \quad (3)$$

3. Results and Discussion

3.1 Characterization and properties of APE and the amphoteric polymer

3.1.1 FT-IR spectrum analysis

The FT-IR spectrum of the corresponding amphoteric polymer is presented in Figure 2a. The wideband nearby 3446 cm^{-1} is attributed to the stretching vibration peak of -NH in the amide group (-CONH-).[26] Two typical peaks at 2926 cm^{-1} and 2855 cm^{-1} are ascribed to the symmetric and asymmetric stretching vibrations of C-H from the $-CH_3$ and $-CH_2$ groups in dodecyl.[27] The absorption peak at 1731 cm^{-1} belongs to the stretching vibration of C=O in the ester group (-COOR), while the peak at 1657 cm^{-1} is related to the stretching vibration of C=O in the amide group (-CONH-).[28,29] The characteristic peaks appeared at 1183 cm^{-1} and 1039 cm^{-1} are

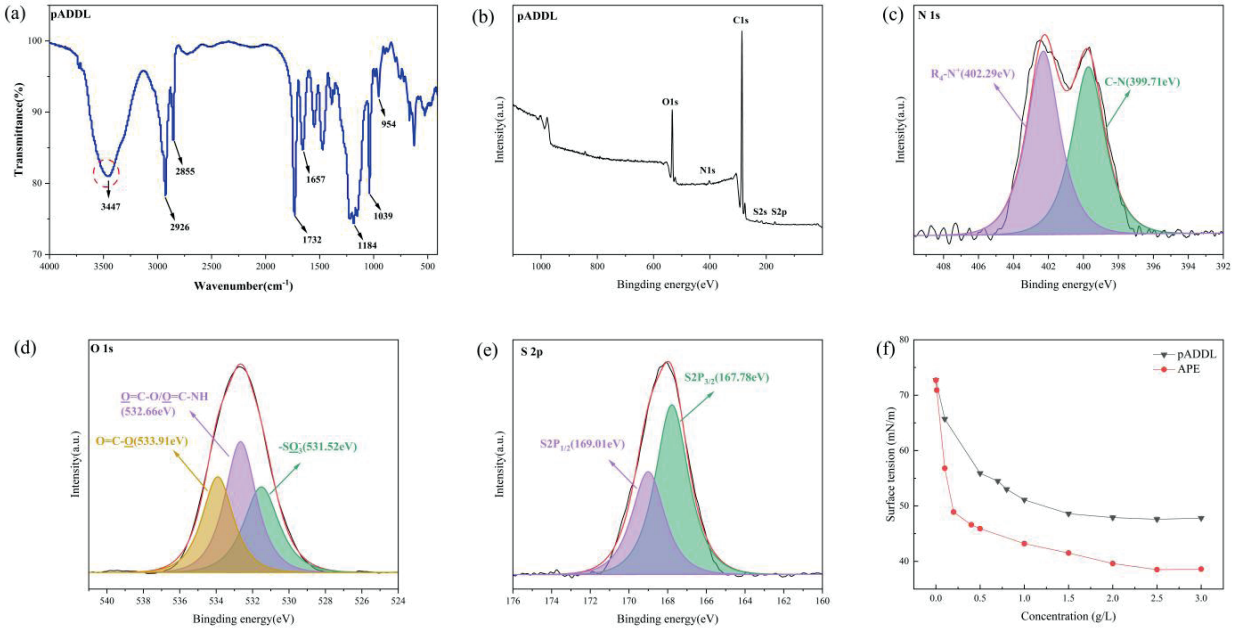

Figure 2. (a) FT-IR spectrum, **(b)** full XPS spectrum of the amphoteric polymer; High-resolution XPS spectra of the amphoteric polymer: **(c)** N1s, **(d)** O1s, **(e)** S2p; **(f)**Surface tension versus concentration of the amphoteric polymer and APE, respectively.

due to the stretching vibration and asymmetric deformation of S=O in the sulfonic acid group ($R\text{-}SO_3^-$).[30] The absorption peak at 957 cm^{-1} corresponds to the stretching vibration of the quaternary ammonium group (N^+).[31] In addition, the absorption peak near 1640 cm^{-1} corresponding to C=C is absent. Therefore, these results preliminarily confirmed the success of copolymerization.

3.1.2 XPS analysis

The structure of the corresponding amphoteric polymer was further confirmed by XPS analysis. As expected, Figure 2b shows that it was composed of C, N, O, and S elements. Particularly, the existence of S2s peak and S2p peak indicated the incorporation of AMPS. In addition, the high-resolution deconvolution peaks of N1s, O1s and S2p (Figure 2c-e) shows that the N1s peak can be deconvoluted into two corresponding sub-peaks of C-N at 399.71 eV (coming from DMAEMA) and quaternary N at 402.29 eV (coming from DMC).[32] Moreover, individual contributions of O1s peak were located at 531.52 eV, 532.66 eV and 533.91eV, which corresponds to $-S\underline{O}_3^-$, $\underline{O}$=C-O and O=C-$\underline{O}$, respectively.[33,34] The S2p was divided into two peaks namely $S2p_{1/2}$ and $S2p_{3/2}$ with the binding energies of 169.01 eV and 167.78 eV.[33,35] Taking together, all these above well further illustrated the successful copolymerization of AMPS, DMAEMA, DMC and LMA.

3.1.3 Surface tension

Surface activity is the ability of amphiphilic molecules to reduce the surface tension (or interfacial tension) at low concentration, which is the cornerstone of their formation of kinetically stabilized emulsions. Surface tension measurement is a usual way to evaluate the surface activity of amphiphilic materials.[36] Curves of surface tension versus concentration for APE and the amphoteric polymer aqueous solution are shown in Figure 2f. It can be clearly seen that the surface tension of amphoteric polymer aqueous solution decreases with the increase of its concentration, and reaches the minimum value of 47.6 mN/m at the concentration of 2.5 g/L. The significant reduction in surface tension indicates that amphoteric polymer has amphiphilic structure, which also proves the successful copolymerization of hydrophilic and hydrophobic monomers to some extent. Similarly, with the increase of APE concentration, the surface tension of water solution decreases, which also confirms the surface activity of APE. Compared with the aqueous solution of amphoteric polymer, the surface tension of APE dropped more dramatically with increasing concentration, reaching a lower value of 38.6 mN/m, which is mainly due to the existence of small amount of emulsifiers (SDS and AEO-9) in APE.[28] Thus, APE has good surface activity. On the one hand, it has the potential of emulsifying castor oil to ensure the stability of COAPE; On the other hand, it would make fatliquoring liquid easier to wet and penetrate into leather.

3.1.4 Zeta potential and pI, particle size and its distribution

The pI is defined as the pH value of amphoteric materials when they are electrically neutral, which can be determined by the zeta potential change at different pH values.[14,34] The zeta potential of APE as a function of pH is presented in Figure 3a. It can be clearly observed that with the increase of pH value, the potential of APE gradually changes from positive to negative, which may be mainly related to the neutralization of the positive charge carried by DMC, the exposure of the negative charge carried by AMPS, and the deprotonation of the tertiary amine group in DMAEMA.[37] This obviously revealed the amphoteric characteristics of APE, and the pI is 8.22, which indicated the successful copolymerization of cationic and anionic monomers. In addition, the pI of SATL leather can also be figured out from Figure 3a, was 4.62. Fortunately, the difference of the pI values of APE and SATL is beneficial for us to master the situation that APE and SATL are charged with same/opposite sign under different pH environments, and further adjust the ability of penetration and combination of APE in SATL leather.

In addition, particle size is one of the crucial parameters of fatliquoring agent, which is directly related to the penetration into leather.[38] The average particle size and poly dispersion index (PDI) of APE at different pH values are summarized in Figure 3b, and the corresponding particle size distribution is shown in Figures 3c-j. From Figure 3b, there is little fluctuation in average size values of APE at different pH, with a range of 150 - 185 nm. On the one hand, the small particle size of APE can ensure better permeability and avoid surface deposition,[11] on the other hand, it also means that the surface area of emulsion per unit volume increases, which is helpful for chemical reactions and increases the combination of APE and leather fibers.[39] However, the PDI increased initially and then decreased as the pH increased, exhibiting a dramatically high value near the pI of APE. Especially, when the pH is 7.15, 8.11 or 8.52, the existence of particles even larger than 1000 nm can be conspicuously observed, as shown in Figures 3f-h, which directly indicates that some particles in APE have obviously agglomerated near the pI of APE, forming larger particles. This is mainly because the closer to pI, the lower the absolute value of zeta potential, and the smaller the electrostatic repulsion between particles in APE, so that particles will agglomerate together.[40]

The above results comprehensively proved the success of copolymerization, and the emulsion APE with amphoteric and amphiphilic characteristics was obtained. The pI values of APE and SATL leather were also measured, which were 4.62 and 8.22 respectively. Based on this, we then will try different pH regulation schemes to explore the interaction mechanism between amphoteric polymer and SATL leather from the perspective of their surface charge states.

3.2 Insight into interaction between amphoteric polymer and silicic acid tanned leather

3.2.1 Effect of fixing pH value at the end of fatliquoring

In Schemes 1, 2 and 3, the absorption rate of APE in SATL leather at different fixing pH values at the end of fatliquoring and physical properties of fatliquored SATL leather are compared and represented

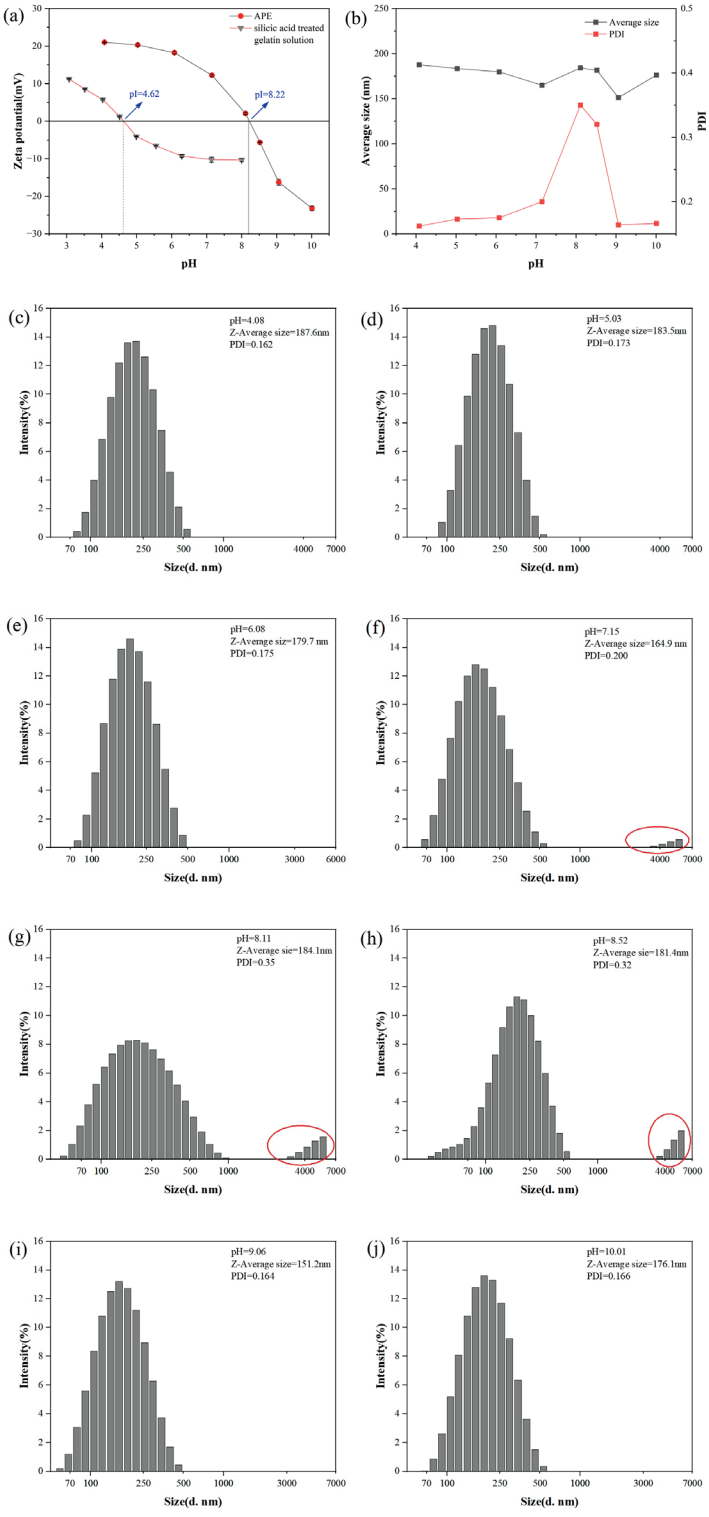

Figure 3. (a) Zeta potentials of APE and silicic acid treated gelatin solution at different pH values; **(b)** average size and poly dispersion index of APE at different pH values; Particle size distribution of APE at **(c)** pH=4.08, **(d)** pH=5.03, **(e)** pH=6.08, **(f)** pH=7.15, **(g)** pH=8.11, **(h)** pH=8.52, **(i)** pH=9.06, **(j)** pH=10.01.

in Figure 4. Figure 4a shows that APE was well absorbed at different fixing pH values, which may be mainly due to the fact that: (1) at the beginning of fatliquoring under the initial pH of 4.0 (below the pIs of SATL leather and APE), the leather and APE are both positively charged, thus making APE easier to penetrate into the leather, while at the end of fatliquoring under the fixing pH of 6.0, 7.5 or 8.0 (below the pI of APE, but above the pI of SATL leather), the leather exhibits negative charged surface while APE is still positive charged, thus promoting their interaction with each other through electrostatic attraction. That is, the strategy of penetration at first and then combination was achieved; (2) the plentiful functional groups in APE, such as tertiary amine, N^+ and $-SO_3^-$, can ensure good interaction of APE and collagen fibers. Furthermore, it can also be found that the absorption rate of APE increased with the increase of fixing pH from 6.0 to 8.0. This is mainly related to the amphoteric characteristics of APE. As the pH value approaches the pI of APE, in addition to the electrostatic interaction between leather and APE, proper aggregation of internal particle caused by the instability of APE is also conducive to the absorption of APE.

Meanwhile, the aggregation of particles in APE leads to their easier deposition in the collagen fiber gaps of leather, especially in the loose parts, which is beneficial to better filling effect. Therefore, the thickening rate increases with the increase of the fixing pH value, leading to the highest thickening rate at the fixing pH of 8.0 (Figure 4b). In addition, the softness of leather treated with APE was much better than that of untreated leather (the softness value is 4.6 mm), however, what deserves attention is that the softness reaches the maximum when the fixing pH is 7.5 (Figure 4b). This is mainly because the aggregation and deposition of APE near its pI are double-edged. Typically, the polar groups in APE interacted with collagen fibers of SATL leather through ionic bonds and hydrogen bonds during fatliquoring, while the hydrophobic long alkyl chains in APE arranged and coated on the surface of collagen fiber to form a lubricating layer, thus reducing the sliding friction, enhancing the relative movement between collagen fibers, and showing the softer hand feeling macroscopically. Moreover, the tertiary amine of APE may form hydrogen bonds with Si-OH groups in SATL leather,[8] thus probably inhibiting further intramolecular condensation of Si-OH groups during storage and thereby improving softness of SATL leather. It can be considered that these are the main reasons why the softness of SATL is improved after APE treatment. On the other hand, the excessive filling effect of APE at the fixing pH of 8.0 limited the relative sliding between and inside collagen fibers, resulting in the softness of fatliquored leather being lower than of leather obtained at the fixing pH of 7.5. As for the leather fatliquored at the fixing pH of 6.0, its softness is relatively low, mainly due to the low absorption rate of APE, which leads to insufficient lubrication.

Figure 4c shows the tensile strength and elongation at break of leather after APE treatment. Compared with the tensile strength of leather

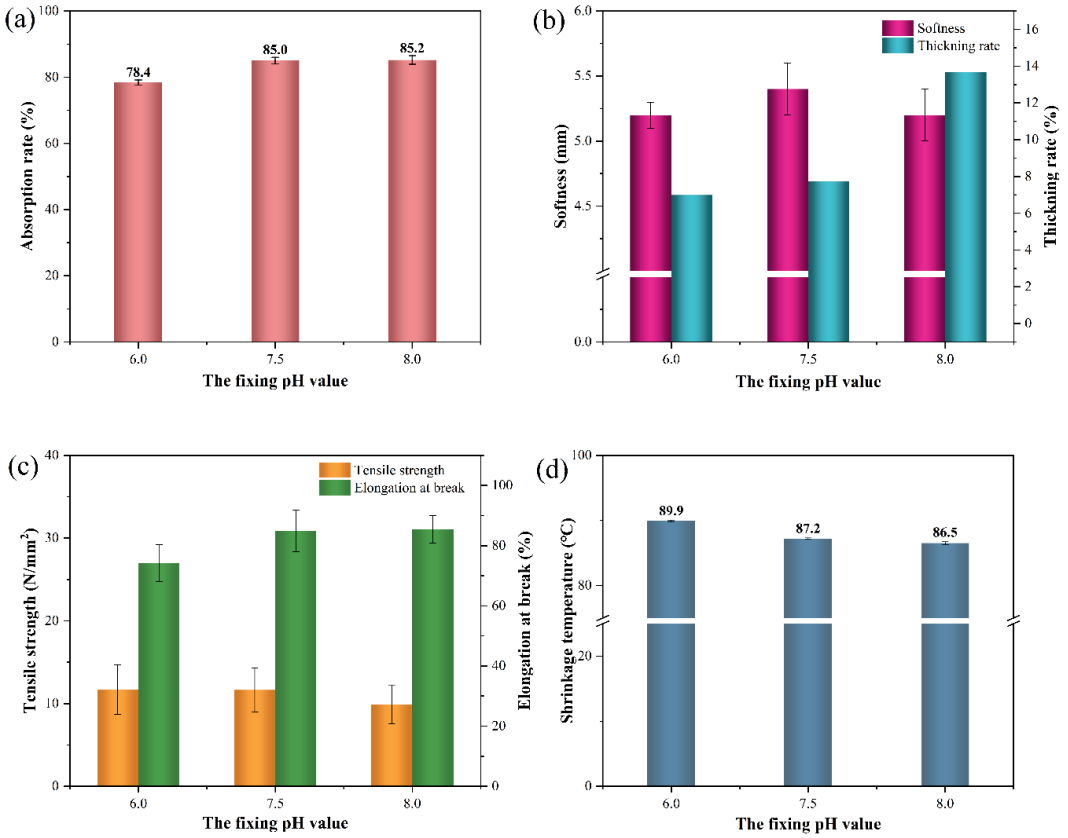

Figure 4. (a) Absorption rate of APE at different fixing pH; **(b)** Thickening rate and softness, **(c)** Tensile strength and elongation at break, **(d)** T_s of SATL leather fatliquored with APE at different fixing pH values

before APE treatment (10.1 N/mm^2), their tensile strength changed slightly. While compared with the elongation at break of untreated leather (49.0%), their elongation at break increased sharply. This can also be attributed to the lubrication function of APE. Briefly, after APE was well-dispersed inside the collagen fibers and well-bonded with fiber chains, the flexible long alkyl chains in APE could stretch the intermolecular spacing and enhance the relative slippage between collagen fibers,[20] thus significantly improving the extensibility of leather. Furthermore, the elongation at break of leather obtained at the fixing pH of 7.5 and 8.0 is very close, and both of them are higher than that of leather obtained at the fixing pH of 6.0, which indicated that the fixing pH of 7.5 is sufficient to ensure the excellent flexibility of leather.

T_s, that reflects the hydrothermal stability of leather, is one of the most important indicators for leather performance. Unfortunately, compared with the T_s of untreated leather, the T_s decreased slightly with the increase of fixing pH. This was mainly because the APE deposited in the gaps between collagen fibers increased the chain spacing between collagen molecules, thus weakened the cross-linking degree of collagen fiber networks.[21,41] In addition, the higher absorption rate of APE, the lower the T_s. However, it is worth mentioning that the T_s of SATL, as a chrome-free tanned leather, is still acceptable after fatliquoring.

To sum up, under the condition of the fixing pH of 7.5 and the initial pH of 4.0, the electrostatic attraction between APE and SATL leather as well as the aggregation and deposition of APE due to its amphoteric characteristics can be fully utilized to balance the filling effect and softening effect, so that APE can be well dispersed and absorbed, the physical and mechanical properties of SATL leather can be significantly improved. It can be speculated that there is almost no obvious negative impact on the cross-linking network after APE treatment.

3.2.2 Effect of initial pH value at the beginning of fatliquoring

In Schemes 4, 5 and 6, the organoleptic status and physico-chemical features of SATL leather fatliquored at different initial pH value of fatliquoring are studied and shown in Figure 5. It can be observed that under the premise of keeping the fixing pH at 7.5, the highest APE absorption rate (86.2%), softness (5.8 mm), thickening rate (8.1%), as well as elongation at break (86.2%) were obtained when the initial pH was 4.0 (Scheme 4). This phenomenon can be explained as follows. In Scheme 5 and Scheme 6 with the initial pH of 5.0 and 6.0 respectively, during the whole fatliquoring process, APE was positively charged, while the SATL leather was negatively charged (Figure 3a). Therefore the strong electrostatic attraction between SATL and APE might lead to excessive combination of fatliquoring agent on the leather surface in the initial stage, blocking the subsequent penetration of APE into the middle layer of

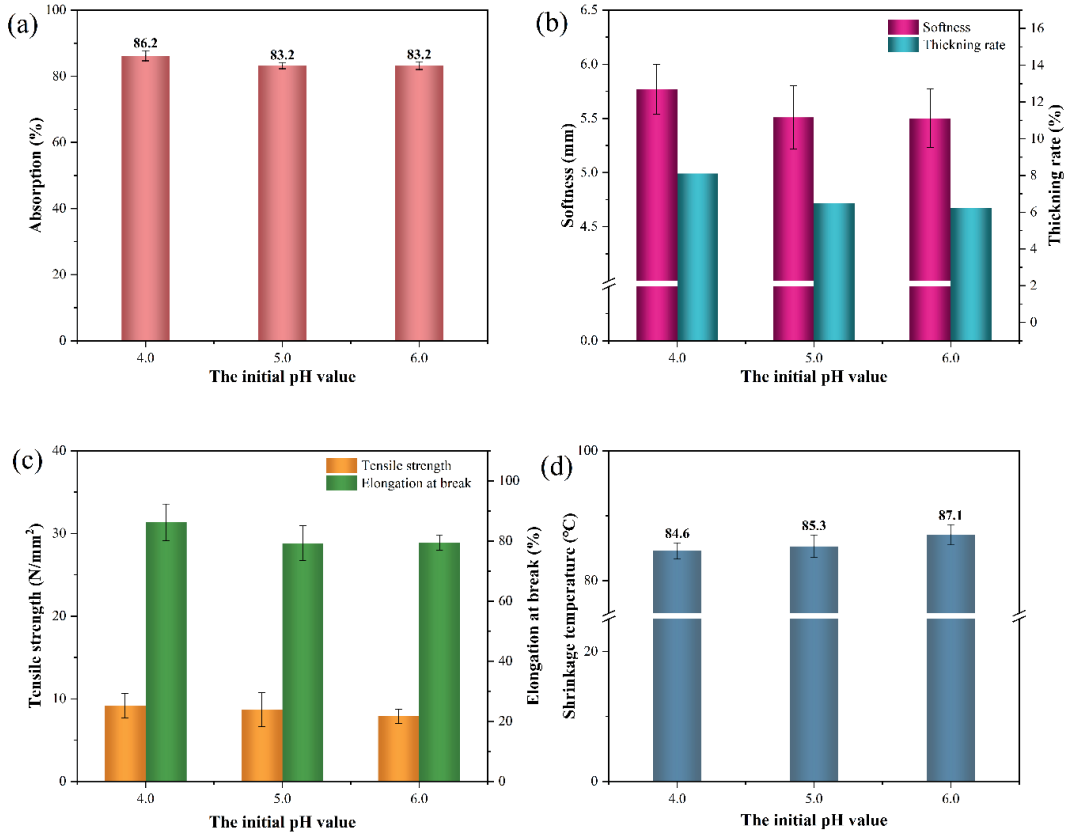

Figure 5. **(a)** Absorption rate of APE at different neutralization pH; **(b)** Thickening rate and softness, **(c)** Tensile strength and elongation at break, **(d)** T_s of SATL fatliquored with APE at different pH values before fatliquoring.

leather, which means that more APE accumulated on the surface of leather, while less APE lubricated the collagen fiber networks inside leather, finally resulting in greasy feeling and inferior mechanical properties.[18] On the contrary, the strategy of first penetration and then combination used in Scheme 4 (the same as Scheme 2) allowed enough APE to penetrate and combine in the leather to play a role in lubrication, thus obtaining better physical and mechanical properties. The lowest T_s (84.6°C) of fatliquored leather in Scheme 4 is also an indirect evidence of preferable lubrication effect. In addition, the T_s of fatliquored leather in Scheme 6 is higher than that in Scheme 5, although they have almost the same APE absorption rate (83.2%), suggesting more combination of APE on the leather surface.

3.2.3 Interaction mechanism model between amphoteric polymer and silicic acid tanned leather

According to the above research results, when the initial pH at the beginning of fatliquoring is 4.0 and the fixing pH at the end of fatliquoring is 7.5, the optimal fatliquoring effect can be achieved, in which the amphoteric characteristics of SATL and APE play a crucial role. Therefore, a possible interaction mechanism between SATL leather and amphoteric polymer is proposed and illustrated in Figure 6. As mentioned above, SATL is a silicic acid-modified collagen fiber matrix with a pI of 4.62, while APE rich in active groups has a pI of 8.22. When adjusting the initial pH to 4.0, the SATL leather and APE are both positively charged, allowing APE to penetrate easily into SATL with the help of mechanical action and its own surface activity and small particle size. Then, in order to maximize the use of the difference between the pI of APE and SATL to enhance the electrostatic interaction between them, the pH value of the bath liquid was adjusted to 7.5. In the meantime, the site binding between amphoteric polymer in APE and collagen can be realized, that is, the quaternary ammonium group and sulfonic acid group in amphoteric polymer are combined with the amino- and carboxyl groups in collagen fibers through ionic bonds respectively, while its tertiary amino groups mainly formed hydrogen bonds with collagen fibers and three-dimensional silica network in SATL. Moreover, the long alkyl chains in amphoteric polymer are arranged outward and distributed between collagen fibers, which plays a lubricating role. Besides, the aggregation of particles inside APE is also conducive to the absorption and filling effect of APE. Consequently, the flexibility and extensibility of silicic acid-modified collagen network are strikingly improved, and SATL leather is softer and more flexible macroscopically.

What's striking is that the pH adjustment mode for fatliquoring in this work is completely opposite to that in the process of fatliquoring chrome tanned leather. For chrome tanned leather, the neutralization pH and fixing pH are generally 6.0 and 4.0 respectively. This is mainly owing to the higher pI of chrome tanned

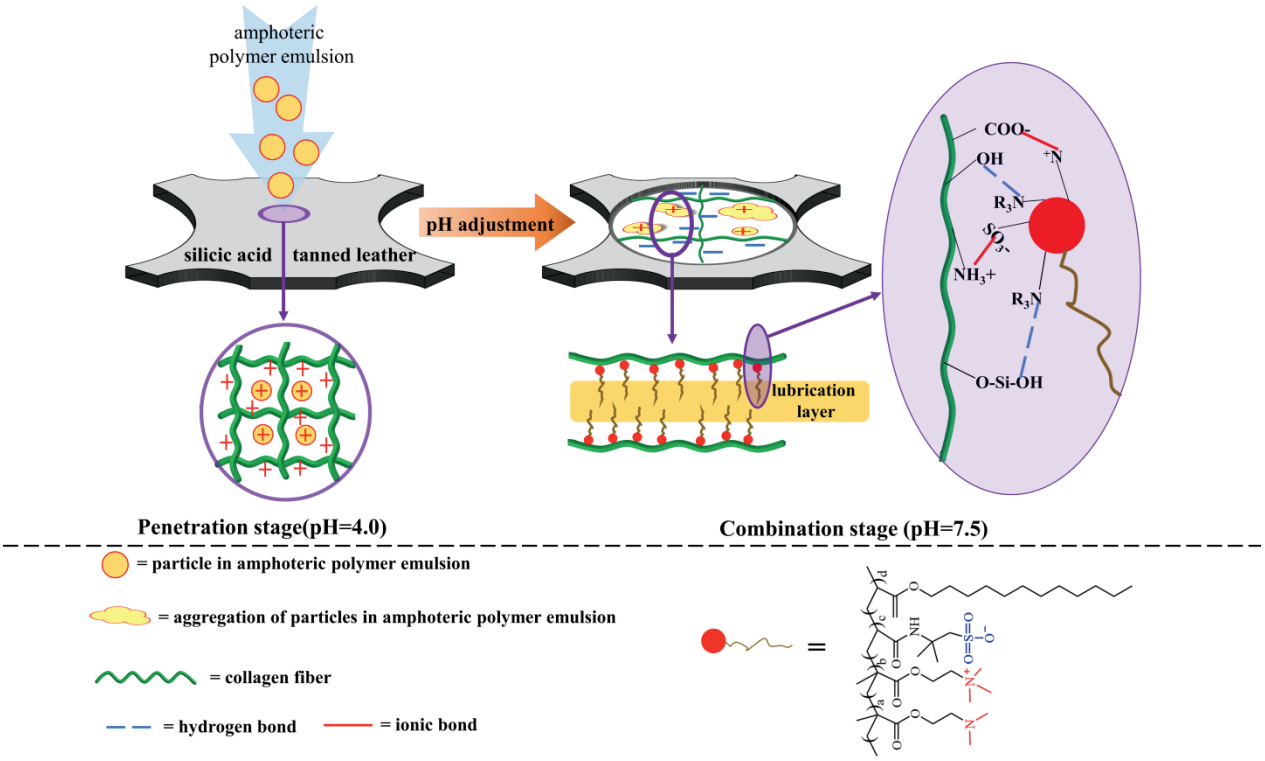

Figure 6. Schematic illustration of the interaction mechanism between amphoteric polymer and silicic acid-tanned leather

leather (between 7.0 to 8.0) as well as the use of anionic fatliquoring agent. That is, the electrostatic interaction between chrome tanned leather and anionic fatliquoring agent is weakened when the initial bath pH is neutralized to 6.0, and then strengthened when the bath pH is adjusted to 4.0 at the end of fatliquoring, so as to achieve the same purpose of penetration first and then combination. It is worth mentioning that these two pH adjustment strategies are different in form, but both of them essentially regulate the surface charge state of leather and fatliquoring agent by changing the environmental pH, thus controlling the mass transfer and combination of fatliquoring agent in leather.

3.3 Adaptability of amphoteric fatliquoring agent to the SATL leather

After understanding the interaction mechanism of amphoteric polymer and silicic acid-modified collagen fiber matrix and obtaining the optimal initial pH and fixing pH, we compared the fatliquoring effects of APE and COAPE, and also compared with a counterpart anionic commercial polymer fatliquoring agent, further explored whether the amphoteric fatliquoring agent was suitable for the fatliquoring process of SATL leather, and designed in Schemes 7, 8 and 9. The physical properties of SATL leather treated with different fatliquoring agents are summarized in Table III.

Table III shows that SATL treated with COAPE exhibits the highest tensile strength, elongation at break, softness and thickening rate. Compared with APE, COAPE contains castor oil, which can assist the filling and lubrication of long alkyl chains, thus obtaining better physical properties. Notably, the absorption rate of the anionic commercial fatliquoring agent is sharply lower than that of APE and COAPE. This is mainly attributed to the fact that there are only anionic groups in the commercial fatliquoring agent, which is detrimental to combination with the relatively electronegative SATL leather. Consequently, poor absorption leads to the lowest tensile strength, elongation at break and thickening rate of SATL treated with commercial fatliquoring agent. In contrast, APE and COAPE, two amphoteric emulsions with abundant cationic groups (-NR_2, N^+), have high positive charge, so they have excellent affinity with SATL leather. What's more, the highest absorption rate of CPOAPE (90.5%) indicates that the application of COAPE can reduce the chemical residue in fatliquoring wastewater, thus alleviating the subsequent waste management. Intriguingly, the T_s value of SATL treated with commercial fatliquoring agent dropped the most, despite the fact that only a small amount of the commercial fatliquoring agent was absorbed to lubricate the collagen fibers. It may have stemmed from the weak interaction of commercial fatliquoring agent and SATL leather caused by the "de-tanning" action, whereas the multi-point combination between APE/COAPE and SATL leather can offset the partial "de-tanning" action.

Since the SATL leather is light white, the color change, especially yellowing, will significantly affect its practical application.[42] Thus, the color difference (ΔE) and yellowness difference (Δb*) of leathers before and after aging were evaluated and recorded in Table III. The ΔE values of unfatliquored and fatliquored leathers are all

quite tiny, which are all less than the minimum color difference of 1.5 that can be distinguished by the naked eye,[41] indicating that silicic acid tannned leather has excellent light fastness, and the addition of APE, COAPE and commercial fatliquoring agent has little negative effect on it. The satisfactory yellowing resistance of untreated leather and all fatliquored leathers was further identified according to the Δb* values. The effects of APE, COAPE and the commercial fatliquoring agent on the favorable light fastness and yellowing resistance of SATL leather can be ignored.

Moreover, the morphology of untreated and treated collagen fibers with APE, COAPE and the commercial fatliquoring agent was observed by SEM at different magnifications (Figure 7), and their pore diameter distributions were tallied in Figure 8. During the fatliquoring process, the separation of collagen fiber bundles is mainly related to the supporting and lubricating functions of fatliquoring agents.[43] As shown in Figure 7a1 and a2, the collagen fibers of untreated SATL leather arranged compactly, whereas the SATL leathers treated with APE, COAPE and the commercial fatliquoring agent all exhibited loose structure (Figure 7b1-d1, b2-d2). Particularly, it can be observed that the adhesive collagen fiber bundles were opened up and separated into smaller bundles, which was consistent with the increase of smaller pores (Figure 8). This evidently proves that these three fatliquoring agents could penetrate into the collagen fiber and lubricate them, thus imparting the SATL leather good flexibility. Moreover, collagen fibers treated by COAPE were looser than the other two treatments, presenting the best filling and lubrication effect.

Overall, the above results clearly prove that COAPE is more suitable for the fatliquoring process of SATL leather than anionic commercial fatliquoring agent, since COAPE can not only greatly improve the physical and mechanical properties, especially softness and elongation at break, but also facilitate the realization of clean technological process for SATL, a chrome-free tanned leather.

Table III

Physical properties of SATL leather treated with different fatliquoring agents

Fatliquoring agent	Untreated	APE	COAPE	Anionic commercial polymer fatliquoring agent
Absorption rate (%)	-	82.7	90.5	63.2
Tensile strength (N/mm^2)	7.9±1.0	11.0±0.5	11.6±1.3	9.0±0.5
Elongation at break (%)	53.2±5.8	83.1±6.8	95.5±7.1	70.4±5.5
Softness (mm)	4.1±0.2	5.7±0.3	6.5±0.3	6.3±0.3
Thickening rate (%)	-	7.3	7.8	5.5
Ts (°C)	90.6±1.1	87.0±0.6	86.5±0.5	85.0±1.3
ΔE	0.3	0.3	0.4	0.3
Δb*	0.2	0.2	0.2	0.2
Average pore diameter (μm)	11.3	8.1	8.7	9.3

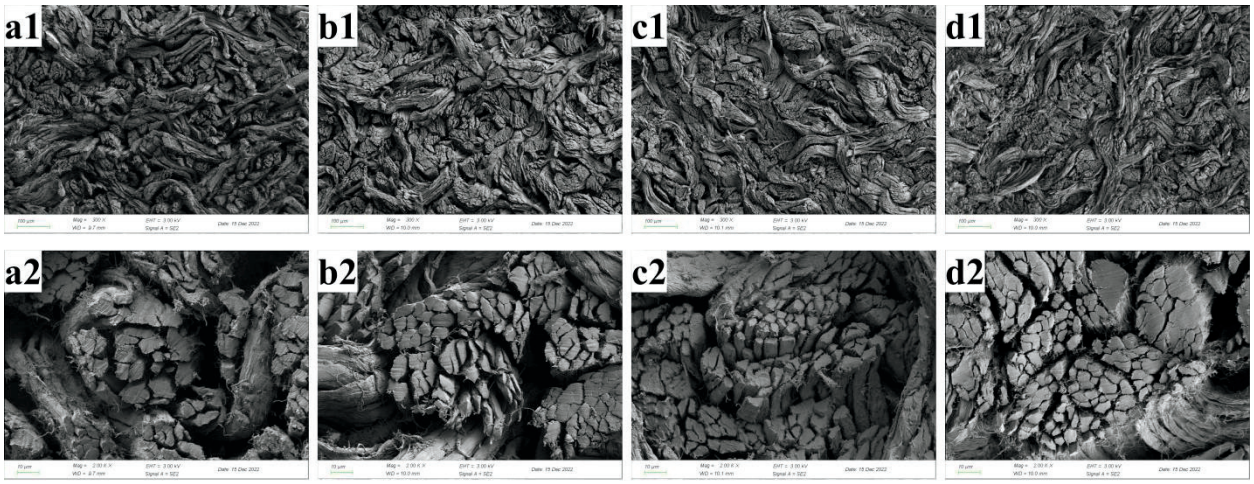

Figure 7. SEM images of SATL leather: **(a1)** unfatliquored, **(b1)** APE fatliquored, **(c1)** COAPE fatliquored and **(d1)** commercial fatliquoring agent fatliquored; **(a2-d2)** were the corresponding high magnification of SEM images of corresponding leathers, respectively

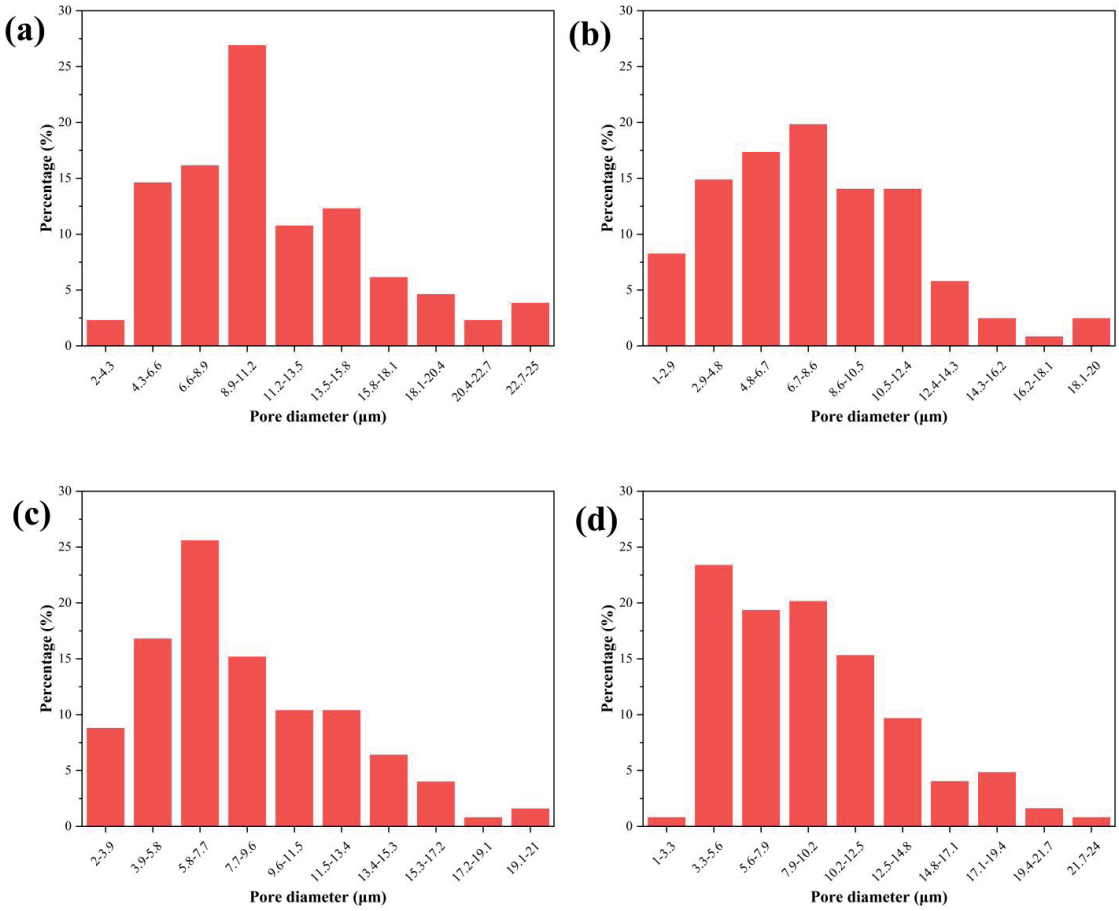

Figure 8. Pore size distribution of SATL leather: **(a)** unfatliquored, **(b)** APE fatliquored, **(c)** COAPE fatliquored, and **(d)** commercial fatliquoring agent fatliquored

4. Conclusion

In this work, an amphoteric polymer emulsion APE was successfully synthesized. The structure of amphoteric polymer was confirmed by FT-IR and XPS characterization. The measurement of surface tension, zeta potential and particle size identified the amphiphilic structure as well as amphoteric nature of APE with a pI of 8.22, which performed obvious aggregation behavior near pI. The interaction between amphoteric polymer and silicic acid-modified collagen fibers can be easily controlled by adjusting the pH value of the fatliquoring bath. When the initial pH value at the beginning of fatliquoring is 4.0, the same surface charge state is conducive to the penetration of APE emulsion particles into SATL leather. Attractively, when the fixing pH at the end of fatliquoring is 7.5, the synergistic effect of the electrostatic interaction between APE and collagen fibers and the aggregation effect of APE particles makes them reach the best combination state, and site binding occurs in the form of hydrogen bonds and ionic bonds, thus forming a molecular layer on the surface of collagen fibers, which isolated and lubricated the collagen fibers. Subsequently, the APE emulsion was compounded with castor oil as an amphoteric fatliquoring agent (COAPE) and applied to silicic acid tanned leather (SATL). Compared with those of the SATL treated with the anionic commercial fatliquoring agent, the mechanical and physical properties of the COAPE-treated SATL leather and the absorption rate of fatliquoring agent were greatly improved, demonstrating that the amphoteric fatliquoring agent is more compatible with SATL leather. Therefore, this work provides a viable strategy for the fatliquoring process of SATL leather, thus facilitating to promote the practical application of silicic acid-based tanning technology, and also provides some theoretical support for the application of amphoteric polymers in natural collagen-based materials.

Acknowledgements

This research was supported by the National Natural Science Foundation of China (No. 21376153), the Fundamental Research Funds for the Central University of China. The authors would thank Jinwei Zhang (College of Biomass Science and Engineering, Sichuan University) for his great help during conducting the leather tanning and fatliquoring process.

References

1. Ding, W., Remon, J.; Jiang, Z.C.; Biomass-derived aldehyde tanning agents with in situ dyeing properties: a 'Two Birds with One Stone' strategy for engineering chrome-free and dye-free colored leather. *Green Chem* **24**, 3750-3758, 2022.
2. Zhu, H.L., Liu, H., Tang, K.Y., et al.; Optimization of dialdehyde soluble soybean polysaccharide: preparation by response surface methodology for cleaner leather tanning. *Rsc Advances* **12**, 7506-7515, 2022.
3. Huang, W., Song, Y., Yu, Y., et al.; Interaction between retanning agents and wet white tanned by a novel bimetal complex tanning agent. *Journal of Leather Science and Engineering* **2**, 8, 2020.
4. Bacardit, A., Gonzalez, M., van der Burgh, S., et al.; Development of a New Leather Intermediate: Wet-Bright with a High Dye Affinity. *JALCA* **111**, 113-122, 2016.
5. Shi, B., Li, J., Liao, X., Zhang, J., Cao, M.; A salt-free and non-picking amphoteric polymer. CN103146850A, 2013-06-12; chrome-free tanning agent patent CN103146850A. 2013-06-12.
6. Beghetto, V., Agostinis, L., Gatto, V., et al.; Sustainable use of 4-(4,6-dimethoxy-1,3,5-triazin-2-yl)-4-methylmorpholinium chloride as metal free tanning agent. *Journal of Cleaner Production* **220**, 864-872, 2019.
7. Zhang, Z.T., Liu, J., Wang, J.C., et al.; Insight into Understanding Incorporation of Glycidoxypropyltrimethoxysilane for Improving Hydrothermal Stability and Porous Structure of Silicic Acid Tanned Leather. *JALCA* **114**, 300-312, 2019.
8. Zhang, Z.T., Liu, J., Gao, W.W., et al.; Action of silicic acid derived from sodium silicate precursor toward improving performances of porous gelatin membrane. *J Appl Polym Sci* **137**, 2020.
9. Zhang, Z., Liu, Y., Wang, J., et al.; A chrome-free combination tanning strategy: based on silicic acid and plant tannin. *Journal of Leather Science and Engineering* **3**, 15, 2021.
10. Kamely, N.; "Fatliquors" for leathers: an application of microemulsion-a review. *Polym Bull* **79**, 1977-2002, 2022.
11. Venkatesh, M., Ashokraj, J., Babu, P.R., et al.; Recycling of used domestic waste oils: A benign emulsifier-free lubricating material for leather process. *Journal of Cleaner Production* 329, 2021.
12. Ding, W.; Bridging-induced densification strategy based on biomass-derived aldehyde tanning integrated with terminal Al(III) crosslinking towards high-performance chrome-free leather production. *Journal of Environmental Management* 307, 2022.
13. Ding, W., Guo, S., Liu, H., et al.; Synthesis of an amino-terminated waterborne polyurethane-based polymeric dye for high-performance dyeing of biomass-derived aldehyde-tanned chrome-free leather. *Materials Today Chemistry* 21, 2021.
14. Lowe, A.B.; McCormick, C.L.; Synthesis and solution properties of zwitterionic polymers. *Chem Rev* **102**, 4177-4189, 2002.
15. Wei, C., Wang, X.C., Wang, W.N., et al.; Bifunctional amphoteric polymer-based ecological integrated retanning/fatliquoring agents for leather manufacturing: Simplifying processes and reducing pollution. *Journal of Cleaner Production* 369, 2022.
16. Wang, X., Sun, S., Zhu, X., et al.; Application of amphoteric polymers in the process of leather post-tanning. *Journal of Leather Science and Engineering* **3**, 9, 2021.
17. Wang, X.C., Wang, W.N., Liu, X.H., et al.; Amphoteric functional polymers for leather wet finishing auxiliaries: A review. *Polym Adv Technol* **32**, 1951-1964, 2021.
18. Hao, D.Y., Wang, X.C., Liu, X.H., et al.; A novel eco-friendly imidazole ionic liquids based amphoteric polymers for high performance fatliquoring in chromium-free tanned leather production. *J Hazard Mater* 399, 2020.
19. Sun, S.W., Wang, X.C., Zhu, X., et al.; Synthesis of an amphiphilic amphoteric peptide-based polymer for organic chrome-free ecological tanning. *Journal of Cleaner Production* 330, 2022.
20. Liu, X.H., Wang, W.N., Wang, X.C., et al.; A "Taiji-Bagua" inspired multi-functional amphoteric polymer for ecological chromium-free organic tanned leather production: Integration of retanning and fatliquoring. *Journal of Cleaner Production* 319, 2021.
21. Jiang, Z.C., Xu, S.G., Ding, W., et al.; Advanced masking agent for leather tanning from stepwise degradation and oxidation of cellulose. *Green Chem* 23, 4044-4050, 2021.
22. Wang, Y.N., Huang, W.L., Zhang, H.S., et al.; Surface Charge and Isoelectric Point of Leather: A Novel Determination Method and its Application in Leather Making. *JALCA* **112**, 224-231, 2017.
23. Wang, Y.-n.; Hu, L.; Essential role of isoelectric point of skin/leather in leather processing. *Journal of Leather Science and Engineering* **4**, 25, 2022.
24. Dong, Q.W., Li, X.; Dong, J.X.; Synthesis of branched surfactant via ethoxylation of oleic acid derivative and its surface properties. *Chem Eng Sci* 258, 2022.
25. Pan, F., Xiao, Y.H., Zhang, L., et al.; Leather wastes into high-value chemicals: Keratin-based retanning agents via UV-initiated polymerization. *Journal of Cleaner Production* 383, 2023.
26. Li, W.Y., Zuo, P., Xu, D.D., et al.; Tunable adsorption properties of bentonite/carboxymethyl cellulose-g-poly(2-(dimethylamino) ethyl methacrylate) composites toward anionic dyes. *Chemical Engineering Research & Design* **124**, 260-270, 2017.
27. Liu, D.T., Yang, X., Liu, P., et al.; Synthesis and characterization of gemini ester surfactant and its application in efficient fabric softening. *J Mol Liq* 299, 2020.
28. Ge, J.J., Zhang, T.C., Pan, Y.P., et al.; The effect of betaine surfactants on the association behavior of associating polymer. *Petroleum Science* **18**, 1441-1449, 2021.
29. Yuan, S.S., Wang, Y.F., Wang, X.J., et al.; Efficient demulsification of cationic polyacrylate for oil-in-water emulsion: Synergistic effect of adsorption bridging and interfacial film breaking. *Colloids and Surfaces a-Physicochemical and Engineering Aspects* 640, 2022.
30. Zhao, J., Cui, L., Wang, X.R., et al.; Dual ionically crosslinked chitosan-based injectable hydrogel as drug delivery system. *Colloid Polym Sci* **300**, 1075-1086, 2022.
31. Wang, S.Y., Gonzales, R.R., Zhang, P.F., et al.; Surface charge control of poly(methyl methacrylate-co-dimethyl aminoethyl methacrylate)-based membrane for improved fouling resistance. *Sep Purif Technol* 279, 2021.
32. An, L., Yu, Y.H., Chen, J., et al.; Synthesis and characterization of tailor-made zwitterionic lignin for resistance to protein adsorption. *Industrial Crops and Products* 167, 2021.
33. Yang, P.P., Zhao, J.Y., Gong, D.R., et al.; Zwitterionic ammonium-sulfonato grafted cellulose for efficient thallium removal and

adsorption mechanism study. *Int J Biol Macromol* **227**, 1059-1069, 2023.

34. Cheng, Q.L., Asha, A.B., Liu, Y., et al.; Antifouling and Antibacterial Polymer-Coated Surfaces Based on the Combined Effect of Zwitterions and the Natural Borneol. *ACS Appl Mater Interfaces* **13**, 9006-9014, 2021.
35. An, Y.Y., Zheng, H.L., Zheng, X.Y., et al.; Use of a floating adsorbent to remove dyes from water: A novel efficient surface separation method. *J Hazard Mater* **375**, 138-148, 2019.
36. Bjerk, T.R., Severino, P., Jain, S., et al.; Biosurfactants: Properties and Applications in Drug Delivery, Biotechnology and Ecotoxicology. *Bioengineering-Basel* 8, 2021.
37. Lv, S., Peng, W.J., Cao, Y.J., et al.; Synthesis and characterisation of a novel pH-sensitive flocculant and its flocculation performance. *J Mol Liq* 348, 2022.
38. Saranya, R., Selvi, A.T., Jayapriya, J., et al.; Synthesis of Fat Liquor Through Fish Waste Valorization, Characterization and Applications in Tannery Industry. *Waste and Biomass Valorization* **11**, 6637-6647, 2020.
39. Yorgancioglu, A.; Emulsification and application of a thymol loaded antibacterial fatliquor for leather industry. *J Ind Text* **51**, 470-485, 2021.
40. Hong, S.J., Garcia, C.V., Shin, G.H., et al.; Enhanced bioaccessibility and stability of iron through W/O/W double emulsion-based solid lipid nanoparticles and coating with water-soluble chitosan. *Int J iol Macromol* **209**, 895-903, 2022.
41. Ding, W., Wang, Y.-n., Zhou, J., et al.; Investigations on the general properties of biomass-based aldehyde tanned sheep fur for its selective post-tanning processing. *Journal of Leather Science and Engineering* **3**, 5, 2021.
42. Rosu, L., Varganici, C.D., Crudu, A.M., et al.; Ecofriendly wet-white leather vs. conventional tanned wet-blue leather. A photochemical approach. *Journal of Cleaner Production* **177**, 708-720, 2018.
43. Du, J.X., Shi, L.; Peng, B.Y.; Amphiphilic acrylate copolymer fatliquor for ecological leather: Influence of molecular weight on performances. *J Appl Polym Sci* 133, 2016.

Biomass-based Tanning Agent for Sustainable Leather Manufacture via Cyanuric Chloride Modified Chitooligosaccharide

by

Min Jiang,[a] Yuanhang Xiao,[a] Jun Sang,[b] Chunhua Wang,[a,c] Jiajing Zhou[a,c*] and Wei Lin[a,c*]

[a]*Department of Biomass and Leather Engineering, Key Laboratory of Leather Chemistry and Engineering of Ministry of Education, Sichuan University*, Chengdu, China, 610065

[b]*Sinolight Inspection & Certification Co., Ltd.*, Beijing, China, 100015

[c]*National Engineering Research Center of Clean Technology in Leather Industry, Sichuan University*, Chengdu, China, 610065

Abstract

Developing alternative tanning agents to avoid the potential environmental and human health risks from the conventional chrome tanning is essential for the leather industry. In this work, we prepared an eco-friendly biomass-based tanning agent dichlorotriazinyl chitooligosaccharide (DTCS) by modifying chitooligosaccharide (COS) with cyanuric chloride (CC) for chrome-free leather manufacture. The synthesis of such biomass-based tanning agent was systematically optimized to obtain the target product with high grafting degree of 67% and weight-average molecular weight (M_w) of 1465 g/mol. The non-pickling tanning procedure using DTCS was investigated, and the interactions between DTCS and collagen fibers were studied. Our results showed that the hydrothermal stability of the tanned leather was significantly increased, i.e., the shrinkage temperature (T_s) exceeding 82.0 °C, and the mechanical properties were improved. Moreover, the organoleptic properties of leather (e.g., fullness, softness and grain tightness) exhibited obvious improvement. This research not only offers a reliable approach for cleaner leather manufacturing while addressing the underlying ecological pressure, but also highlights the emerging use of biomass materials in the leather industry.

1. Introduction

Chrome tannage has catalyzed the advance of modern leather industry for more than 120 years.[1] These Cr(III) salts endow the leather with high hydrothermal stability, light resistance and versatile performance, which are virtually suitable for various types of leather products. However, Cr(III)-containing sludges and solid wastes from chrome tanning processing may pose potential environmental burdens and have been listed in the "Directory of National Hazardous Wastes (Version 2021)" in China.[2,3] Moreover, possible conversion of Cr(III) into hazardous and carcinogenic Cr(VI) under certain conditions has drawn public health concern worldwide.[4,5] Several regulations have been published to strictly limit the content of Cr(VI) in leather articles.[6] The European Commission requires the content of Cr(VI) in leather products in contact with skin to be below 3 mg/kg (Annex XVII of REACH regulation). Therefore, the development of chrome-free tanning agents has become a critical research topic in the leather industry.

Currently, chrome-free tanning techniques can be mainly categorized into non-chrome metal tanning (e.g., aluminum tanning and zirconium tanning) and organic tanning (e.g., aldehyde tanning and vegetable tanning).[7] However, the weak coordination stability of non-chrome metal tanning agents endows the tanned leather with poor properties[8]. Besides, the content of metal in metal-free leather has been restricted by international standards (i.e. Leather Standard by OEKO-TEX)[9], which promotes the development of metal-free tanning agents. The common metal-free agents, including modified glutaraldehyde, oxazolidine and organic phosphine), are derived from non-renewable petrochemicals and have been restricted owing to the release of formaldehyde during their preparation and leather production.[10-12] Therefore, efficient and eco-friendly metal-free tanning agents are still rare.

Polysaccharides such as starch, cellulose and sodium alginate have received extensive interest to produce green chemicals due to their versatile chemistry, biocompatibility, and biodegradability.[13-15] Chemical modification of polysaccharides has allowed the introduction of active groups (e.g., aldehyde groups, hydroxyl groups and alkenyl groups) for leather tanning.[16-18] However, the oxidative modification of polysaccharides may involve free formaldehyde during the process.[19] Moreover, the low isoelectric point of the obtained leather leads to the poor absorption and fixing efficiency of subsequent anionic materials (e.g., anionic dyes and fatliquors).[10]

Chitooligosaccharide (COS) is the degradation product of chitosan with the degree of polymerization (DP) less than 20.[20] The relatively low molecular weight, less chain entanglement and steric hindrance of COS lead to good water solubility and diffusion kinetics.[21,22] Recently, triazine moiety has emerged as an attractive crosslinker alternative for metal-, formaldehyde-, and phenol-based moieties in leather manufacture due to its biocompatible nature.[23] For example, Granofin® Easy F-90 liquid (F-90) is a commercialized triazine tanning agent, which can produce the light colored leather via the efficient

*Corresponding Author email: wlin@scu.edu.cn, jjzhou@scu.edu.cn

Manuscript received March 12, 2023, accepted for publication May 10, 2023.

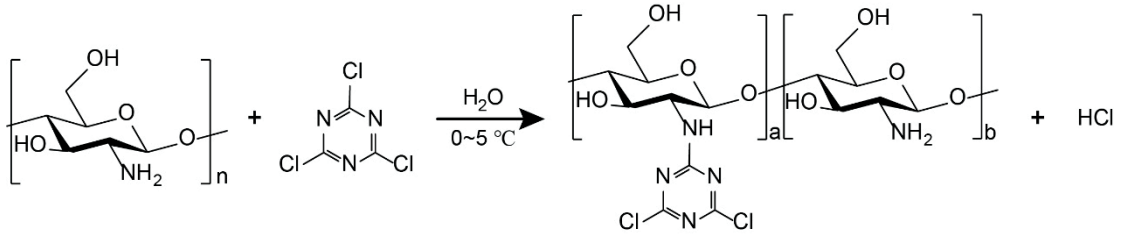

Scheme 1. The preparation of DTCS from chitooligosaccharide and cyanuric chloride.

crosslinking between active chlorines in the benzenesulphonate and the amino groups in collagen.[24] This tanning process can start from bated pelt without the pickling process, thus reducing the pollution of neutral salts[25] and simplifying the tanning process. However, F-90-tanned leather suffers from low shrinkage temperature, poor softness and undesirable fullness. Therefore, we hypothesize that novel tanning materials can be obtained by combining the advantage of cationic COS and biocompatible triazine to exert a synergistic effect, which can contribute to sustainable and reliable leather manufacture.

In this work, we developed a biomass-based chrome-free tanning agent by modifying COS with CC and evaluated its performance. The biomass-based tanning agent (i.e., dichlorotriazinyl chitooligosaccharide, DTCS) possesses active chlorines which serve as the active sites to crosslink collagen fibers, while the adequate molecular weight endows the tanned leather with satisfactory organoleptic properties such as fullness and softness. The synthesis of DTCS was optimized to provide sufficient reactive chlorines and the chemical structure of DTCS was characterized in detail. The important parameters affecting the tanning effect (e.g., tanning temperature, tanning pH, tanning time and the dosage of DTCS) were evaluated in the non-pickling tanning process. This work provides a theoretical and practical reference for clean production of leather using COS-based tanning agent, demonstrating the immense potential of biomass-based materials for sustainable development.

2. Materials and Methods

2.1 Materials

Wet salted cattle hides used for preparation of pickled and bated pelt were supplied by Zhangpu Zhiyuan Leather Co., Ltd, and the average weight of the raw materials was about 33 kg. Chitooligosaccharide (COS) was purchased from Xi'an Benfeng Biotechnology Co., Ltd. Cyanuric chloride (CC) was obtained from Aladdin Reagent Co., Ltd. The reagents used for synthesis were of analytical grade, and the other chemicals used for leather processing were commercial products.

2.2 Synthesis of DTCS

Cyanuric chloride and deionized water were first added into a three-necked flask reactor and stirred for 10 min to fully dispersion. Then COS was dissolved in deionized water, and the solution was added dropwise into reaction system over 30 min. The mass ratio of CC to COS (i.e., 0.1, 0.2, 0.3, 0.4, 0.5, 0.6) was regulated, and the reaction took placed at 2 °C for 10 h under stirring. Meanwhile, different amounts of sodium carbonate aqueous solution (20wt%) (i.e., the mass ratio of sodium carbonate to CC at 0, 0.1, 0.2, 0.3 and 0.4) was continuously added dropwise to neutralize hydrogen chloride generated in the reaction system over 10 h. Finally, the biomass-based tanning agent dichlorotriazinyl chitooligosaccharide (DTCS) was obtained through freeze drying of the supernatant for 48 h. The reaction formula is depicted in Scheme 1.

2.3 Determination of grafting degree (GD) of DTCS

O-phthaldialdehyde (OPA) spectrophotometric assay, where o-phthaldiadehyde and β-mercaptoethanol react with primary amine to form adduct with strong absorption at 340 nm,[26] was adopted to determine the grafting degree (GD) of DTCS. Specifically, the OPA reagent was prepared by combining the following solutions and diluting to a final volume of 50 mL with deionized water: 0.1 M sodium tetraborate (25 mL), 20wt% SDS (2.5 mL), 40 mg OPA (dissolved in 1 mL of methanol) and 100 μL of β-mercaptoethanol. 0.1 g/L COS/DTCS aqueous solution (5 mL) was mixed with OPA reagent (5 mL) and the mixture was incubated for 10 min at ambient temperature. Then the absorbance values at 340 nm were measured by UV-visible spectrometer (Hitachi U-3900H, Japan). The absorbance-concentration curve of glucosamine hydrochloride was plotted as calibration curve to obtain the amino content of the samples. The GD of DTCS was calculated by the following formula (1):

$$GD = \frac{(C_0 - C_S)}{C_S} \times 100\% \quad (1)$$

Where C_0 and C_s represent the amino concentration of the COS and DTCS solution, respectively.

2.4 Characterization of DTCS

2.4.1 Fourier transform infrared (FT-IR) spectroscopy

The CC, COS and DTCS samples were collected and mixed with potassium bromide. FT-IR spectra of the samples were recorded in the range from 400 to 4000 cm^{-1} with a resolution of 4 cm^{-1} on a Nicolet IS10 infrared spectrometer.

2.4.2 Nuclear magnetic resonance (NMR) spectroscopy

^{13}C-NMR spectra of CC, COS and DTCS were recorded on a 400 MHz Brucker ARX400 NMR spectrometer (Bruker, Switzerland) using $CDCl_3$, D_2O and D_2O as solvent at a concentration of 50

mg/mL, respectively. Tetramethylsilane (TMS) was adopted as an internal reference.

2.4.3 X-ray diffraction (XRD) measurement

The crystallinity of COS and DTCS was analyzed by an X-ray diffractometer (Rigaku Ultima IV, Japan) with a voltage of 40 kV and a current of 40 mA at Cu-Kα irradiation. The samples were scanned in the diffraction angle (2θ) ranging from 5° to 55° with a scanning rate of 5°/min.

2.4.4 X-ray photoelectron spectroscopy (XPS)

The elements composition and molecular structure on the surface of COS and DTCS samples were analyzed using X-ray photoelectron spectrometer (ThermoFischer, ESCALAB 250Xi, USA) with Al Kα ray as the excitation source under a vacuum degree of 8×10^{-10} Pa.

2.4.5 Gel permeation chromatography (GPC) analysis

The average molecular weight and corresponding polydispersity indexes of COS and DTCS were determined by GPC equipped with refractive index detector (Shimadzu Rid-20A, Japan), $TSK_{gel}GMPW_{XL}$ chromatographic column (Tosoh Bioscience, Japan) and high-performance liquid chromatography (HPLC) pump (Shimadzu LC20, Japan). The COS and DTCS aqueous solution (20 mg/mL) were filtered to eliminate the influence of the dust particles before injection. A solution of 0.1 M $NaNO_3$ was used as mobile phase and the flow rate was 0.6 mL/min with elution temperature at 40 °C.

2.5 DTCS tanning trials

The bated cattle hides were prepared according to the conventional process.[27] The bated cattle hide samples from back part (30 cm × 30 cm) were first immersed in 100wt% water, and then 5, 10, 15, 20, 25 and 30wt% of DTCS was added as tanning agent. The pH of the tanning bath was adjusted to 3.0, 4.0, 5.0, 6.0, 7.0 and 8.0, respectively. The tanning system was operating at 25, 30, 35, 40, 45 and 50 °C for different periods (i.e., 1, 2, 3, 4, 5, 6, 7 and 8 h). The tanned leather was washed and piled overnight. The dosage of chemical materials in the tanning process were based on the weight of limed pelt. The specific process recipe is given in Table I.

The commercially available active chlorine tanning agent (i.e., Granofin® Easy F-90 liquid from Stahl Company, abbreviation as F-90) and conventional chrome tanning agent were used to treat leather as control groups. The tanning process of F-90 is shown in Table II and chrome tanning process was carried out according to the conventional process.

The fatliquoring process of tanned leather was performed by introducing natural+synthetic fatliquor combination (3%), lecithin fatliquor (3%), synthetic fatliquor (3%), lanolin fatliquor (1%) and synthetic neatsfoot oil (1%). The fatliquored leather was dried and softened at room temperature to prepare crust leather for further evaluation.

2.6 Leather properties analysis

2.6.1 Determination of shrinkage temperature

Shrinkage temperature (T_s) of tanned leather was measured by a shrinkage temperature tester (Sunshine electronic institute, Shaanxi University of Science & Technology) according to the ASTM

Table I

Tanning process for DTCS.

Process	Chemical	Dosage/%	Temperature/°C	Time/min	Remarks
Wash	Water	400	25	5	
Tanning	DTCS	0-30	25-50		
	Water	100		0-480	pH 3-8
Wash	Water	400	25	20	Overnight
Horse up					

Table II

Tanning process for F-90.

Process	Chemical	Dosage/%	Temperature/°C	Time/min	Remarks
Wash	Water	400	25	5	
Tanning	Water	40			
	F-90	15		120	
	Water	30	35	120	
	Water	30	45	240	Overnight
Wash	Water	400	25	20	
Horse up					

method.[28] Samples (60 mm × 3 mm) were cut out from tanned leather and suspended vertically in water. The heating rate was kept at 2 °C/min. The temperature when samples shrink was recorded as T_s of tanned leather.

2.6.2 Morphology observation

The microstructure of the cross section of lyophilized leather samples was observed to analyze the dispersion of collagen fibers using a scanning electron microscope (SEM, Thermo scientific Apreo 2C, USA) with an accelerating voltage of 15 kV. The grain surface morphologies of lyophilized leather samples were observed to analyze the gain flatness by a stereomicroscope (M205 C, LEICA, Germany).

2.6.3 Determination of thickening rate

Thickening rate of tanned leather (i.e., DTCS, F-90 and Cr(III)-tanned leather) was determined by a thickness gauge (PEACOCK, Japan) according to the standard recommended by International Union of Leather Technologists and Chemists Societies.[29] The thickening rate could be calculated according to the following formula (2), in which the T (mm) is the thickness of tanned leather and the T_0 (mm) is the thickness of the pelt prepared for tanning.

$$\textit{Thickening rate}\ (\%) = \frac{(T-T_0)}{T_0} \times 100\% \quad (2)$$

2.6.4 Physical and organoleptic properties measurement

Physical properties of crust leather were measured according to the official standards recommended by International Union of Leather Technologists and Chemists Societies. Test items include tensile strength and elongation at break,[30] tear strength,[31] burst strength[32] and softness.[33]

3. Results and Discussion

3.1 Optimization of DTCS synthesis condition

The nucleophilic substitution reaction rate of CC onto COS is mainly related to the concentration of CC and the available nucleophile at different pH.[34] Therefore, effects of the CC dosage and sodium carbonate dosage on the GD of DTCS were explored.

The effect of different mass ratio of sodium carbonate to CC on the GD of DTCS was first investigated (Figure 1a). When maintaining the mass ratio of CC to COS at 0.5, the GD of DTCS increased first and then decreased with the increase of the mass ratio of sodium carbonate to CC. It reached the maximum (i.e., ~64%) when the mass ratio was 0.3. Sodium carbonate was continuously added to neutralize the hydrogen chloride generated along with the nucleophilic substitution reaction between COS and CC, which promoted the forward reaction. However, continuous addition of excess sodium carbonate caused the enhancement of the alkalinity of the reaction system, which intensified the hydrolysis reaction of cyanuric chloride, leading to the decline of the GD of DTCS. Therefore, the optimal mass ratio of sodium carbonate to CC is 0.3.

Keeping the mass ratio of sodium carbonate to CC at 0.3, the effect of different mass ratio of COS to CC on the GD of DTCS was studied (Figure 1b). The GD of DTCS increased when the mass ratio of CC to COS increased from 0.1 to 0.5, and the maximum GD was obtained (i.e., ~67%). This was attributed to the fact that the increase of CC dosage in the reaction system was conducive to the occurrence of nucleophilic substitution reaction between CC and COS. However, if the mass ratio of CC to COS exceeded 0.5, the GD of DTCS decreased. We speculated that the increase of CC dosage also promoted the hydrolysis of CC, which led to the generation of excessive HCl, thus leading to the decline of the GD of DTCS.[34] Therefore, the optimal mass ratio of CC to COS is 0.5.

3.2 Characterization of DTCS

FT-IR, ^{13}C NMR, and UV-vis analyses were performed to confirm the formation of DTCS. In the FT-IR spectrum of DTCS (Figure 2a), the broad absorption peaks between 3650 cm^{-1} and 3100 cm^{-1} were assigned to the stretching vibration of –NH_2 and –OH groups, while the relatively weak peak between 3000 cm^{-1} and 2800 cm^{-1} was attributed to C–H band stretching vibration. This indicated that the basic structural unit of COS existed in DTCS. Besides, the characteristic absorption bands of CC also appeared in DTCS, where the C=N and C–N stretching vibration of triazine ring were at around 1544 cm^{-1} and 1326 cm^{-1}, and the stretching vibration of

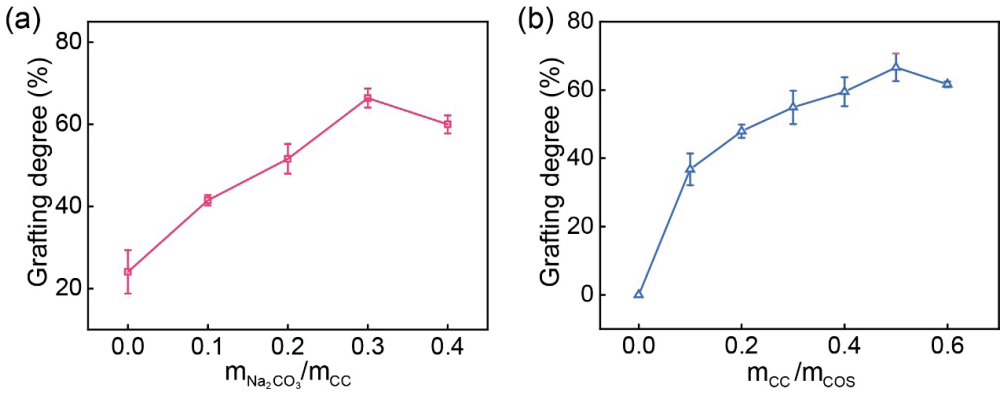

Figure 1. The GD of DTCS under **(a)** different mass ratio of sodium carbonate to CC and **(b)** different mass ratio of CC to COS.

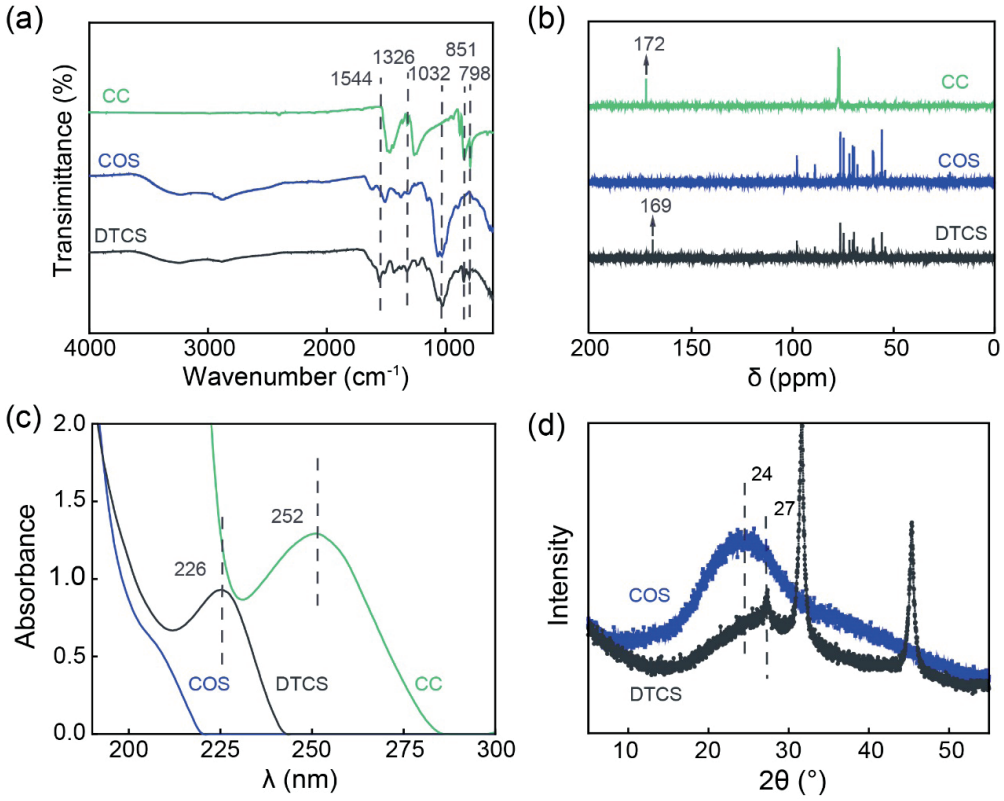

Figure 2. FT-IR spectra **(a)**, ^{13}C NMR spectra **(b)**, UV-vis absorption spectra **(c)** of CC, COS and DTCS; XRD spectra of COS and DTCS **(d)**.

C–Cl bond was at 851 cm^{-1} and 798 cm^{-1}. Collectively, FT-IR spectra indicated that CC could react with COS.

^{13}C-NMR spectra of CC, COS and DTCS were then obtained (Figure 2b). In the spectrum of CC, the carbon signal appearing at δ=172 ppm was ascribed to triazine ring. The signals of C1 (98.1 ppm), C2 (55.9 ppm), C3 (70.0 ppm), C4 (88.8 ppm), C5 (76.4 ppm), C6 (60.0 ppm) were observed in the spectrum of COS.[35,36] These peaks remained after the formation of DTCS, where the typical carbon signal of CC appeared at 169 ppm. Therefore, ^{13}C-NMR spectra confirmed that the substitution reaction of CC occurred successfully.

The UV-vis absorption spectra of CC, COS and DTCS were also collected (Figure 2c). There was no maximum absorption peak in the range of 200 nm to 400 nm for COS. The maximum absorption peaks of DTCS and CC were located in 226 nm and 252 nm, respectively. The difference was attributed to the inductive effect of imine on triazine ring which caused the λ_{max} of DTCS to move towards the shorter wavelength (i.e., blue shift). These results also demonstrated the presence of the triazine structure in DTCS.

The crystal structures of COS and DTCS were characterized (Figure 2d). XRD patterns exhibited well crystallinity of COS with a distinct 2θ peak at 24°, associated with the intermolecular and intra-molecular hydrogen bonding.[37] In contrast, the broad peak at 27° weakened significantly, owing to the introduction of dichlorotriazinyl and breakdown of hydrogen bonds, while the peaks at 31° and 45° were assigned to residual sodium chloride after the modification process. These also indicated that DTCS was more amorphous than COS, which can promote water solubility as well as penetration in tanning process.

The XPS spectra were also performed to determine the surface element composition of COS and DTCS (Figure 3). The XPS survey spectra of COS (Figure 3a) and DTCS (Figure 3d) both contained carbon, nitrogen and oxygen elements. Two obvious signal peaks of sodium and chlorine elements appeared in the spectrum of DTCS, related to the introduction of sodium chloride and dichlorotriazinyl in the modification process. Spectra of C 1s and N 1s were fitted to further estimate the functional groups on the surface of COS and DTCS. The C 1s peaks of COS (Figure 3b) were attributed to the contribution of C–C/C–H, C–O/C–N and O–C–O bonds, corresponding to the peak positions at 284.8 eV, 286.3 eV and 287.8 eV. In contrast, the C 1s of DTCS (Figure 3e) showed two additional peaks at 288.7 eV and 289.8 eV, assigned to C=N and C–Cl bonds, respectively.[38] Besides, the N 1s spectrum of COS (Figure 3c) was decomposed into two component peaks at 399.3 eV and 401.6 eV, corresponding to free amino groups and protonated amino groups.[39] In contrast, the two peaks in the N 1s spectrum of DTCS (Figure 3f) (389.9 eV and 400.6 eV) were attributed to C–N and C=N.[38]

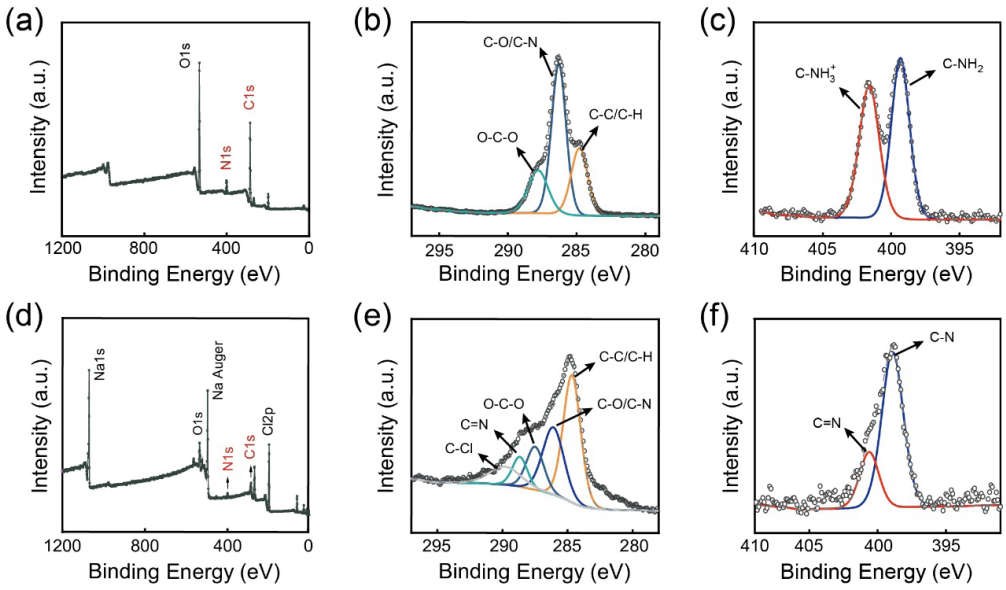

Figure 3. The wide scan XPS survey spectra of COS **(a)** and DTCS **(d)**, and the corresponding XPS spectra of C 1s and N 1s of COS **(b, c)** and DTCS **(e, f)**.

Therefore, the results of XPS analysis could further confirm the successful synthesis of DTCS.

The tanning properties of tanning agent are closely related to the size of the tanning agent molecule In order to ensure the penetration of tanning agent molecule into the inner structure of three-dimensional leather matrix and effective crosslinking with collagen fibers, the molecular weight distribution of tanning agents is generally controlled in the range of 500-3000 Da.[40] The molecular weight and the distribution of COS and DTCS were determined (Table III) using GPC. The molecular weight of DTCS was higher than COS and the M_w increased from 1077 g/mol to 1465 g/mol, which indicated the successful grafting of CC onto COS. Besides, the polydispersity (M_w/M_n) increased from ~1.4 to ~1.9. This data indicated that DTCS has suitable molecular weight and broad molecular weight distribution, which can penetrate into the collagen fibers for tanning process.

3.3 Optimization of DTCS tanning process

Tanning processes have great influence on the properties of tanned leather. We investigated the effects of the different factors (e.g., temperature, pH, time and dosage of tanning agent) on tanning properties by evaluating the hydrothermal stability of the tanned leather, which is the critical criterion for leather products.

3.3.1 Tanning temperature

The substitution of active chlorine on CC is largely controlled by temperature.[41] For example, the di-substitution of chloride occurs while the temperature exceeds 25 °C. Hence, the effect of temperature on the tanning property of DTCS was explored at different temperatures (i.e., 25 °C, 30 °C, 35 °C, 40 °C, 45 °C and 50 °C) (Figure 4a). When the tanning temperature was adjusted to 25 °C, 30 °C and 35 °C, the T_s of tanned leather was close to 75.5 °C. The highest T_s (i.e., 78.5 °C) was obtained at 40 °C. However, there was no significant contribution to the T_s by further increasing the tanning temperature. These results demonstrated that the efficient binding of DTCS and collagen fibers had already happened at 25 °C, and could be strengthened at 40 °C.

3.3.2 Tanning pH

The pH of reaction system is related to the availability of reactive groups from collagen and tanning agents, which has a significant influence on the tanning reactivity. We revealed the effect of pH on the T_s of tanned leather (Figure 4b). The T_s of tanned leather increased along with the increase of pH and achieved the highest value (~81.2 °C) when the pH was controlled at ~6.0, while it decreased slightly by further raising the pH of the reaction system. The increase of tanning pH facilitated the covalent interaction between C–Cl and $-NH_2$ under acidic conditions (i.e., pH<6.0), while the alkaline conditions (i.e., pH>7.0) promoted the hydrolysis reaction of chlorine

Table III

The average molecular weight and molecular-weight distribution of COS and DTCS.

Sample	M_n	M_w	M_z	M_w/M_n
COS	765	1077	1948	1.4
DTCS	789	1465	3836	1.9

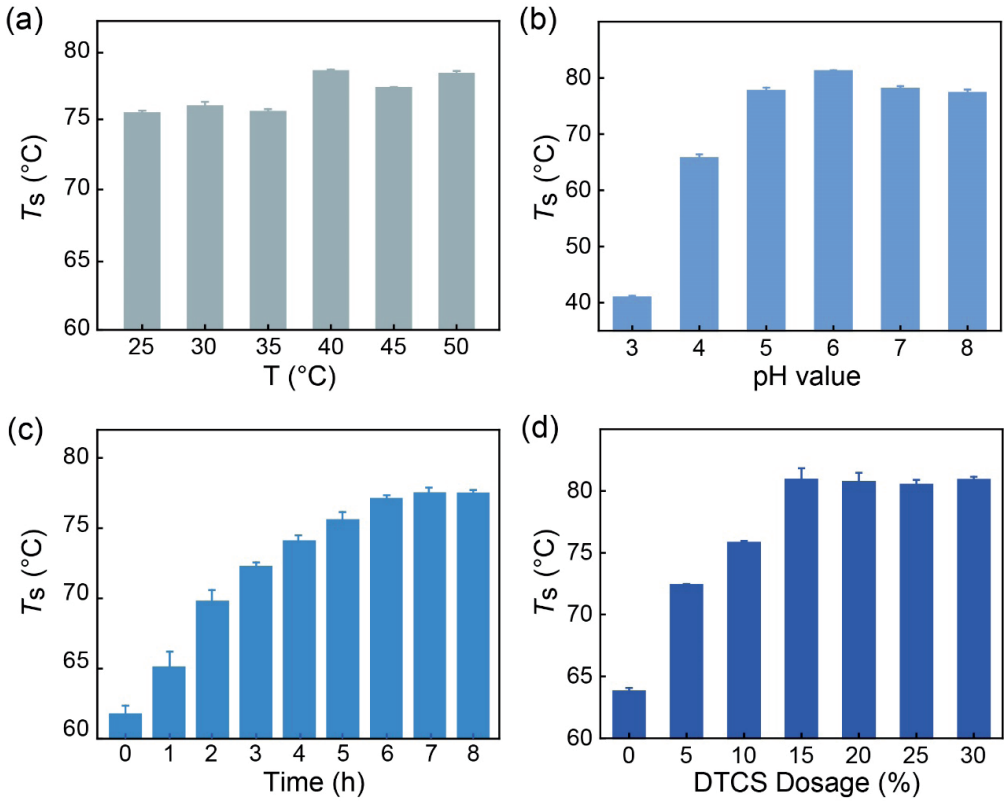

Figure 4. (a) T_s of leather tanned at different temperature, **(b)** T_s of leather tanned at different pH, **(c)** T_s of leather tanned at different time, **(d)** T_s of leather tanned with different dosage of DTCS tanning agent.

groups in DTCS and inhibited the effective covalent interaction between DTCS and collagen fibers.[42] Therefore, the pH in tanning process is optimized as ~6.0.

3.3.3 Tanning time

We further investigated the relationship of tanning time to the T_s of tanned leather (Figure 4c). The T_s elevated gradually with the extension of tanning time, while the T_s of tanned leather was nearly constant (~77.5 °C) after 7 h of tanning time. This indicated that sufficient crosslinking between DTCS tanning agent and collagen fibers occurred. Hence, the optimum tanning time is 7 h.

3.3.4 Dosage of DTCS tanning agent

The T_s of tanned leather was also evaluated by using various dosages of DTCS tanning agent (Figure 4d). The T_s of 5% DTCS-tanned leather reached 72.4 °C, suggesting that the substantial crosslinking between DTCS and collagen fibers was formed to significantly improve the hydrothermal stability of DTCS-tanned leather. Notably, tanning with 15% DTCS provided DTSC-tanned leather with significant increase in the T_s (~80.9 °C). Further increasing the DTCS dosage (>15%) showed no obvious effect on the T_s of tanned leather, due to the saturated absorption of DTCS. The use of 15% DTCS in tanning process can improve the hydrothermal stability of tanned leather with reasonable utilization rate of the tanning agent.

Overall, the optimum tanning process is obtained and summarized in Table IV by optimizing the tanning conditions. Specifically, 15% DTCS tanning agent is used in the tanning system and the tanning process is conducted at pH ~6.0 and 40 °C for 7 h, raising the T_s of DTCS-tanned leather to ~82.0 °C.

Table IV

The optimum tanning process of DTCS.

Process	Chemical	Dosage/%	Temperature/°C	Time/ h	Remarks
Wash	Water	400	25		
Tanning	Water	100			
	DTCS	15	40	7	pH ~6.0
Wash	Water	400	25		Overnight
Horse up					

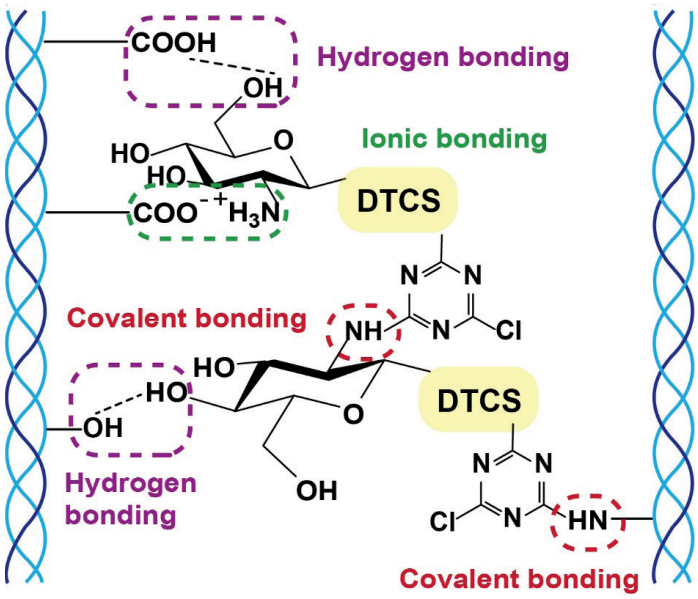

Figure 5. The possible interactions of DTCS in the tanned leather matrix.

3.4 The proposed tanning mechanism of DTCS

We proposed the possible interactions between DTCS and collagen fibers in the tanning system (Figure 5). The active chlorine groups on DTCS can not only react with amino groups of collagen fibers by covalent bonding, but also form intermolecular crosslinking with amino groups of DTCS molecules. Substantial number of hydroxyl groups of DTCS molecules can also interact with hydroxyl, carboxyl and amino groups of collagen fibers by hydrogen bonding.[43] In addition, the carboxyl groups ($-COO^-$) on collagen may bond with $-NH_3^+$ of DTCS by ionic interaction.[44] Collectively, the robust crosslinking effects within collagen fibers are formed, which consequently contribute to the enhanced hydrothermal stability of the tanned leather.

3.5 Leather morphology analysis

The dispersion of collagen fibril and fibrous network structure of leather can reflect the crosslinking/tanning effect of tanning agent.[45] The microstructure of bated pelt, DTCS-tanned leather, Cr(III)-tanned leather and F-90-tanned leather were analyzed (Figure 6). The dispersion degree of collagen fibers of DTCS-tanned leather was higher than that of bated pelt, and was comparable to those of Cr(III)-tanned leather and F-90-tanned leather. This was due to the increased degree of the crosslinking within the collagen fibers (i.e., tanning effect), which makes the collagen fibers of tanned leathers arrange regularly and disperse distinctly.[45,46] The results demonstrated that the DTCS has good tanning property and can form effective crosslinking between collagen fibers.

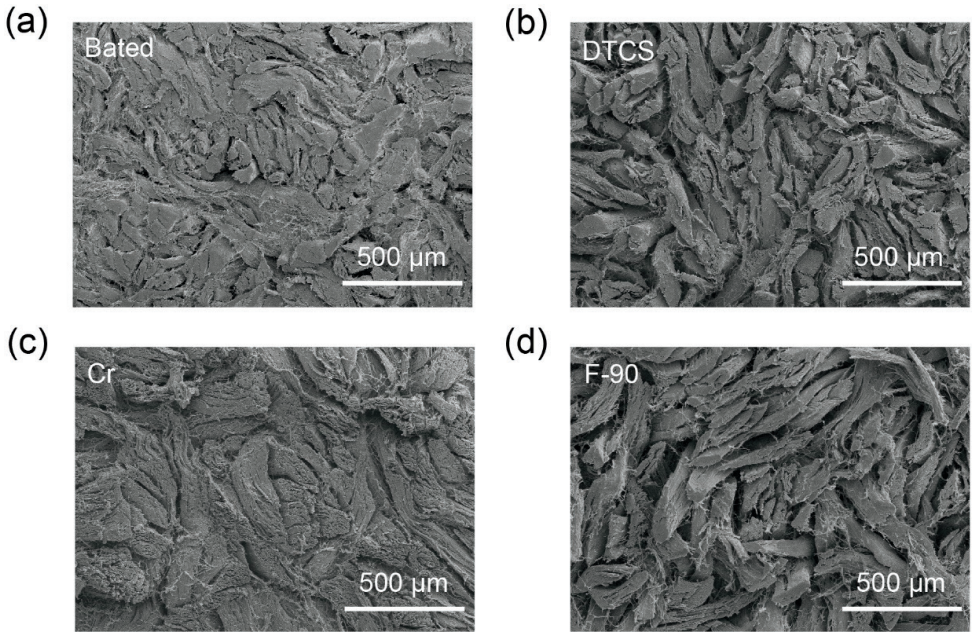

Figure 6. SEM observation of cross section microtopography of **(a)** bated pelt, **(b)** DTCS-tanned leather, **(c)** Cr(III)-tanned leather and **(d)** F-90-tanned leather.

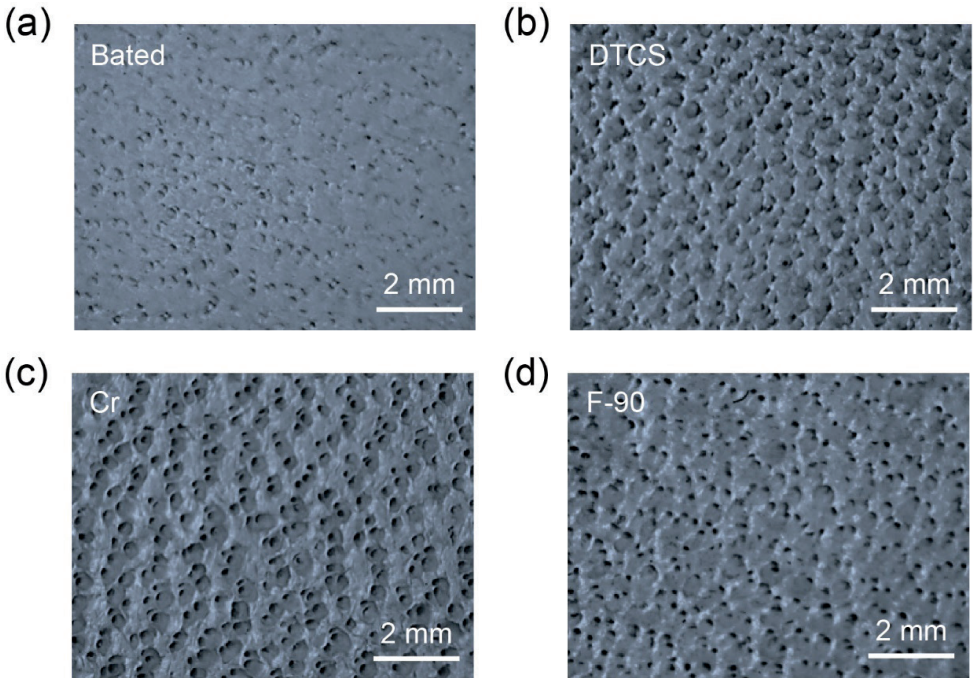

Figure 7. Stereomicroscope images of grain surface of leather tanned by different processing strategies: **(a)** bated pelt, **(b)** DTCS-tanned leather, **(c)** chrome-tanned leather and **(d)** F-90-tanned leather.

The morphology features of grain surface of leathers are the important evaluation parameters of leather performance. The grain surface morphologies of bated pelt and tanned leather were observed by a stereomicroscope (Figure 7). The bated pelt exhibited irregular grain with disordered and indistinct pores. In contrast, the grain surface of all tanned leathers presented clearer pores without apparent surface deposition of tanning agents. This could ascribe to the well penetration of tanning agent and the efficient crosslinking network forming between collagen fibers.[46] In addition, the grain of DTCS-tanned leather was smoother with relatively small aperture than that of Cr(III)-tanned leather and F-90-tanned leather, suggesting the DTCS exhibited better filling ability.[47]

3.6 Thickening rate analysis

The thickening rate of leather tanned with DTCS, F-90 and Cr(III) was determined, respectively (Figure 8a). The thickening rate of DTCS-tanned leather (~64.4%) was significantly higher than that of F-90-tanned leather (~30.2%) and Cr(III)-tanned leather (~27.6%) owing to the large molecular weight of DTCS, suggesting the DTCS exhibited better filling ability.

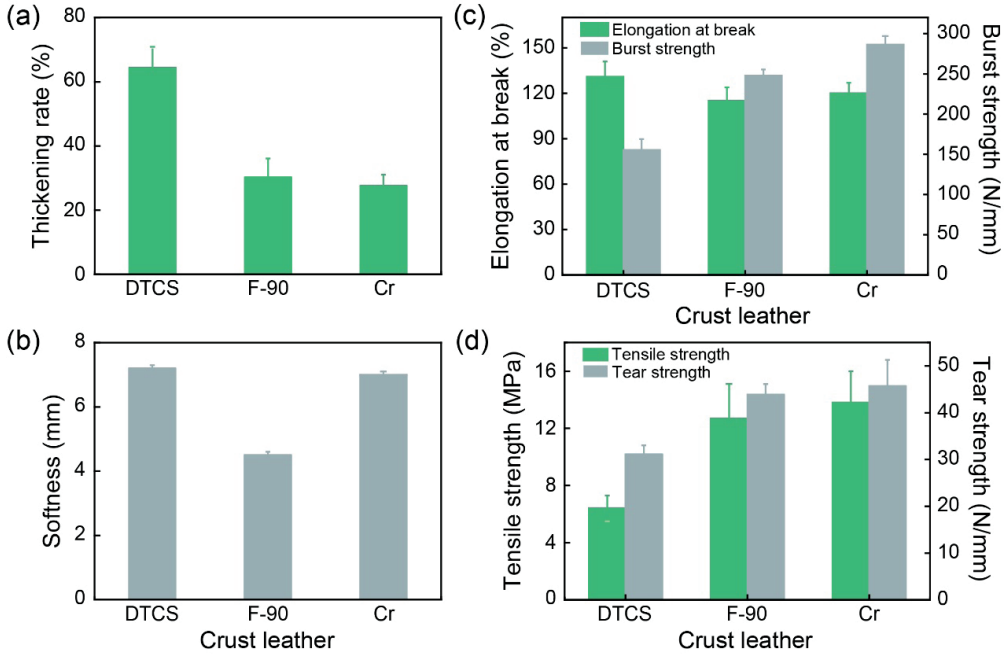

Figure 8. (a) Thickening rate of different tanned leather. **(b-d)** Physical and organoleptic properties of different crust leathers.

3.7 Physical and organoleptic properties analysis

The physical and organoleptic properties of crust leather can be determined to characterize the intrinsic quality and machinability of leather. We evaluated the physical properties (i.e., softness, tensile strength, elongation at break, tear strength and burst strength) of crust leathers tanned with DTCS, F-90 and Cr(III), respectively (Figure 8b-d). The softness of DTCS-tanned leather (7.2 mm) was similar to that of Cr(III)-tanned leather (7.0 mm) and much higher than F-90-tanned leather (4.5 mm) (Figure 8b). This might due to the flexible molecular chains of DTCS.[10] The elongation at break of DTCS-tanned leather (131%) was higher than Cr(III)-tanned leather (120%) and F-90-tanned leather (115%) (Figure 8c), indicating that DTCS-tanned leather had great extensibility. Even though the tensile strength, tear strength and burst strength of DTCS-tanned leather were not as good as crust leathers tanned with Cr(III) or F-90 (Figure 8c, d), DTCS endowed the leather with good sensory and acceptable physical properties, suggesting that DTCS had promising application in leather manufacturing.

4. Conclusions

A biomass-based tanning agent (i.e., DTCS) was prepared by conjugating COS with CC. The characteristic structure and physical properties of DTCS were characterized by several techniques including FT-IR, ^{13}C NMR, UV-vis, XRD, and XPS. The optimum synthesis protocol was obtained when the mass ratio of sodium carbonate to CC was 0.3 and the mass ratio of CC to COS was 0.5. The DTCS tanning agent was used in delimed and bated cattle hides without pickling process, aiming at eco-leather manufacturing. The tanning system using DTCS conferred the tanned leather with satisfactory T_s (~82.0 °C), improved thickness (by 64.4%), light color and good sensory. We confirmed the interaction between collagen fibers and DTCS tanning agent, which resulted in the dispersed structure of collagen fibers and the improvement of grain smoothness and porosity of tanned leather. This biomass-based tanning agent DTCS shows great potential in chrome-free tanning technology and provides a promising approach for cleaner leather manufacture.

Acknowledgment

The financial support of National Natural Science Foundation of China (21978177) and Key research and development project of Sichuan Province (22ZDYF2761) are gratefully acknowledged. The authors would like to thank Jinwei Zhang from Sichuan University for his help in tanning experiments.

References

1. Lin, W., Mu, C., Zhang, M.; Chrome tanning —— a sustainable process. *China Leather.* **29**, 27-33, 2000. doi: 10.13536/j.cnki.issn1001-6813.2000.07.007.
2. Zhao, J. , Wu, Q. , Tang, Y., Zhou, J., Guo, H.; Tannery wastewater treatment: conventional and promising processes, an updated 20-year review. *J. Leather Sci. Eng.*, 4,1-22, 2022. doi: 10.1186/s42825-022-00082-7.
3. Dixit, S., Yadav, A., Dwivedi, P. D., Das, M.; Toxic hazards of leather industry and technologies to combat threat: a review. *J. Clean. Prod.* 87, 39-49, 2015. doi: 10.1016/j.jclepro.2014.10.017.
4. Moretto, A.; Hexavalent and trivalent chromium in leather: What should be done? *Regul. Toxicol. Pharmacol.* **73**, 681-686, 2015. doi: 10.1016/j.yrtph.2015.09.007.
5. Hedberg, Y. S.; Chromium and leather: a review on the chemistry of relevance for allergic contact dermatitis to chromium. *J. Leather Sci. Eng.* **2**, 16-30, 2020. doi: 10.1186/s42825-020-00027-y.
6. Xiao, Y.; Ren, K.; Sang, J.; Lin, W.; Limitation of hexavalent chromium in leather products, its risk in business and response measures. *China Leather.* **48**, 28-34, 2019. doi: 10.13536/j.cnki.issn1001-6813.2019-008-004.
7. Covington, A.D., Wise, W.R.; Current trends in leather science. *J. Leather Sci. Eng.* **002**, 344-352, 2020. doi: 10.1186/s42825-020-00041-0.
8. Zhang, M.; The expaination of the differences in tanning properties of complexing tanning agents such as Cr^{3+}, Zr^{4+}, Al^{3+}, Ti^{4+}, Fe^{3+} through ligand field theory. *China Leather.* **09**, 19-28, 1985.
9. OEKO-TEX. Leather standard by OEKO-TEX (2021). 2021.
10. Ding, W., Yi, Y., Wang, Y., Zhou, J., Shi, B.; Peroxide-periodate co-modification of carboxymethylcellulose to prepare polysaccharide-based tanning agent with high solid content. *Carbohydr. Polym.* **224**, 2019. doi: 10.1016/j.carbpol.2019.
11. Inbasekar, C., Rao, J.R., Fathima, N.N.; trategizing the development of a metal- and formaldehyde-free tanning process using (3,5-dimethyl-1H,3H,5H-oxazolo [3,4-c] oxazol-7a(7H)-yl) methanol heterocyclic derivative oxazolidine and polyallylamine. *ACS Sustainable Chem. Eng.* **9**, 15053-15062, 2021. doi: 10.1021/acssuschemeng.1c06091.
12. Shao, S., Shi, K., Li, Y., Jiang, L., Ma, C.; Mechanism of chrome-free tanning with tetra-hydroxymethyl phosphonium chloride. *Chinese J Chem Eng.* **16**, 446-450, 2008. doi: 10.1016/S1004-9541(08)60103-2.
13. Liu, X., Chang, P.R., Zheng, P., Anderson, D.P., Ma, X.; Porous cellulose facilitated by ionic liquid [BMIM]Cl: fabrication, characterization, and modification. *Cellulose.* **22**, 709-715, 2015. doi: 10.1007/s10570-014-0467-0.
14. Mahmoudian, S., Wahit, M.U., Ismail, A.F., Yussuf, A.A.; Preparation of regenerated cellulose/montmorillonite nanocomposite films via ionic liquids. *Carbohydr. Polym.* **88**, 1251-1257, 2012. doi: 10.1016/j.carbpol.2012.01.088.
15. Qiao, C., Chen, G., Zhang, J., Yao, J.; Structure and rheological properties of cellulose nanocrystals suspension. *Food Hydrocolloids.* **55**, 19-25, 2016. doi: 10.1016/j.foodhyd.2015.11.005.

16. Ariram, N., Madhan, B.; Development of bio-acceptable leather using bagasse. *J. Cleaner Prod*. **250**, 2020. doi: 10.1016/j.jclepro.2019.119441.
17. Hua, L.S., Zhong, M.J., Qiang, L.Q., Sui, Y.Z.; Synthesis and application of graft copolymer of degraded starch and vinyl monomers. *J. Soc. Leather Technol. Chem*. **89**, 63-66, 2001.
18. Lv, S., Gong, R., Yan, X., Hou, M., Zhang, G.; Structure and properties of graft copolymer of starch and resorcinol synthesized using HRP. *J. Appl. Polym. Sci*. **125**, 541-547, 2012. doi: 10.1002/app.35686.
19. Yi, Y., Jiang, Z., Yang, S., Ding, W., Wang, Y., Shi, B.; Formaldehyde formation during the preparation of dialdehyde carboxymethyl cellulose tanning agent. *Carbohydr. Polym*. **239**, 2020. doi: 10.1016/j.carbpol.2020.116217.
20. Mourya, V.K., Inamdar, N.N., Choudhari, Y.M.; Chitooligosaccharides: synthesis, characterization and applications. *Polym. Sci., Ser. A*. **53**, 583-612, 2011. doi: 10.1134/s0965545x11070066.
21. Dou, J., Xu, Q., Tan, C., Wang, W., Du, Y., Bai, X., Ma, X.; Effects of chitosan oligosaccharides on neutrophils from glycogen-induced peritonitis mice model. *Carbohydr. Polym*. **75**, 119-124, 2009. doi: 10.1016/j.carbpol.2008.07.005.
22. Jeon, Y.J., Kim, S.K.; Production of chitooligosaccharides using an ultrafiltration membrane reactor and their antibacterial activity. *Carbohydr. Polym*. **41**, 133-141, 2000. doi: 10.1016/s0144-8617(99)00084-3.
23. Gatto, V., Conca, S., Bardella, N., Beghetto, V.; Efficient triazine derivatives for collagenous materials stabilization. *Materials*. **14**, 2021. doi: 10.3390/ma14113069.
24. Xiao, Y., Wang, C., Sang, J., Lin, W.; A novel non-pickling combination tanning for chrome-free leather based on reactive benzenesulphonate and tannic acid. *JALCA*, **115**, 16-22, 2020.
25. Liang, W., Wang, Y.; Application of A Novel Chrome-free Tanning Agent. *Leather and Chemicals*. **30**, 10-14, 2013.
26. Church, F.C., Swaisgood, H.E., Porter, D.H., Catignani, G.L.; Spectrophotometric assay using o-phthaldialdehyde for determination of proteolysis in milk and isolated milk proteins. *J. Dairy Sci*. **66**, 1219-1227, 1983. doi: 10.3168/jds.S0022-0302(83)81926-2.
27. Liao, L.; Tanning chemistry and technology. Science Press, 2005.
28. Shi, J., Zhang, R., Mi, Z., Lyu, S., Ma, J.; Engineering a sustainable chrome-free leather processing based on novel lightfast wet-white tanning system towards eco-leather manufacture. *J. Cleaner Prod*. **282**, 2021. doi: 10.1016/j.jclepro.2020.124504.
29. ISO 2589: Leather — Physical and mechanical tests — Determination of thickness. 2016.
30. ISO 3376: Measurement of tensile strength and percentage elongation. 2020.
31. ISO 3377-2: Physical and mechanical tests — Determination of tear load — Part 2: Double edge tear. 2016.
32. ISO 3379: Leather — Determination of distension and strength of surface (Ball burst method). 2015.
33. ISO 17235: Leather — Physical and mechanical tests — Determination of softness. 2015.
34. Yan, Z., Xue, W., Zeng, Z., Gu, M.; Kinetics of cyanuric chloride hydrolysis in aqueous solution. *Ind. Eng. Chem. Res*. **47**, 5318–5322, 2008. doi: 10.1021/ie071289x.
35. Zhang, C., Ping, Q., Ding, Y.; Synthesis and characterization of chitosan derivatives carrying galactose residues. *J. Appl. Polym. Sci*. **97**, 2161-2167, 2005. doi: 10.1002/app.21975.
136. Zhang, H., Li, P., Wang, Z., Cui, W., Zhang, Y., Zhang, Y., Zheng, S., Zhang, Y.; Sustainable disposal of Cr(VI): adsorption-reduction strategy for treating textile wastewaters with amino-functionalized boehmite hazardous solid wastes. ACS Sustainable Chem. Eng. **6**, 6811-6819, 2018. doi: 10.1021/acssuschemeng.8b00640.
37. Maity, J., Ray, S.K.; Chitosan based nano composite adsorbent—synthesis, characterization and application for adsorption of binary mixtures of Pb(II) and Cd(II) from water. *Carbohydr. Polym*. **182**, 159-171, 2018. doi: 10.1016/j.carbpol.2017.10.086.
38. Guo, S., Ma, L., Song, G., Li, X., Li, P., Wang, M., Shi, L., Gu, Z., Huang, Y.; Covalent grafting of triazine derivatives onto graphene oxide for preparation of epoxy composites with improved interfacial and mechanical properties. *J. Mater. Sci*. **53**, 16318-16330, 2018. doi: 10.1007/s10853-018-2788-0.
39. Benitez, J.J., San-Miguel, M.A., Dominguez-Meister, S., Heredia-Guerrero, J.A., Salmeron, M.; Structure and chemical state of octadecylamine self-assembled monolayers on mica. *J. Phys. Chem. C*. **115**, 19716-19723, 2011. doi: 10.1021/jp203871g.
40. Ding, W., Yi, Y., Wang, Y., Zhou, J., Shi, B.; Preparation of a highly effective organic tanning agent with wide molecular weight distribution from bio-renewable sodium alginate. *Chemistryselect*. **3**, 12330-12335, 2018. doi: 10.1002/slct.201802540.
41. Blotny, G.; Recent applications of 2,4,6-trichloro-1,3,5-triazine and its derivatives in organic synthesis. *Tetrahedron*. **62**, 9507-9522, 2006. doi: org/10.1016/j.tet.2006.07.039.
42. Jia, X., Tan, R., Peng, B.; Preparation and application of polyethylene glycol triazine derivatives as a chrome-free tanning agent for wet-white leather manufacturing. *Environ. Sci. Pollut. Res*. **29**, 7732-7742, 2022. doi: 10.1007/s11356-021-16133-1.
43. Lim, S.H., Hudson, S.M.; Review of chitosan and its derivatives as antimicrobial agents and their uses as textile chemicals. *J. Macromol. Sci., Polym. Rev*. **43**, 223-269, 2003. doi: 10.1081/mc-120020161.
44. Zargarkazemi, A., Sadeghi-Kiakhani, M., Arami, M., Bahrami, S.H.; Modification of wool fabric using prepared chitosan-cyanuric chloride hybrid. *J. Text. Inst*. **106**, 80-89, 2015. doi: 10.1080/00405000.2014.906097.
45. Li, X., Wang, Y., Li, J., Shi, B.; Effect of sodium chloride on structure of collagen fiber network in pickling and tanning. *JALCA*. **111**, 230-237, 2016.
46. Xu, S., Shi, Bi.; A green and sustainable strategy for leather manufacturing: Endow dehydrated hide with consistent and durable hydrophobicity. *J. Cleaner Prod*. **383**, 2023. doi: 10.1016/j.jclepro.2022.135526.
47. Pradeep, S., Sundaramoorthy, S., Sathish, M., Jayakumar, G. C., Rathinam, A., Madhan, B., Saravanan, P., Rao, J. R.; Chromium-free and waterless vegetable-aluminium tanning system for sustainable leather manufacture. *Chem. Eng. J. Adv*. **7**, 2021. doi: 10.1016/j.ceja.2021.100108.

Effect of Electrostatic Interaction between Collagen and Enzymes on Permeation of Protease into the Pelt during Leather Bating Process

by
Yiwen Zhu,[1,2] Jinzhi Song,[1,2] Xu Zhang,[1,2] Mengchu Gao,[1,2] Biyu Peng[1,2*] and Chunxiao Zhang[1,2]
[1]*National Engineering Research Center of Clean Technology in Leather Industry, Sichuan University,* Chengdu 610065, China
[2]*Key Laboratory of Leather Chemistry and Engineering of Ministry of Education, Sichuan University,* Chengdu 610065, China

Abstract

The enzymatic delimed pelts bating process using proteases is critical to improving the overall performance of the leather. Bating effectiveness is determined not only by the properties but also by the permeation behavior of the proteases. Imperfect methods to control protease permeation often results in uneven distribution of enzyme proteins in the pelts, leading to excessive enzymolysis of the surface layer and inadequate opening-up of the inner layer. In this study, the relative size of proteases and delimed pelts were analyzed, the permeation behavior of fluorescein-labeled proteases in the pelt was observed using a confocal laser scanning microscope (CLSM), and the effect of electrostatic interaction between protease and collagen proteins on the permeation of protease into the pelt was investigated. The results showed that, after dehairing, liming and deliming operations, the enzyme can easily permeate into the pelts due to the formation of large cavities and interfibrillar gaps. The permeation of protease within the delimed pelt is significantly influenced by the affinity (electrostatic interactions) between the collagen and protease proteins. The isoelectric point (pI) of the protease protein, the collagen and the pH of the solution directly influence the electrostatic properties and interactions. When the enzyme and collagen are similarly charged (electrostatic repulsion), the enzyme can easily permeate into the pelts; when the enzyme and collagen are oppositely charged (electrostatic attraction), the permeation of the enzyme into the inner layer is difficult, resulting in the accumulation of protease on the grain and excessive hydrolysis of the grain layer. Therefore, the established permeation regulation mechanism of protease based on electrostatic interactions between enzyme and collagen could serve as an important basis for the selection of protease and the regulation of the enzymatic bating process.

Introduction

Enzymatic bating is an important process performed on delimed pelts to further remove scale, interfibrillar substances and opening-up collagen fibers to obtain clean, smooth, elastic and soft leather products, which cannot be replaced by any chemical and mechanical operations. As the main component of animal hides is protein, protease is the main enzyme used for pelts bating, and trypsin, an endo-protease extracted from the animal pancreas, is taken as the preferred option for pelts bating.[1] However, the disadvantages of animal trypsin limit its application, and the application of microbial proteases in the pelts bating process tends to increase.[2-4]

With the increasing demands for the softness, evenness and properties of leather products, the dosage of proteases and the duration time of the bating process, namely the intensity of the protease treatment, have been increased. The ideal bating effect is that the protease can quickly penetrate into the pelts to avoid the excessive degradation and damage of the grain surface, and to ensure the bating evenness of the inner and outer layers. However, in the practical bating process, protease tends to accumulate on the surface due to the difficulty of permeation of protease into the pelts. In addition, most of the proteases possess a stronger effect on structural proteins and wide-spread substrate specificity, resulting in damage to the grain surface at high dosages and long duration time. Therefore, the current pelts bating process usually takes a conservative method with lower protease dosage and short treatment time. However, the conservative bating method results in the insufficient opening-up of the middle layer due to the difficulty of protease permeation into the inner layer.[5] Consequently, it is crucial to improve the permeation rate and depth of proteases and avoid accumulation on the surface layers, especially on the grain layer, to achieve the desired bating effect.

Several factors may influence the permeation of proteases into the pelts,[6-8] such as the situation of the permeation channels, the relative size of the protease molecule, its aggregates and the interfibrillar space, and the affinity between the pelt fibers and the protease molecules. Our previous enzymatic dehairing research found that,[9] different proteases have significantly different isoelectric points (pI), and the surface charges of the protease molecules and collagen fibers changed with the adjustment of the pH values of the solution, resulting in the various electrostatic interactions between the proteins. The results demonstrated that it is a useful way to speed up protease permeation into the pelts by regulating the surface charges of proteins and its affinity.[9] Wang et al. [10] demonstrated that

*Corresponding author email: pengbiyu@scu.edu.cn ; Tel.+86-28-85401208
Manuscript received April 2, 2023, accepted for publication May 10, 2023.

negatively charged materials can penetrate negatively charged skin/leather faster than positively charged materials. The above results suggest that the electrostatic interaction between the protease and delimed pelts is critical for the permeation of proteases in the pelts bating process, but the mechanism involved is not clear at present.

Fluorescence labeling and confocal laser scanning microscope (CLSM) observation is an effective method to study the permeation behavior of proteases in delimed pelt.[11] However, the purity of the selected proteases has been ignored in some of the reported studies, and the purification of the fluorescein-labeled proteases and the variations of the molecular weight and pI of the proteases have been neglected. All of these deficiencies result in the mass transfer tracking results of the labeled proteases not fully representing the permeation behavior of the unlabeled proteases.

The purpose of this study was to investigate the permeation behavior of proteases in delimed pelts during the enzymatic bating process, the effect of the relative size of proteases and pelt pores and the electrostatic interaction between protease molecules and collagen fibers on the permeation behavior of proteases. Three highly purified proteases with significantly different pI were selected and labeled with fluorescein isothiocyanate (FITC), and the effect of the degree of labeling on the properties of the proteases was evaluated. The permeation behavior of the selected proteases was investigated using fluorescein labeling and CLSM techniques, including the permeation direction, pathway and depth of the proteases in delimed pelts. Then, the effects of different electrostatic interactions on the permeation depth and rate of the proteases were analyzed by adjusting the pH of the solutions to induce the proteases and delimed pelts to carry different charges. In addition, unlabeled protease bating experiments were performed to verify the results of the fluorescein-labeled protease permeation experiments. These studies attempt to clarify the law of the permeation behavior of proteases in the pelts and provide guidance for the selection of proteases and the regulation of the pelt bating process.

Materials and Methods

Materials

Fresh wet-salted bovine hides were purchased from a tannery in Sichuan, China, and subjected to conventional soaking, dehairing, degreasing, liming and deliming processes to obtain delimed pelts. Alkaline protease P-SG-B, trypsin P-NB115-T and P-PTN110-T were purchased from Sichuan Dowell Science and Technology Co, Ltd, China. Sodium dodecyl sulfate (SDS), polyacrylamide and FITC were purchased from Shanghai Sangon Biotech, Co., Ltd, China. Chemicals used in the tanning process were of industrial grade and supplied by Sichuan Dowell Science and Technology Co., Ltd., China. All of the analytical grade reagents were purchased from local suppliers in Chengdu, China. All of the analytical experiments were repeated at least three times and the mean was reported.

Determination of protease particle size and delimed pelts pore diameter

Determination of protease particle size

The concentration of P-SG-B, P-NB115-T and P-PTN110-T was diluted to 10 mg/mL protein with deionized water. The pH of the protease solutions was then adjusted to 7.5, 8.5 and 9.5 using 0.1 mol/L hydrochloric acid and sodium hydroxide, respectively, and filtered through an aqueous filter membrane (0.1 μm). The particle size distribution of the proteases at different pH values was then determined using a particle size analyzer (Zetasizer nano zsp, Malvern, USA) under the following conditions: the dispersion medium was water, the measurement temperature was 25°C, the scattering angle was 173°, the number of measurements was automatic, the equilibration time was 120 s and the particle size calculation model was Protein Analysis.

Determination of pore diameter of delimed pelts[12]

Mercury intrusion porosimetry (MIP) was used to assess the pore diameter distribution of the delimed pelts. The delimed pelts were freeze-dried and cut into uniform pieces (approximately 1 cm^3). The pore diameter distribution of the samples was determined using a fully automated mercury porosimeter (AutoPore VI 9500, Micromeritics, USA) capable of measuring pores in the range of 5.5 nm to 120,000 nm in diameter.

Determination of zeta (ζ) potential and pI of the delimed pelts [13,14]

The delimed pelts were freeze-dried and then ground to powder and passed through a 1 mm diameter sieve. Fifteen grams of the pelt powder obtained was mixed with 500 mL of deionized water in a conical flask. The pH of the solution was adjusted to a certain value using either a 0.1 mol/L hydrochloric acid solution or a sodium hydroxide solution. The pI of the samples was determined as the pH value when the ζ potential on the curve is zero. The ζ potential of the delimed pelt powder was evaluated at different pH values using a solid zeta potential meter (SZP-10, MÜtek, Sweden). The curve of ζ potential versus pH was plotted, and the pH value at which the ζ potential on the curve was zero was determined to be the pI of the samples.

Preparation and characterization of fluorescein-labeled proteases

Preparation and purification of fluorescein-labeled protease

FITC-labeled proteases were prepared according to the reported method.[15] Specifically, P-SG-B, PTN110-T and P-NB115-T proteases were dissolved in carbonate buffer (0.5 mol/L, pH 9.0) to obtain a 5 mg/mL protein solution and mixed with a certain amount of FITC; and the mixture was gently stirred at 4°C for 12 hours under light-free conditions. Then, a certain amount of semi-saturated ammonium sulfate was added to the mixture to precipitate the labeled protease, and the precipitate was immediately separated. Next, the precipitate was dissolved in phosphate buffer solution (PBS, 0.01 mol/L, pH 7.2) and dialyzed with an 8 kDa dialysis bag at 4°C to remove the salt and uncombined fluorescein. The prepared

fluorescein-labeled proteases were designated FITC-P-SG-B, FITC-PTN110-T and FITC-P-NB115-T, respectively, and were temporarily stored at 4°C in the dark.

Determination of UV-Vis and fluorescence spectra

The unlabeled and labeled protease samples were appropriately diluted with a certain volume of PBS buffer. The PBS buffer was prepared as follows: first, 1 mol/L disodium hydrogen phosphate (liquid A) and 1 mol/L sodium dihydrogen phosphate (liquid B) were prepared. Then, 72 mL of liquid A and 28 mL of liquid B were mixed and diluted to a final volume of 1000 mL with deionized water, which was 0.01 mol/L PBS buffer (pH 7.2). The UV-Vis spectra of the unlabeled and labeled protease solutions were analyzed by using a UV-Vis spectrophotometer (V-1100D, Mapada, China) in the wavelength range of 200 nm - 800 nm at a scanning speed of 2 nm/s. The fluorescence intensity of the labeled protease solutions was analyzed by using a fluorescence spectrophotometer (F7000, Hitachi Ltd., Japan) with an excitation wavelength of 495 nm, slit width of 5 nm and integral time of 0.1 s.

Determination of the combined amount of FITC to protease protein 16

The combined rate of fluorescein was defined as the amount of combined FITC (mg) per milligram of labeled protease protein. The concentration of proteins was determined by the Lowry method [17] and the concentration of FITC was calculated according to the FITC concentration-absorbance standard curve, measured at 490 nm.

Determination of the pI and molecular weight (Mw) of the proteases

The pI of the protease was determined by isoelectric focusing polyacrylamide gel electrophoresis (IEF-PAGE) (Model 111 Mini IEF Cell, Bio-Rad, American). The electrophoresis steps were as follows: 100 V for 30 minutes, 200 V for 15 minutes, and 450 V for 60 minutes.

The M_w of the protease was determined by sodium dodecyl sulfate-polyacrylamide gel electrophoresis (SDS-PAGE) (Mini-PROTEAN® Tetra, Bio-rad, American) with a separating gel concentration of 12%. The electrophoresis steps were as follows: 100 V to move the samples to the boundary between the concentrate and the separating gel, then 150 V until the samples migrated to the bottom of the separating gel.

After IEF-PAGE and SDS-PAGE, the gels were fixed and stained with a Coomassie Blue solution and washed with deionized water to eliminate the background color. The pI and M_w of the proteases were calculated using Quantity One software (Bio-Rad, USA).

Permeation behavior of labeled proteases in the delimed pelts at various pH values

The pH values of the delimed pelts were adjusted to 7.5, 8.5 and 9.5 by using Britton-Robinson buffer (B-R buffer, 0.1 mol/L), respectively. Then, pieces (4 cm × 4 cm) with adjusted pH were mixed with 50% (w/w) of labeled protease solution (containing 0.5 mg/mL protein) in a 250 mL brown bottle and rotated in a drum to mimic the mechanical action of the actual pelt bating process. Samples (0.5 cm × 0.5 cm) were cut and washed at intervals of 5 min, 1 h, 3 h and 5 h, and sectioned longitudinally at 20 μm thickness using a freezing microtome (CM1950, Leica, Germany) and observed using a confocal laser scanning microscope (Stellaris, Leica, American).

The fluorescence of FITC was excited by an argon ion laser at a wavelength of 488 nm, resulting in green fluorescence. The distribution of FITC-labeled proteins on the longitudinal section of the pelts was visualized in the *xy* plane, and the confocal images were captured and analyzed; the fluorescence intensity was also quantitatively analyzed.

Delimed pelts bating effectiveness of proteases at various pH values

Six pieces of delimed pelts were sampled adjacent and symmetrically and weighed. One piece of the pelt was used as a control without subsequent bating, with only 50% (w/w) deionized water and simultaneously rotated. The rest (five pieces of pelts) were mixed with 50% (w/w) of B-R buffer solution (0.1 mol/L, containing 50% of P-NB115-T) at pH 7.5, 8.1, 8.8, 9.6 and 10.5, and rotated at 35°C for 6 h, respectively. The bated samples were then subjected to standard pickling, Cr-tanning and post-tanning operations, and the grain surface of the crust leather was observed using a stereoscopic microscope (TIPSCOPE, China).

Results and Discussion

The particle size of protease in solution and pore diameter of delimed pelts

Animal hides are primarily composed of collagen fibers. After the removal of hair and glands in the dehairing and liming processes, the pores and interfibrillar spaces provided channels for chemical permeation in the subsequent processes. While the permeation of protease molecules into the hides is very important in the enzymatic leather making process, it is still a challenge for protease proteins to permeate into the inner layer of the hides due to their relatively large molecular size. It can be speculated that the relative size of the protease molecules, their aggregations and the pore diameter of the pelts are the main factors influencing the permeation of proteases.

The particle size of protein molecules is influenced by their structure and molecular weight, temperature, pH and ionic strength of the solution, and the protein molecules may also aggregate into masses of different sizes. Protein bating is performed under weak alkaline conditions, mainly using trypsin and alkaline proteases. In this study, three widely used highly-pure proteases (animal trypsin P-PTNP110-T, microbial trypsin P-NB115-T and microbial alkaline protease P-SG-B) were selected, and the particle size of these proteases was investigated at the same pH and ionic strength of the bating conditions. The results are shown in Figure 1.

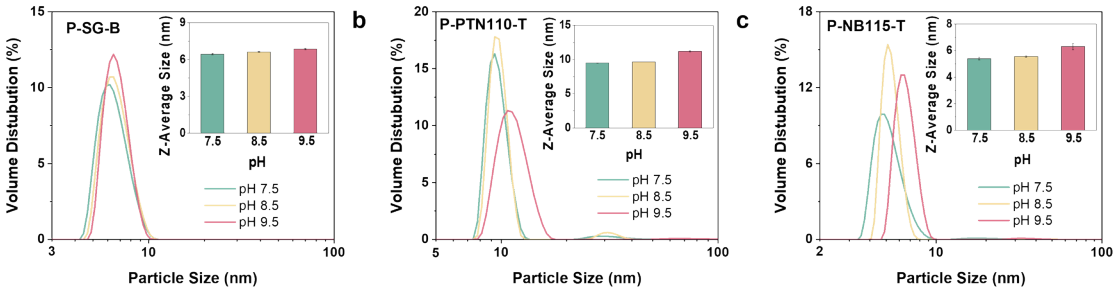

Figure 1. Particle size and distribution of proteases at various pH values (10 mg/mL of protein)

As shown in Figure 1, all of the selected proteases had similar particle sizes and distributions in an aqueous solution (pH 7.0), except for protease P-PTNP110-T, which was slightly larger but also less than 13 nm. The average size of the protease particles increased slightly with increasing pH values, with a size difference of less than 2 nm.

The relative molecular weight of the selected proteases was approximately 25 kDa (see Figure 6b), and it has been reported in the literature that the particle size of protein molecules with a relative molecular weight of around 25 kDa is approximately 5 nm.[18] Therefore, the degree of aggregation of the selected protease proteins is expected to be low at a protein concentration of 10 mg/mL (pH 7.5 - 9.5). In the practical bating process, the dosage of proteases is very low and the concentration of proteins is usually less than 0.5 mg/mL; therefore, it can be speculated that the selected proteases will not aggregate into large masses during the actual bating process.

As the enzymatic bating process uses enzymes to dispose of the delimed pelts, it was necessary to further analyze the pore diameter and distribution of the delimed pelts produced by the conventional beamhouse process. The results are shown in Figure 2.

As shown in Figure 2, the pore diameter-log differential intrusion curve shows that the most prevalent pore diameter in the delimed pelts was 12500 nm; the pore diameter cumulative curve shows that the total pore volume increased significantly between 4000 and 24000 nm, indicating that the majority of the pores in the delimed pelts are in this range. The proportion of macropores with pore diameters larger than 4000 nm was over 74% of the total pore volume, which means that the majority of the pores in the delimed pelts are microporous. In the literature,[19,20] it is reported that the pore diameter of the soaked hides is mainly in the range of 5 - 55 nm, which is much smaller than the pore diameter of the delimed pelts measured in this experiment. Despite the difference in results obtained from different methods and hides,[21] it is evident that the porosity and pore diameter of the delimed pelts are significantly higher than those of the soaked hides. This is because the removal of unwanted tissues, such as hair and glands, during dehairing, liming and deliming creates a large cavity in the grain surface layer and increases the interfibrillar gap by removing interfibrillar substances. The increased porosity and pore diameter of delimed pelts is conducive to protease permeation. During the enzymatic bating process, the small particle size of the protease (less than 13 nm) allows it to easily permeate the pelts through the large channels. However, the inner granular and reticular layers are woven by finer collagen fibers with smaller fiber gaps. When proteases pass through the small channels, the affinity interaction between the collagen fibers and the protease proteins may have a more pronounced effect on protease permeation.

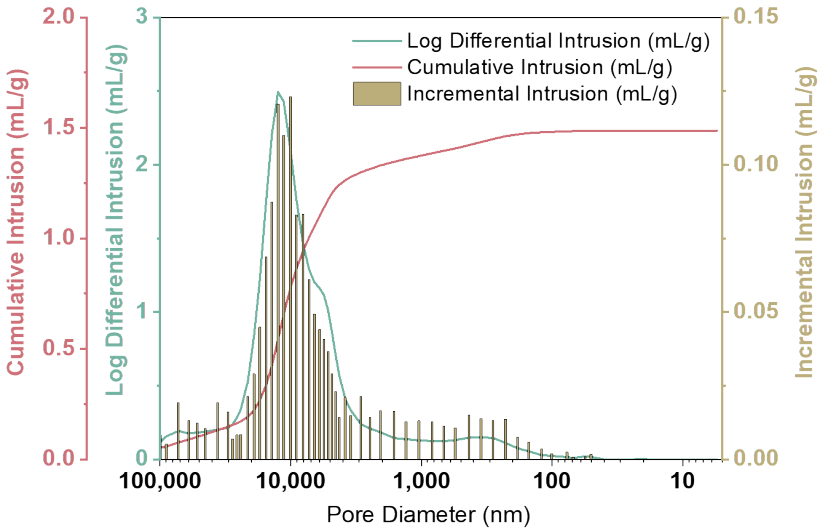

Figure 2. Pore diameter distribution of delimed pelt

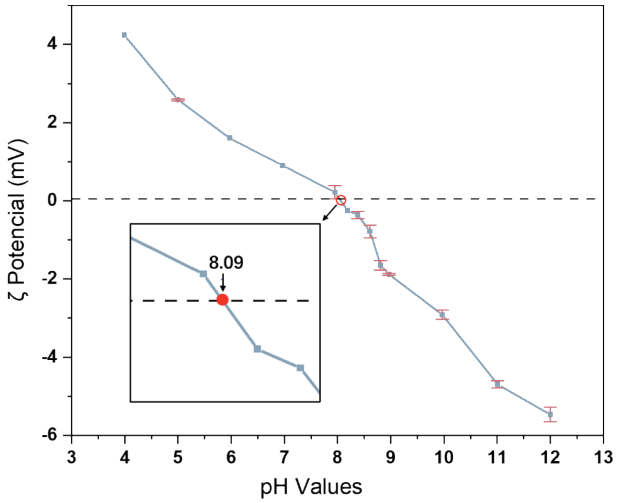

Figure 3. ζ potential of the delimed pelts at various pH values

Determination of the pI of the delimed pelts

In addition to the particle size of the protease molecules and the diameter of the permeation channels, the permeation of proteases into the pelts may also be influenced by the affinity between the protease molecules and the collagen fibers of the pelts. The charge state of the protease proteins and collagen fibers has a major influence on the affinity between them. The charge state of proteins mainly depends on their pI and the pH value of the solutions. Herein, the ζ potential of the delimed pelts was determined at various pH values and the results are shown in Figure 3.

The results in Figure 3 show that the ζ potential of the delimed pelts gradually decreased with the increasing of pH values, and the ζ potential is 0 mV when the pH of the solution is 8.09, indicating that the pI of the delimed pelts is 8.09.

Characterization of the FITC-labeled proteases

The permeation behavior of proteases in the pelts is difficult to observe directly. Fluorescein labeling is a widely used visualization technique for proteins,[22] the covalent combination of fluorescein to protease proteins imparts fluorescence properties to the proteases, allowing them to be localized and tracked. In this study, the labeling conditions and the basic properties of the labeled proteases were investigated.

The amount of fluorescein combined with a protease molecule has a large effect on the fluorescence intensity and properties of the labeled protease. Typically, the more fluorescein that binds to a protease molecule, the greater the variation in the M_w, pI and enzyme activity properties. Conversely, a low binding rate may result in a weak fluorescence signal, making it difficult to observe in subsequent permeation experiments. Therefore, as a substitute for unlabeled proteases, fluorescein-labeled proteases should have an appropriate fluorescein binding rate to allow their detection in permeation tracing experiments without dramatically affecting the properties of the protease molecules.

Labeled proteases with varying amounts of fluorescein were prepared by adjusting the amounts of both fluorescein and protease. The binding rate of fluorescein to protease is defined as the amount (mg) of combined FITC per milligram of protease protein. Based on the results of the permeation pre-experiment, when the fluorescein binding rates of FITC-P-SG-B, FITC-P-PTN110-T and FITC-P-NB115-T reached 0.009, 0.023 and 0.006, respectively, fluorescence signals were significantly observed in the labeled protease-treated pelts sections. However, if the binding rate was lower than the above values, the fluorescence signal has to be amplified by software, which might lead to the detection of autofluorescence of the collagen and affect the accuracy of the experimental results. Therefore, the fluorescein binding rates of the above-labeled proteases were used in the subsequent experiments.

UV-Vis spectroscopy characterizations of FITC-labeled proteases

The prepared fluorescein-labeled protease solutions were likely to contain uncombined fluorescein monomers and fluorescein-labeled small-molecule non-enzyme proteins, which could rapidly enter the pelts and interfere with the observation of the permeation of the actual protease molecules into the pelts, leading to erroneous conclusions. Therefore, the crude FITC-labeled protease solutions were dialyzed to remove the impurities. The proteases were examined before and after labeling using a UV-Vis spectrophotometer in the wavelength range of 200 - 800 nm.

As shown in Figure 4, The absorption peaks of the three labeled proteases are comparable. The characteristic absorption peak of FITC is known to be at 490 nm, whereas the peaks of the three labeled proteases migrate to 495 nm, indicating that FITC is combined with the proteases, which is consistent with the reported results.[23]

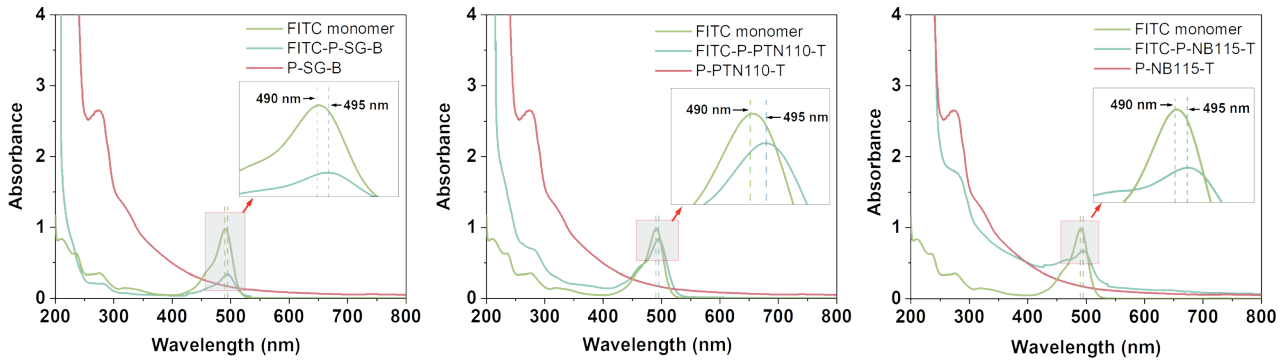

Figure 4. UV-Vis spectra of FITC monomer, proteases and FITC labeled proteases

Fluorescence spectroscopy characterizations of FITC labeled proteases

Since FITC can generate intense fluorescence under alkaline conditions and bating is typically performed in the pH range of 7.5 - 9.5, it is necessary to investigate the effect of pH on the fluorescence intensity of the labeled proteases. Figure 5 shows that the fluorescence spectra of the three labeled proteases are similar at different pH values, obtaining maximum fluorescence intensity at a wavelength of 520 nm. Although the maximum fluorescence intensity of the labeled proteases increased with the increasing of pH value, the difference is not significant.

pI and relative molecular weight of labeled proteases

The isoelectric point and molecular weight of the protease proteins are critical factors that influence their mass transfer in pelts.[24,25] The covalent cross-linking of fluorescein to proteases may alter their molecular properties, therefore, it is important to compare the pI and molecular weight values of the proteases before and after fluorescein labeling. The IEF-PAGE and SDS-PAGE results in Figure 6 show that the pI and molecular weight of the labeled and unlabeled proteases are similar, and all of the selected proteases showed high purity with only a single electrophoretic band. IEF-PAGE (Figure 6a) showed that the pI of FITC-P-SG-B, FITC-P-PTNP110-T and FITC-P-NB115-T were 7.1, 8.2 and 9.6, respectively. SDS-PAGE (Figure 6b) showed that the molecular weight of the selected proteases is all close to 25 kDa. Therefore, these labeled proteases can be used to substitute the original protease to investigate the permeation behavior of the protease in the pelts through a visualization way.

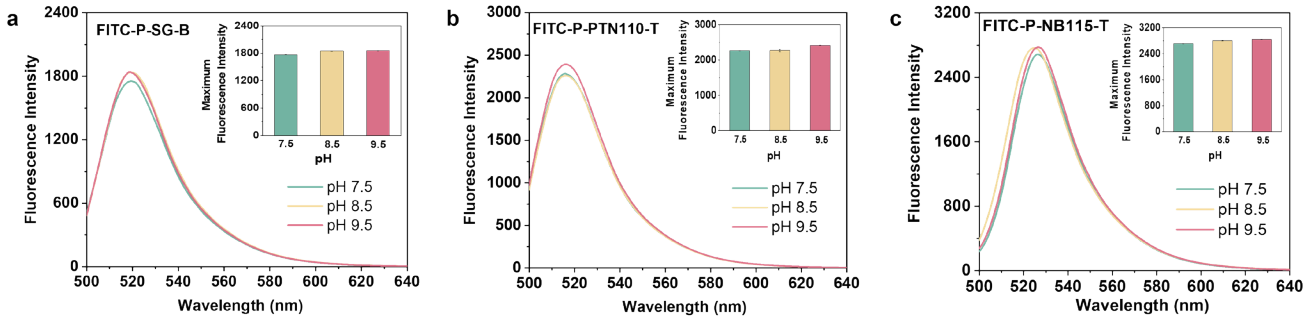

(a) FITC-P-SG-B; **(b)** FITC-P-PTN110-T; **(c)** FITC-P-NB115-T

Figure 5. Fluorescence spectra and maximum fluorescence intensity of fluorescein-labeled proteases

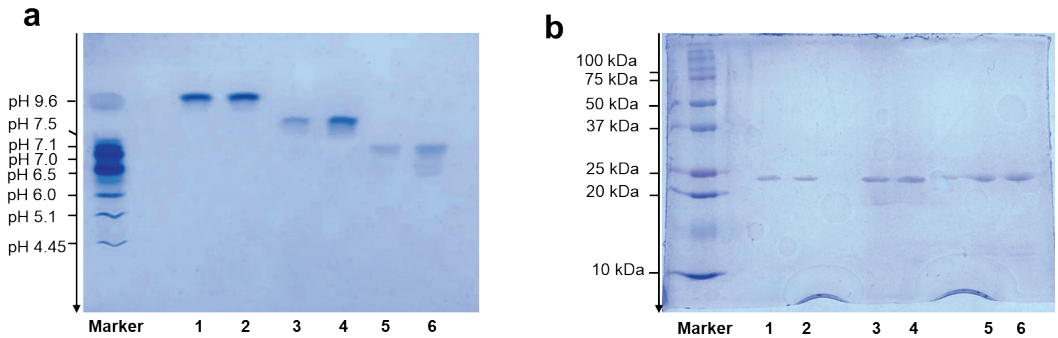

(**1:** P-NB115-T; **2:** FITC-P-NB115-T; **3:** P-PTN110-T; **4:** FITC-P-PTN110-T; **5:** P-SG-B; **6:** FITC-P-SG-B)

Figure 6. IEF-PAGE **(a)** and SDS-PAGE **(b)** electrophoretogram of the proteases before and after fluorescein labeling

Effect of proteins affinity on proteases permeation behavior in delimed pelts

The permeation behavior of FITC-labeled proteases at various pH values in the delimed pelts was observed using a confocal laser scanning microscope (CLSM), and the results are shown in Figures 7 - 9. The results show that proteases permeated into the pelts from both the grain and flesh surfaces, and the flesh side absorbed more proteases and exhibited higher fluorescence intensity than the grain side due to its greater specific surface area than the tightly woven grain side. As the channels for protease permeation are not continuous, the proteases are mainly distributed around the channel walls at the beginning of the bating process, resulting in a discontinuous fluorescence signal in the longitudinal section. The fluorescence intensity distribution in the longitudinal section (1h) shows an obvious "fluorescent circle" around the hair follicles, and strong fluorescence signals can be detected at a distance of about 0.5 mm from the top and bottom surfaces of the pelt, which are the hair follicles and the villi of the flesh, respectively, indicating that during the early stages of bating, the permeation of proteases into the pelts through large cavities is relatively easy, such as the pores.

As the permeation time increased, the proteases transferred from both the grain and flesh sides to the inner layer of the pelts. However, pH had a significant effect on the permeation rate and depth of the proteases. Figure 7 shows that FITC-P-SG-B (pI 7.1) permeated into the pelt at pH 9.5 after 5 hours of treatment, strong fluorescein signals were detected at 1.2 mm and 2.0 mm from the grain and flesh surfaces respectively, showing a significantly better protease permeation rate and depth than those at pH 7.5 and 8.5. Figure 8 shows that the permeation rate and depth of FITC-P-PTN110-T (pI 8.2) at pH 7.5 and 9.5 were superior to those at pH 8.5. Figure 9 shows that the permeation rate and depth of FITC-P-PTN115-T (pI 9.6) at pH 7.5 were better than those at pH 8.5 and 9.5.

The pI values of the delimed pelts and FITC-P-SG-B were 8.09 (Figure 3) and 7.1 (Figure 6a), respectively. At pH 7.5, the protease molecules are negatively charged while the collagen is positively charged. As a result, the strong electrostatic attraction between the protease and the pelt surface and channel walls inhibits protease permeation. When the pH is higher than the pI of the protease and collagen, both are negatively charged and the electrostatic attraction is weakened. Therefore, protease permeation is enhanced at pH 8.5 and 9.5, especially at pH 9.5, where both molecules are more negatively charged, resulting in electrostatic repulsion that prevents protease adsorption to collagen and promotes its permeation rate and depth.

The pI of FITC-P-PTN110-T was found to be 8.2. At pH 7.5, which is significantly lower than the pI of both protease and collagen, the positively charged protease and collagen repel each other. Correspondingly, at pH 9.5, which is significantly higher than the pI of both protease and collagen, the negatively charged protease and collagen also repel each other. Therefore, at pH 7.5 or 9.5, where there is strong electrostatic repulsion between the protease and collagen, the proteases could permeate more effectively than that at pH 8.5, which is slightly higher than the pI of the protease and collagen and results in fewer negative charges, leading to weaker electrostatic repulsion.

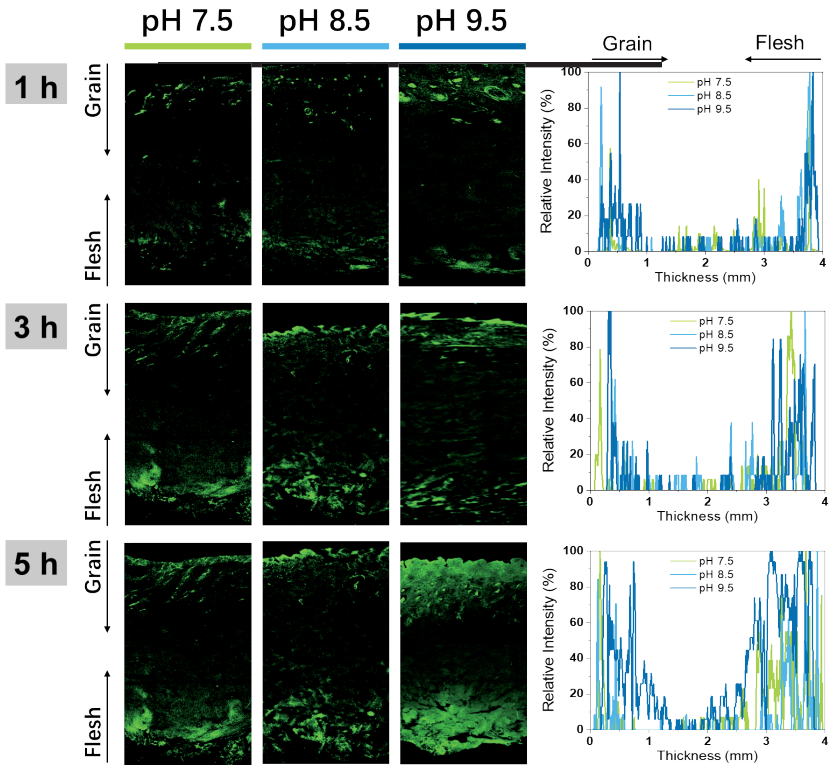

Figure 7. Permeation behavior of FITC-P-SG-B at various pH values

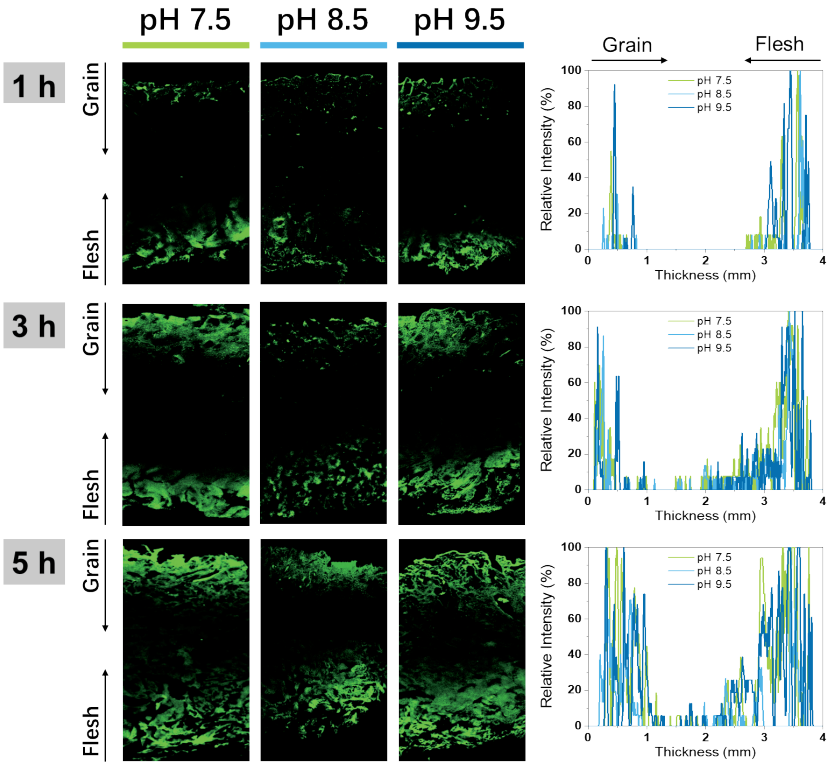

Figure 8. Permeation behavior of FITC-P-PTN110-T at various pH values

The pI of FITC-P-NB115-T was found to be 9.6. At pH 7.5, both protease and collagen carried a large number of positive charges, resulting in strong electrostatic repulsion. However, at pH 8.5 and 9.5, between the pI of the protease and collagen, the protease was positively charged while the collagen was negatively charged, resulting in electrostatic attraction. Therefore, the protease has better permeability at pH 7.5.

The three proteases have comparable molecular weights and particle sizes but different pI values. The apparent difference in their permeation behavior into pelts at different pH values is mainly due to the difference in affinity between protease and collagen due to their different charge states. As a result, the oppositely charged protease protein and the collagen fiber create a strong electrostatic attraction, which causes the protease to tend to remain on the surface

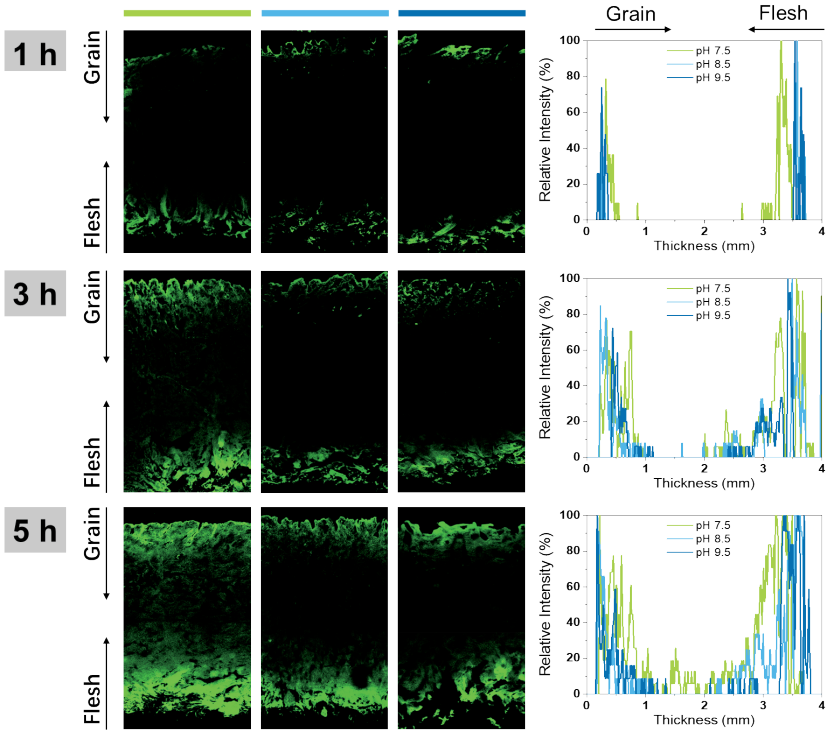

Figure 9. Permeation behavior of FITC-P-NB115-T at various pH values

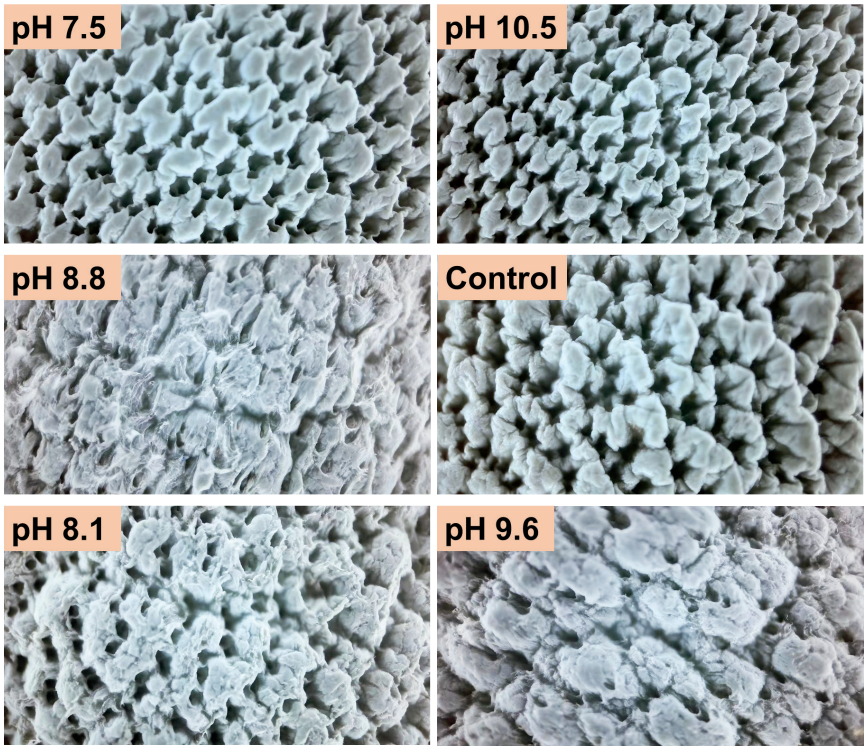

Figure 10. Grain surface of the crust leather after bated at different pH values

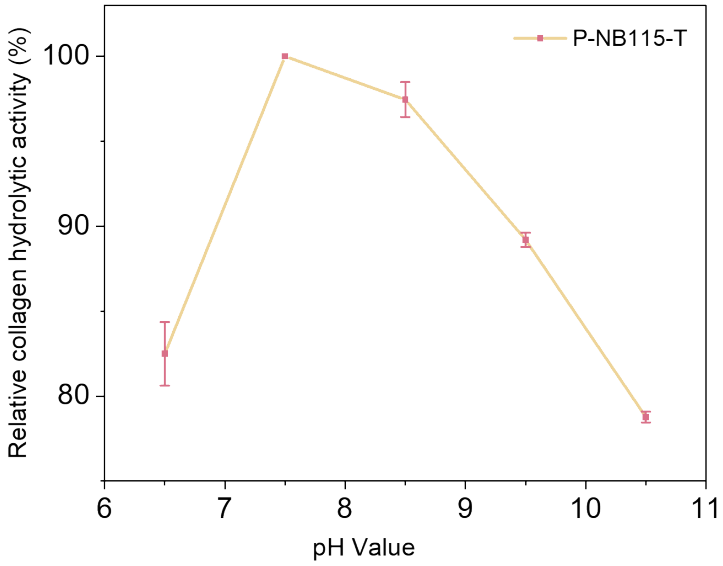

Figure 11. Relative collagen hydrolysis activity of P-NB115-T at different pH values

of the pelts, impeding its penetration. Conversely, if the proteins are similarly charged, the electrostatic repulsion reduces the attraction and facilitates the permeation of the proteases.

Effect of pH on the surface of the pelts during enzymatic bating

Bating experiments were carried out with unlabeled protease P-NB115-T to verify the results of the above permeation experiments using fluorescein-labeled proteases. The delimed pelts were bated for 6 hours at the same protease dosage and temperature under different pH conditions, followed by conventional pickling, Cr-tanning and post-tanning operations, the grain surface of the crust leather is shown in Figure 10.

The results in Figure 10 show that the grain surface of the crust leather after being bated at different pH values is significantly different. The grain surface of the pelt bated at pH 7.5 and 10.5 was intact with no damage, whereas the pelts bated at pH 8.1, 8.8 and 9.6 showed significant damage, particularly at pH 8.8. Figure 11 shows that the collagen hydrolysis activity of P-NB115-T decreases with the increasing of pH value in the range of 7.5 to 10.5. At the same

protease dosage, pH 7.5, with higher collagenolytic activity, resulted in weak hydrolysis of the grain surface collagen and left the grain intact; whereas pH 8.1, 8.8, and 9.6, with lower collagenolytic activity, resulted in apparent hydrolysis of the grain surface collagen and caused grain damage. Apparently, the hydrolysis of grain surface collagen was related to the permeation behavior of proteases in the pelts bating process.

At pH 7.5 or 10.5, P-NB115-T (pI 9.6) and delimed pelts (pI 8.09) were similarly charged (positively or negatively), and the electrostatic repulsion between the protease and the collagen promoted the permeation of the protease into the inner layer of the pelts and avoided the accumulation of the protease on the surface, resulting in weaker hydrolysis of the grain surface. At pH 8.8, the protease and delimed pelts are oppositely charged, the strong electrostatic attraction between the proteins facilitated the accumulation of protease on the grain surface and impeded its permeation into the inner layer, resulting in grain damage. At pH 8.1 and 9.6, corresponding to the pI of the collagen fiber and the protease, the electrostatic interaction is somewhere between the above two situations, and the protease permeation and the state of the grain surface are also somewhere between them. The results of the softness and organoleptic properties of the crust leather showed that the crust leather treated at pH 7.5 and 10.5 had better softness and uniformity than the samples treated at pH 8.8, which was attributed to the permeation of proteases into the inner layer and the uniformity of the bating process.

Charge regulation mechanism of protease permeation in delimed pelts

From the above results of the labeled and unlabeled protease permeation experiments, it can be concluded that the permeation of protease within the delimed pelt is significantly influenced by the electrostatic interactions between the collagen and protease proteins. And the interactions depend on the charge characteristics of the collagen and protease proteins, which are determined by both the pH of the solution and the pI of the proteins.

Various electrostatic interactions may occur between proteases and delimed pelts, such as (1) Strong electrostatic repulsion: as shown in Figure 12a, when the pH value of the solution is higher or lower than the pI values of both the protease and the delimed pelts, the protease and the delimed pelt are similarly charged, resulting in strong electrostatic repulsion. This repulsion is further enhanced by the mechanical force of the drum. Therefore, the protease molecules could easily permeate into the inner layers of the delimed pelt via the hair follicles and interfibrillar pathways, leaving only a small amount of protease on the surface layer, thereby avoiding the excessive degradation of grain collagen fibers. (2) Strong electrostatic attraction: as shown in Figure 12b, when the pH of the solution is between the pI of the protease and the delimed pelt, the protease and collagen carried opposite charges, resulting in strong electrostatic attraction; Therefore, the protease proteins tend to adhere and accumulate on the surface of the pelts, reducing the permeation rate and depth of the protease into the pelt, resulting in a damaged grain surface and inadequate opening-up of the inner layer. (3) Weak electrostatic interaction: when the pH value of the solution is close to the pI of either the protease or the collagen, as shown in Figure 12c, the electrostatic interaction between them is slight. Hence, the permeation performance of the protease into the pelt and the degree of action on the grain surface is intermediate between the two cases discussed above.

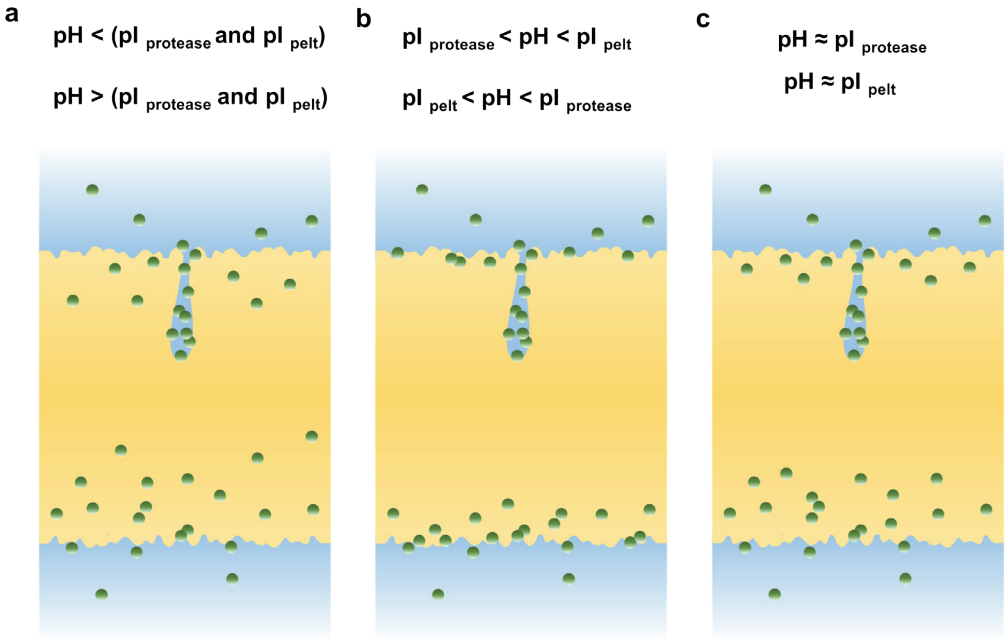

Figure 12. Schematic of the charge regulation of protease permeation into the pelts

Conclusion

The permeation behavior of typical proteases in the delimed pelts, the relative size of proteases and pelt pores, and the electrostatic interaction between protease molecules and collagen fibers were studied. The results indicated that, after dehairing, liming and deliming operations, which remove hair and interfibrillar substances, the enzyme can easily permeate into the pelts due to the formation of large cavities and interfibrillar gaps. The electrostatic interaction between protease and collagen proteins plays an important role in the permeation of protease into the delimed pelts. When the protease and collagen proteins are similarly charged, with electrostatic repulsion and weak affinity between the proteins, the proteases can easily permeate into the pelts; when the protease and collagen proteins are oppositely charged, with less electrostatic attraction, the permeation of protease into the pelts is difficult, which usually results in damage to the grain surface. Therefore, according to the electrostatic regulation mechanism of protease permeation in the pelt bating process, the permeation behavior of proteases can be regulated by selecting protease with appropriate pI and adjusting the pH value of the bating solution.

Acknowledgements

This work was financially supported by the Fundamental Research Funds for the Central Universities (2023SCU12104), the Fundamental Science on Nuclear Wastes and Environmental Safety Laboratory (22kfhk04) and the Opening Project of the Key Laboratory of Leather Chemistry and Engineering (Sichuan University), Ministry of Education (20826041D4237). We would like to particularly thank Qingshuang Song, Jinwei Zhang, Zhonghui Wang, Xiu He and all our other group mates at Sichuan University for their kind help.

References

1. Peng, B.Y. and Yu, Z.M.; Application of enzyme to leather manufacture. *China Leather* **28**, 19-22, 1999.
2. Xian, J., Bu, D.Y., Tian, Y.X., et al.; Properties and bating effects of trypsins from different sources. *Leather Science and Engineering* **30**, 40-46, 2020.
3. Zhang, X., Chattha, S.A., Song, J.Z., et al.; An integrated pickling-bating technology for reducing ammonia-nitrogen and chloride pollution in leather manufacturing. *Journal of Cleaner Production* **375**, 134070, 2022.
4. Zhang, X., Gao, M.C., Chattha, S.A., et al.; Application of acidic protease in the pickling to simplify the pelt bating process. *Journal of Leather Science and Engineering* **3**, 27, 2021.
5. Song, Y., Wu, S.Q., Yang, Q., et al.; Factors affecting mass transfer of protease in pelt during enzymatic bating process. *Journal of Leather Science and Engineering* **1**, 4, 2019.
6. Ma, J.Z., Hou, X.Y., Gao, D.D., et al.; Diffusion and reaction behavior of proteases in cattle hide matrix via FITC labeled proteases. *JALCA* **109**, 138-145, 2014.
7. Zhang, Y.H., Dan N.H., Jiang, Q.Q., et al.; Cattle hide histologic structure and penetration model of fluorescence labeling enzyme unhairing process. *China Leather* **47**, 23-26, 2018.
8. Liu, C., Chen, X.Y., Zeng, Y.H., et al.; Effect of the surface charge of the acid protease on leather bating performance. *Process Biochemistry* **121**, 330-338, 2022.
9. Gao, M.C., Song, J.Z., Zhang, X., et al.; Key mechanism of enzymatic dehairing technology for leather-making: permeation behaviors of protease into animal hide and the mechanism of charge regulation. *Collagen and Leather* **5**, 9, 2023.
10. Wang, Y.N. and Hu, L.Y.; Essential role of isoelectric point of skin/leather in leather processing. *Journal of Leather Science and Engineering* **4**, 25, 2022.
11. Meldan, V.M.; Method for quantifying intrafollicular drug delivery: a critical appraisal . Expert Opinion on Drug Delivery **7**, 1095-1108, 2010.
12. Giesche, H.; Mercury porosimetry: a general (practical) overview. *Particle and Particle Systems Characterization* **23**, 9-19, 2006.
13. Tadros, Th.F. Solid/liquid dispersions. *Academic Press*, London, 1987.
14. Sonnefeld, J.; On the influence of background electrolyte concentration on the position of the pI and the point of zero charge. *Colloids and Surfaces A: Physicochemical and Engineering Aspects* **190**, 179-183, 2001.
15. Tian, Q., Zhang, C.N., Wang, X.H., et al.; Glycyrrhetinic acid-modified chitosan/poly (ethylene glycol) nanoparticles for liver-targeted delivery. *Biomaterials* **31**, 4748-4756, 2010.
16. Yang, Q., Zeng, Y.H., Zhang, W.H., et al.; Investigation of mass transfer characteristics of protease in bating process using fluorescence tracing. *China Leather* **14**, 16-19, 2014.
17. Redmile-Gordon, M.A., Armenise, E., White, R.P., et al.; A comparison of two colorimetric assays, based upon Lowry and Bradford techniques, to estimate total protein in soil extracts. *Soil Biology and Biochemistry* **67**, 166-173, 2013.
18. Fleming, P.J. and Fleming K.G.; Hullrad: fast calculations of folded and disordered protein and nucleic acid hydrodynamic properties. *Biophysical journal* **114**, 856-869, 2018.
19. Fathima, N.N., Kumar, M.P., Rao, J.R., et al.; A DSC investigation on the changes in pore structure of skin during leather processing. *Thermochimica Acta* ***501,*** 98-102, 2010.
20. Sanjeevi, R., Ramanathan, N. and Viswanathan, B.; Pore size distribution in collagen fiber using water vapor adsorption studies. *Journal of Colloid and Interface Science* **57**, 207-211, 1976.
21. He, X., Wang, Y.N., Zhou, J.F., et al.; Suitability of pore measurement methods for characterizing the hierarchical pore structure of leather. *JALCA* **114**, 41-47, 2019.
22. Liu, J. and Cui, Z.Q.; Fluorescent labeling of proteins of interest in live cells: beyond fluorescent proteins. *Bioconjugate Chemistry* **31**, 1587-1595, 2020.
23. Liu, A.P.; Fluorescence principles and practice for cell biology. 1st ed. Press of University of Science and Technology of China, Hefei, 2007.
24. Song, Y., Ma, Y., Zeng, Y.H., et al.; Effect of molecular weight of protease on its mass transfer in leather processing. *Leather Science and Engineering* **28**, 5-10, 2018.
25. Elmowafy, M.; Skin penetration/permeation success determinants of nanocarriers: Pursuit of a perfect formulation. *Colloids and Surfaces B: Biointerfaces* **203**, 111748, 2021.

Use of Long-Chain Synthetic Phenolic Antioxidants to Produce Chromium-Tanned Leather without Risk of Hexavalent Chromium Formation

by

Irene Compte,[1]* Quim Torras,[1] Francina Izquierdo,[2] Rosa Cuadros[1] and Anna Bacardit[1]

[1]*A3 Leather Innovation Center-UdL. Avda. Pla de la Massa 8, 08700* Igualada, Barcelona, Spain.

[2]*Asociación Química Española de la Industria del Cuero (AQEIC).* Avda. Pla de la Massa 8, 08700 Igualada, Barcelona, Spain.

Abstract

Chromium tanned leather is the widest form of leather tanning across the world, but it might involve a risk of hexavalent chromium formation, which is restricted in leather products above 3 mg/kg. Among other conditions, certain processes might lead to the oxidation of natural fats or fatliquoring agents with unsaturated carbon-carbon bonds, thus generating free radical molecules that can contribute to the Cr(III) oxidation to Cr(VI). The auto-oxidation of unsaturated lipids is promoted by exposure to high temperatures and light, specifically UV radiation. Among other relevant manufacturing practices, the addition of synthetic phenolic antioxidants (SPAs) during the synthesis of fatliquoring agents or during leather manufacturing can be a relevant tool for preventing lipid auto-oxidation.

The efficiency of the long-chain synthetic antioxidant 1135 (AO1135, CAS RN® 125643-61-0) has been assessed for Cr(VI) prevention. The performance of AO1135 has been tested in two different skin types (sheepskin, woolly sheepskin), with two different fatliquoring agents (unprotected and protected against oxidation). The protected fatliquoring agent was formulated with AO1135. Also, two commercial products that contain the AO1135 in its formulation have been applied to leathers. Upon completion of the post-tanning process, the leathers have undergone two different thermal ageing processes.

AO1135 has been verified an effective SPA for Cr(VI) prevention and its application during the post-tanning process does not alter the visual aspect of the leathers. Otherwise, if the post-tanning recipe does not contain well-sourced raw materials or Cr(VI) prevention tools, unsaturated fatliquoring agents or natural fats present in the skins can be a cause for Cr(VI) formation.

Introduction

Leather goods have been used for centuries by human beings, and nowadays they still constitute a valuable asset, due to their unique physical properties and their longevity. The process of obtaining leather in order to prevent collagen degradation is the tanning of animal hides, a by-product of meat consumption. In modern life, leather is used to manufacture footwear and clothing articles, handbags and other fine leather goods, automobile seats and upholstery.[1]

Different types of leather tanning have been developed and improved over time. Still, chromium tanning is the most widely used method since its adoption around mid-19th century. Nowadays, it represents 85% of genuine leather production, mainly due to the properties that the trivalent chromium confers to the finished leather: durability, hydrothermal resistance, fastness of the dyestuffs, pleasant feel and look, fullness, etc., but also due to the lower environmental impact of its production along its life cycle.[2,3]

The use of chromium salts during the tanning process might involve an indirect risk of hexavalent chromium formation. Hexavalent chromium could lead to contact dermatitis for the final consumer of leather articles, hence the European Commission issued the Regulation No 301 in 2014 that limits the amount of Cr(VI) present in leather to a maximum of 3 mg/kg. After being active for over four years, studies carried out in Denmark show that the cases of contact dermatitis related to hexavalent chromium have substantially decreased.[4] The 3 mg/kg value is the limit of quantification of this analyte when determined in a leather matrix, which typically contains about four thousand times more free trivalent chromium than hexavalent chromium.

Commission Regulation No 301/2014 brought the need for the implementation of a variety of widespread good manufacturing practices in tanneries that use chromium in their tanning or retanning processes, which allow for Cr(VI) amounts to be below the restricted limit.

1.1 Origins of Cr(VI) in leather - hexavalent chromium containing substances

A source for hexavalent chromium in leather could be the use of Cr(VI)-containing products, such as the use of lead chromate pigments. However, nowadays this practice is obsolete due to the clear and direct risk of Cr(VI) detection in leather.

*Corresponding author email: irene.compte@udl.cat

Manuscript received March 21, 2023, accepted for publication May 10, 2023.

Cr(VI) can also originate from the oxidation of free, non-bonded, trivalent chromium, most likely after the exposure to peroxides or peroxide radicals.[5] Other practices that might involve a risk for Cr(VI) formation and further detection in leather are the use of harsh whitening oxidant products, such as bleach, hydrogen peroxide, potassium permanganate or sodium hypochlorite. Those products provide an oxidizing environment which might lead the free non-bonded Cr(III) to oxidize into Cr(VI).[6]

Although hexavalent chromium is not purposely used in leather production at present time, the conversion of unbound Cr(III) in chromium-tanned leather could generate traces of Cr(VI). This is a reaction influenced by different factors related to production and even storage conditions of finished articles.[7] Differently from other ageing processes, the amount of Cr(VI) formed under certain conditions can be reversed, and the present Cr(VI) could usually be reduced simply by increasing humidity.

1.2 Influence of the pH value

The pH value of the leather is another relevant parameter that can interfere with the Cr(III)-Cr(VI) redox equilibrium. pH has to be controlled and adjusted in certain tannery processes. Otherwise, if pH values are too high, the risk of Cr(VI) detection increases as the equilibrium might be displaced towards Cr(VI) formation.[6,8,9]

For a finished chromium-tanned leather, the most common pH range is usually within the range 3.5 – 4.5. In the market there are also restrictions regarding to pH value for leather from international organizations such as the AFIRM Group, which stablishes the range between 3.2 – 4.5.[10] The common pH range and the values listed by AFIRM are a compromise between the prevention of Cr(VI) formation and the optimization of dying fastness, which are aligned; and also acidic dermatitis in some customers, which increases as a consequence of lower pH values in leather; hence the need for establishing the lower limit for pH value.[11-13]

The appropriate regulation of pH is not the only tool for a tanner to prevent Cr(VI) formation. Tanners might implement other measures that minimize the risk of Cr(VI) formation.

1.3 Oxidation of fatliquoring agents

The fatliquoring step is crucial in the wet-end process of leather production. It will give the leather the touch and flexibility required for the final article. Fat is, next to the tanning agent, the most important component of a finished leather besides the fiber structure. With the exception of sole leather, any kind of softer leather contains remarkable amounts [5 - 20 %] of fat. Fat prevents the sticking, gluing or adhesion of fibers to themselves, and it is said that this is the basis of the leather flexibility.[14]

A general overview of the fatliquoring process can be summarized as follows: First, during the fatliquoring step, the mixture of fatliquoring agents is emulsified in warm water with the support of emulsifying additives. Then, the mixture is incorporated in the rotating drum containing leather and water, which has been preheated to facilitate the penetration of the fatliquoring into the leather. After the drum has rotated for a sufficient amount of time, the effect of mechanical action, together with the temperature, will have ensured proper fatliquoring penetration. Finally, the emulsion of the mixture of fatliquoring agents is broken by means of small acid additions which, in turn, allow for the fixation of fats and oils into the leather. A homogeneous distribution might be difficult to achieve both among the surface of the leather and through its cross-section, thus, making sure that the fatliquoring mixture penetrates well and is evenly distributed is of paramount importance to ensure the desired flexibility in the final article.

Among the variety of wet-end processes, and as early as 1997 - 2000, different research conducted independently concluded that the fatliquoring process can have the largest incidence in Cr(VI) formation due to the auto-oxidation of unsaturated lipids.[15-18]

Some raw materials used for fatliquoring agents' manufacture, or also unsaturated natural fats remaining in a leather, can undergo the process of lipid auto-oxidation in the presence of free radicals, especially unsaturated fatty acids. The bis-allylic hydrogen between the double bonds is readily abstracted in presence of a radical, resulting in the formation of conjugated alkenes due to the rearrangement of the double bonds. Atmospheric oxygen can rapidly be added to the carbon-centered radical to form a peroxy radical. The peroxy radical will capture a new bis-allylic proton, forming a hydroperoxide and a new carbon-centered radical on another fatty acid. This process continues with exponential formation of hydroperoxides and conjugated dienes.[19]

Lipid auto-oxidation can be a risky chain reaction process as it might lead to the formation of hexavalent chromium due to the fact that it provides hydrogen peroxides, that can oxidize the unbonded trivalent chromium.[20,21]

Given the relationship between the double bonds of an unsaturated fatty acid and auto-oxidation, the iodine value test was used in the past as a quality control tool for the raw and unprocessed oils used to make fatliquors. However, the iodine value varies along the different processing steps in which a raw oil is converted into a commercial fatliquoring agent. Nowadays, the iodine value of a properly formulated commercial fatliquor has limited value in terms of predicting Cr(VI) formation and should not be used to compare fatliquoring agents.[22]

1.4 Natural extracts as a way for reducing formed Cr(VI)

Vegetable tanning uses natural vegetable extracts for tanning or retanning leather, which are conformed by high molecular weight

compounds that bond with the collagen fibers, helping in stabilizing them and preventing skin degradation.

The polyphenol molecules that conform the vegetable extracts can also act as a neutralizer of free radicals, and this is the reason why vegetable extracts can be incorporated in some chromium-tanning formulations. Polyphenols can reduce the hydrogen peroxides formed by lipid auto-oxidation (Section 1.3), thus reducing the probabilities of molecules of free Cr(III) being oxidized.

It is worth noting that the use of vegetable extracts entails a certain risk for a change of color, due to the slight browning that this natural material undergoes, especially if it is exposed to light.[12,23,24]

1.5 Synthetic phenolic antioxidants as a tool for preventing lipid auto-oxidation

The auto-oxidation of unsaturated lipids is promoted by its exposure to high temperatures and light, specifically under UV radiation. The presence of free radicals can eventually oxidize free trivalent chromium to hexavalent chromium, so lipidic auto-oxidation involves a risk of Cr(VI) formation in leather, especially if it is exposed to the aforementioned extreme conditions.[16,19,25]

However, there are ways of protecting a fatliquoring agent during its manufacture in order to prevent its oxidation. First of all, the chemical nature of the fatliquoring agent has an important role on whether it can be easily oxidized. Thus, compounds with double-bonded carbon chains are the ones that entail a higher risk. Some synthetic fatliquoring agents that are based on sulphited or sulphated and partially chlorinated linear carbon chains might involve a lesser risk of oxidation. Also, carefully selecting a quality source of raw materials free from risky impurities and following adequate processing methods of the materials to achieve stabilization can certainly play a role in reducing the probability of oxidation.

In some cases, chemical companies consider the addition of synthetic phenolic antioxidants (SPAs) during the synthesis of fatliquoring agents, besides other practices like the aforementioned careful selection of raw materials and implementing certain stabilization processes. Another approach is to add a commercial product that contains SPAs in its formulation directly in the leather fatliquoring process. These additions can be beneficial to counterbalance and prevent lipid auto-oxidation.

SPAs have been used in several industrial sectors to retard oxidative reactions and lengthen product shelf life. Most of the commercially available SPAs are grouped under the name of primary antioxidants, as they share a main structure conformed by a hindered phenol, which interrupts oxidation by donating the -OH hydrogen. On the other hand, secondary antioxidants usually decompose hydroperoxides into thermally stable compounds. The efficiency of

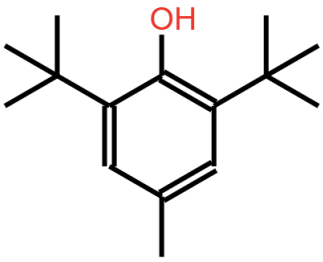

Figure 1. Butylated hydroxytoluene (BHT)

different structures of primary antioxidants has been widely studied in different industries.[25-29]

SPAs have been proposed in the past for the leather sector as a mixture of phenolic and amine antioxidants.[12,25] However, it has been found that the shortest synthetic phenolic antioxidant available, the butylated hydroxytoluene (Figure 1, BHT) tends to create a yellowing effect on the substrate it is applied to, due to its conversion to a quinonemethide (CAS RN® 10396-80-2, 2,4-di-tert-butyl-6-ethylidene-2,5-cyclohexadien-1-one) and then to a stilbenequinone (3,3',5,5'-Tetra-tert-butyl-4,4'-stilbenequinone, CAS RN® 809-73-4) [30], [31].

The antioxidant 1135 (AO1135, octadecyl 3-(3,5-di-tert-butyl-4-hydroxyphenyl)propionate, CAS RN® 125643-61-0) is a synthetic phenolic antioxidant that shows good potential for lipid auto-oxidation prevention in leather and does not have a strong yellowing effect, probably avoided by the longer octadecylpropionate chain attached to the hydroxyphenyl. It has been successfully implemented in different industrial sectors.[26,27,32]

Assessing the ability of SPAs to effectively reduce lipid auto-oxidation rates might be done via several pathways. As mentioned, fatty acid oxidation might involve a light yellowing effect on finished leather, particularly after sunlight exposure. Other sources for detecting oxidized fatty acids could be the rancid smell they release. But the most representative one is Cr(VI) absence or formation due to lipid oxidation in chromium-tanned leathers. This specific indicator can be quantified via Cr(VI) determination in leather, which allows for an accurate conclusion regarding

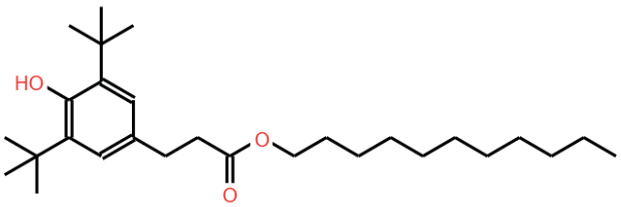

Figure 2. Structure of Antioxidant 1135 (AO1135), octadecyl 3-(3,5-di-tert-butyl-4-hydroxyphenyl) propionate, CAS RN® 125643-61-0

fatliquoring stability and thus, Cr(VI) protection efficiency, especially if the leather sample has been exposed to some form of ageing prior to the analysis.

Aside from hexavalent chromium determination,[33] there is no other current tool that can indicate whether leather has been treated with SPAs. However, both GC-MS and HPLC-DAD have been used to determine SPAs in different matrixes, such as polyurethane foams, polyamide, wastewater and sludge, among others.[26,34-36]

Finally, the fact that fatliquoring agents, lipidic molecules as they are, need to be properly applied and fixed in order to ensure proper distribution, leads to the idea that synthetic phenolic antioxidants may also require adequate distribution and uniformity when used in a formulation.[14]

1.6 Forcing lipid auto-oxidation in leather

Lipid auto-oxidation can be a natural occurring phenomenon. However, some conditions can either trigger or enhance the radical reaction. Sun light, and in particular, its UV wavelengths, has been proven to be a triggering factor for lipid auto-oxidation in leather, along with heat.[37] Leather that was produced with no apparent initial hexavalent chromium could result in Cr(VI) detection when exposed to sun light or heat.

All these different exposure factors lead to a need for a unified treatment of the sample prior to Cr(VI) determination, in order to assess the tendency of a leather to Cr(VI) formation.

The most widespread pre-treatment for leather samples at the moment is to expose them to continuous heat for a specific period of time. In this line, protocols for leather exposure to these type of stress conditions have been developed. The consolidated ISO standard 10195:2018 describes an ageing process consisting of placing leather samples in an oven at 80ºC for 24 hours prior to the Cr(VI) analysis. No other standardized tests have been developed at the moment.

Tanned leather can be stored in a variety of conditions along the supply chain, and such conditions might not be optimal for preventing lipid auto-oxidation. In this work, a new ageing pre-treatment was evaluated as a tool to identify leathers with long-term risk of Cr(VI) formation.

1.7 Determining the efficiency of Antioxidant 1135 to prevent Cr(VI) formation

The main aim of this work is to assess the performance of a long chain lipidic SPA, specifically the AO1135, when applied to leather matrixes as an additive to reduce potential lipidic auto-oxidation that could eventually lead to Cr(VI) formation after being exposed to extreme conditions such as the ones described in Section 1.6. To evaluate AO1135 performance, the approach is to assess its ability to prevent Cr(VI) formation in leather after samples are exposed to conditions that might trigger lipid auto-oxidation (Section 1.6)

1.8 Commercial products with synthetic phenolic antioxidant

There are two main groups of commercial products in the market that contain AO1135. The difference lays in the composition. The simplest way of formulating such products is to dissolve the AO1135 in a solvent, relying on the fatliquoring agent's formulation or other auxiliaries as driver agents for its dispersion and penetration. By contrast, some products contain the AO1135 mixed together with dispersants and emulsifiers so that the emulsion with water and the fatliquoring agent is smooth and good penetration and levelling is ensured along the cross-section and the surface of the leather.

Experimental

Design of the experiment

For assessing the performance of AO1135 in different leather matrixes, two different types of skin origins have been studied. Semi-manufactured wet blue leathers were acquired in an already tanned state, so the difference between the samples laid only in the fatliquoring formulation.

Two different types of fatliquoring agents were assessed. One of them was a fatliquoring agent formulated with a base of sulphited fish oil and with the addition of small amounts of SPA, as well as manufactured according to best manufacturing practices described in Section 1.2. A non-protected fatliquoring agent was used on the second set of leathers.

In order to evaluate the efficiency of AO1135, two commercial antioxidant products (named respectively "Product 01" and "Product 02") that contain this compound were applied to the leathers according to the instructions of the manufacturer. A set of leathers, both with unprotected and protected fatliquors, were treated as a process blank, without the addition of extra amounts of AO1135. Product 01 and Product 02 were selected amongst the increasing variety of commercial products that contain SPAs. Product 01 is a blend of AO1135 with emulsifiers and dispersants, which gives it auto-emulsifyable characteristics that allow for good dispersion along the cross-section of the leather and its surface. Product 02 is a blend of AO1135 with a solvent. In that case, proper penetration and dispersion are ensured by means of adding extra compounds to the mixture or by relying on the fatliquoring agent's auxiliaries. Both products are designed to be applied during the fatliquoring process; emulsified together with the main fatliquoring mixture. The amount applied for each commercial product, according to recommendations of its suppliers, was equal to 0.1% of AO1135 in relationship to the shaved weight of the skin.

Table I

Structure of the study

Type of leather	Type of fatliquoring agent used	Type of extra treatment	Reference
SHEEP-SKIN	Non-Protected fatliquoring agent (U)	Without extra AO1135	01-UB
		With extra AO1135 Product 01	02-U1
		With extra AO1135 Product 02	03-U2
	Protected fatliquoring agent (P)	Without extra AO1135	04-PB
		With extra AO1135 Product 01	05-P1
		With extra AO1135 Product 02	06-P2
WOOLLY SHEEP-SKIN	Non-Protected fatliquoring agent (U)	Without extra AO1135	07-UB
		With extra AO1135 Product 01	08-U1
		With extra AO1135 Product 02	09-U2
	Protected fatliquoring agent (P)	Without extra AO1135	10-PB
		With extra AO1135 Product 01	11-P1
		With extra AO1135 Product 02	12-P2

Table I shows a scheme of all the leather outcomes that were studied.

It has been demonstrated that rechroming a leather might lead to higher Cr(VI) formation when risky fatliquors are used.[38] The unbounded Cr(III) offer is increased in the leather, thus leading to higher chances of oxidation. In this work, all the leathers were rechromed.

2.2 Samples

The risk for Cr(VI) formation is increased if a thorough degreasing process has not been carried out in initial stages of the tanning, as natural fat might lead to lipid auto-oxidation. Good manufacturing practices during tanning are advisable, although in many cases, the early stages of tanning processes (the so-called beamhouse) and the wet end processes take place in different locations. In consequence, they cannot be exhaustively controlled by the intermediate buyer. Taking this information into account, for this study, two types of sheep-skin have been selected and studied.

WS stands for Wooly Sheep-Skin, and these skins belong to an African race of goat. SS stands for Sheep-Skin, also a type of sheep, which usually presents natural fat irregularly distributed. Sheep and wooly sheep-skins, commonly used for shoe or leather goods manufacturing, show higher risk of Cr(VI) formation, probably due to high initial fat percentage and more interfibrillar space.

The wet-end process was applied to the samples, following a simple scheme such as the one described herein.[38] The difference between the samples lies in the fatliquoring formulation, as described in Section 2.1. The process did not involve the application of surface finish coating(s).

It has been shown that the sampled zone of the leather might have an impact on Cr(VI) content.[39] As both types of leather might have higher amounts of natural fats, the Cr(VI) determinations in order to assess the efficiency of each treatment was performed in three zones of the leather; the neck, the flank and the butt, for each of the leathers and processes studied in Section 2.1.

2.3 Chemicals and apparatus

All the chemicals used in the analysis of Cr(VI) were of analytical reagent grade.

Fatliquoring and the rest of wet-end processes have been carried out in common stainless steel pilot plant drums (Simplex 2 from InoxVic, Spain).

The thermal ageing was performed in a DigiHeat TFT drying oven, from Selecta.

2.4 Methods

2.4.1 Method of Cr(VI) determination

The amount of Cr(VI) in leather was determined according to the ISO 17075-2:2017, which has a limit of quantification of 3 mg/kg of Cr(VI). In this case, the analyses were performed in a laboratory accredited by ISO 17025:2015.

2.4.2 Thermal methods to expose the leathers to, prior to Cr(VI) testing

The tanned leathers were tested for Cr(VI) content directly after the fabrication and also after being exposed to certain ageing conditions. The stress of said conditions might trigger Cr(VI)

Table II

Conditions of sample exposure prior to Cr(VI) testing

Thermal ageing	24 h at 80 °C, <10% of relative humidity (ISO 10195:2018)
Lower-temperature / longer-term ageing	40 days at 40 °C, <10% of relative humidity

formation if the fatliquoring agents were not adequately protected against the effects of the auto-oxidation, or also if the additional SPAs added in the formulation would not work properly. Thus, the amount of Cr(VI) is a good indicator of the performance of both the fatliquoring agent and the SPA added. If the leather has a content of Cr(VI) above 3.0 mg/kg, the performance of the fatliquoring agent or the AO1135 would not be considered suitable, as this amount of Cr(VI) is above the limit specified in EU Regulation No 301/2014.

To date, the process of thermal ageing described in ISO 10195:2018 is the only official method to test for the propensity of a leather to develop Cr(VI). In order to evaluate alternative methods of ageing and obtain a deeper insight about how Cr(VI) content could evolve, a lower-temperature, longer-term thermal ageing was also assessed. It consisted of keeping the leather samples for 40 days at 40°C, a condition that could occur if finished leathers are stored in warehouses without temperature control, especially in certain latitudes and hot climates.

Table III

Cr(VI) content according to ISO 17075-2:2017 of Sheep-Skins produced.

Reference	Part of the leather	Cr(VI) content in mg/kg after different exposure to external conditions		
		Initial testing without ageing	Thermal ageing ISO 10195	Lower-temperature / longer-term ageing
01-UB	Shoulder	19.8	43.2	29.4
	Flank	18.6	38.1	22.2
	Butt	17.5	30.8	19.2
02-U1	Shoulder	< 3.0	< 3.0	< 3.0
	Flank	< 3.0	< 3.0	< 3.0
	Butt	< 3.0	< 3.0	< 3.0
03-U2	Shoulder	< 3.0	< 3.0	< 3.0
	Flank	< 3.0	< 3.0	< 3.0
	Butt	< 3.0	< 3.0	< 3.0
04-PB	Shoulder	< 3.0	< 3.0	< 3.0
	Flank	< 3.0	< 3.0	< 3.0
	Butt	< 3.0	< 3.0	< 3.0
05-P1	Shoulder	< 3.0	< 3.0	< 3.0
	Flank	< 3.0	< 3.0	< 3.0
	Butt	< 3.0	< 3.0	< 3.0
06-P2	Shoulder	< 3.0	< 3.0	< 3.0
	Flank	< 3.0	< 3.0	< 3.0
	Butt	< 3.0	< 3.0	< 3.0

Table IV

Cr(VI) content according to ISO 17075-2:2017 of Wooly sheep leathers produced.

Reference	Part of the leather	Cr(VI) content in mg/kg after different exposure to external conditions		
		Initial testing without ageing	Thermal ageing ISO 10195	Lower-temperature / longer-term ageing
07-UB	Shoulder	20.5	30.8	23.9
	Flank	19.8	30.7	25.1
	Butt	20.7	29.6	22.1
08-U1	Shoulder	< 3.0	< 3.0	< 3.0
	Flank	< 3.0	< 3.0	< 3.0
	Butt	< 3.0	< 3.0	< 3.0
09-U2	Shoulder	< 3.0	< 3.0	< 3.0
	Flank	< 3.0	< 3.0	< 3.0
	Butt	< 3.0	< 3.0	< 3.0
10-PB	Shoulder	< 3.0	< 3.0	< 3.0
	Flank	< 3.0	< 3.0	< 3.0
	Butt	< 3.0	< 3.0	< 3.0
11-P1	Shoulder	< 3.0	< 3.0	< 3.0
	Flank	< 3.0	< 3.0	< 3.0
	Butt	< 3.0	< 3.0	< 3.0
12-P2	Shoulder	< 3.0	< 3.0	< 3.0
	Flank	< 3.0	< 3.0	< 3.0
	Butt	< 3.0	< 3.0	< 3.0

2.4.3 Determination of natural fat content in leather

The initial natural fat content in wet-blue leather was determined in the wet-blue samples according to ISO 4048:2018. It was verified that the fat content was below 3% for both the wooly sheep and the sheep-skins.

Results

3.1 Cr(VI) content in the tanned leathers

Once all the leathers were manufactured, Cr(VI) content was determined without any previous treatment, and then it was also determined after the exposure of samples to the described conditions.

The specific post-tanning recipes for the 12 leathers can be obtained by contacting the author.

3.2 Dispersion of the Cr(VI) content depending on the different parts of the leather

Being a natural material, leather can show some irregularities or dispersion among fiber distribution, for example, the flank part tends to have more interfibrillar space due to the movements the animal performs during its life. If a fatliquoring agent with auto-oxidation tendencies is unevenly distributed, it could lead to an irregular Cr(VI) content across leather surface.

Three zones were tested for Cr(VI) for each type of leather and process. This lead to the possibility of assessing how disperse the Cr(VI) content can be, even within the same leather, in both sheep-skin and wooly sheep-skins.

Most of the leather treatments led to the non-detection of Cr(VI). Results of the Relative Standard Deviation (%RSD) for the leathers

Table V
Average and %RSD of leathers with Cr(VI) detection

Reference		Variation of the Cr(VI) content in the same leather		
		Initial testing without ageing	Thermal ageing	Lower-temperature / longer-term ageing
01-UB	Average (mg/kg)	18.6	37.3	23.6
	%RSD	6.2	17	22
07-UB	Average (mg/kg)	20.3	30.4	23.7
	%RSD	2.3	2.2	6.4

that were treated with non-protected fatliquoring agents are shown in Table 5.

Discussion

Influence of the fatliquoring agent on the Cr(VI) content, for Sheep-Skin and Wooly sheep leathers

Tables III and Table IV show the Cr(VI) results for all the conditions described in Section 2.1. Both Sheep-Skin and Wooly Sheep-Skin obtain similar results regarding Cr(VI) content when an unprotected fatliquoring agent is applied during the fatliquoring process. In these two cases (References 01-UB and 07-UB), values around 20 mg/kg or higher are obtained. It can be seen that all the leathers treated with protected fatliquoring agents or both commercial synthetic phenolic antioxidants show very good performance against any of the prior ageing treatments applied to them. These results highlight the importance of the quality of raw materials used in the production process.

4.2 Use of synthetic phenolic auxiliaries (AO1135) and its consequences on the Cr(VI) content

When the fatliquoring agent used is not protected, the addition of small amounts of AO1135 has demonstrated to be effective for preventing Cr(VI) formation. This conclusion is extracted from the fact that all the produced leathers with non-protected fatliquoring agents that contained extra additions of AO1135 have successfully prevented Cr(VI) formation, even after being exposed to a conventional thermal ageing process or a soft ageing process.

Results below 3.0 mg/kg of Cr(VI) were obtained with leathers treated with Product 01 and Product 02, even if the leathers were treated with unprotected fatliquoring agents and even after being exposed to the conventional thermal ageing (References 02-U1, 03-U2, 08-U1 and 09-U2), therefore concluding that the two ways of formulating the chemical products are effective for Cr(VI) prevention. Both chemical products, the blend of AO1135 with emulsifiers and dispersants and one with higher AO1135 concentration mixed with a solvent have been demonstrated to exhibit good performance related to Cr(VI) prevention.

When using a fatliquoring agent that included extra protection from the beginning, Cr(VI) content was found to be less than 3 mg/kg in each type of leather. This group of leathers (04-PB and 10-PB) has been useful for assessing the effectiveness of using a commercial product that has been formulated in a way that includes protection against lipid auto-oxidation, thus avoiding hexavalent chromium formation.

If the fatliquoring agent was not protected against auto-oxidation, when those leathers were exposed to thermal ageing, high amounts of Cr(VI) in leather were found, thus restating the aforementioned conclusion.

The results indicate that when using a protected fatliquoring agent or an extra addition of a chemical product that contains AO1135, the Cr(VI) content is below the regulated limit of 3 mg/kg.

4.3 Zone of the leather and Cr(VI) distribution

Cr(VI) distribution was only evaluated in the leathers treated with the unprotected fatliquoring agent, without AO1135 additions, as the Cr(VI) was above 3 mg/kg for all the samples and leather zones (01-UB and 07-UB). Cr(VI) formation according to the tested part of the leather shows higher dispersion in general for Sheep-skins, and lower dispersion for Wooly sheep-skins, although results vary between the range of 2.2 to 22% of RSD.

Several factors contribute to the high values of relative standard deviation obtained. On one hand, it can be seen in Table V that disperse results in Cr(VI) content are linked to a difference in the sampling site, indicating that irregular distribution of the fibers across the leather surface can contribute to uneven Cr(VI) content across the surface. As unbonded Cr(III) oxidation does not depend exclusively on the fiber distribution, other factors have to be balanced in this issue. Fat-liquoring agents are known to be distributed in empty spaces between fibers. This might lead to an increase of Cr(VI) formation due to an exposure to free radicals from the lipid auto-oxidation, if no AO1135 or other SPA additives are added, and it is clear that this phenomenon takes place in references 01-UB and 07-UB.

When using a protected fatliquoring agent or an extra addition of a manufactured chemical product with AO1135 in its formulation, the protection against Cr(VI) is effective no matter the leather zone sampled.

4.4 Effect of different ageing treatments in Cr(VI) content

Two ageing treatments were applied to each zone of the 12 references that had been prepared. Cr(VI) formation has increased for all the leathers after the samples were submitted to the treatments.

The thermal ageing according to ISO 10195:2018 was designed to simulate the propensity of a leather to form Cr(VI) and in this work it has been proven to be an effective method, as Cr(VI) content increased drastically after the treatment in leathers that were not treated with any sort of SPA addition. For leathers treated with SPAs (References 02-U1, 03-U2, 04-PB, 05-P1, 06-P2, 08-U1, 09-U2, 10-PB, 11-P1 and 12-P2), the thermal ageing did not generate Cr(VI) above the regulated limit.

The lower-temperature / longer-term ageing conditions were designed as a simulation of a long-term storage of the leathers. Again, hexavalent chromium in leathers 01-UB and 07-UB clearly increased after the treatment. For the rest of the leathers, the results are not quantifiable because they are below 3.0 mg/kg, the quantification limit of the testing method. The response in the chromatogram appeared to be higher for the aged samples in comparison to the non-aged leather samples, however, the assumption that Cr(VI) had increased cannot be scientifically confirmed.

Conclusions

This study has thoroughly assessed the efficiency of three methods that are currently used for preventing fatliquoring auto-oxidation: using a protected fatliquoring agent that contains a long-chain synthetic phenolic antioxidant (SPA) on its formulation, using an auxiliary product with a specific SPA (AO1135) in a solvent (Product 02), or using a commercial product that contains a SPA (AO1135) amongst other additives such as dispersants and emulsifiers (Product 01). All three options have been proven effective for Cr(VI) prevention, even when the two different types of leather (Sheep-Skin and Wooly Sheep-Skin) were exposed to the conventional thermal ageing (in a laboratory oven at 80ºC for 24 h, <10% relative humidity).

Besides the conventional thermal ageing (ISO 10195:2018), another ageing treatment was applied to the 12 produced leathers, in order to evaluate the AO1135 efficiency for a simulated long lasting storage condition in hot climate countries. The treatment showed the same tendency as the ISO Standard.

For each one of the 12 tanned leathers and the different tested conditions, three zones were assessed in order to evaluate Cr(VI) distribution in leather. The percent RSD was between 2.2 and 22%, showing a wide dispersion and leading to conclude that Cr(VI) distribution may depend on many factors, one of which being the natural origin of this particular material and another one, the free radicals generated from the auto-oxidation of unsaturated lipid that unbonded Cr(III) to which the leather might be exposed.

The addition of AO1135 to either the fatliquoring formulation or to the recipe has shown to be a very good tool for hexavalent chromium prevention. Cr(VI) below the regulated limit was achieved when AO1135 was included in some way, even if an un-protected fatliquor was used or if thermal ageing was performed to the leathers, restating the relationship between lipid auto-oxidation and Cr(VI) formation.

Cr(VI) below the regulated limit was achieved when AO1135 was included in some way during the wet-end process. Even if an un-protected fatliquoring agent was used or if a thermal ageing was performed to the leathers, the Cr(VI) content was less than 3 mg/kg if the aforementioned SPA was used. This work leads to two main conclusions: AO1135 is an effective SPA for Cr(VI) prevention and unsaturated fatliquoring agents can be a cause for Cr(VI) formation if the recipe does not contain well-sourced raw materials and/or additional Cr(VI) preventing tools.

Acknowledgement

The authors would like to acknowledge the insight provided by Dr. Joaquim Font during the planning and performance of the study, and also his valuable ideas regarding the structure of the manuscript.

References

1. M. Jones, A. Gandia, S. John, and A. Bismarck; Leather-like material biofabrication using fungi, *Nat Sustain*, vol. 4, no. 1, pp. 9–16, 2021, doi: 10.1038/s41893-020-00606-1.
2. A. Bacardit, G. Baquero, S. Sorolla, and L. Ollé; Evaluation of a new sustainable continuous system for processing bovine leather, *J Clean Prod*, vol. 101, pp. 197–204, 2015, doi: 10.1016/j.jclepro.2015.04.012.
3. A. Bacardit, F. Combalia, J. Font, and G. Baquero; Comparison of the sustainability of the vegetable, wet-white and chromium tanning processes through the life cycle analysis, *JALCA* vol. 115, no. 3, pp. 105–111, 2020, doi: 10.34314/jalca.v115i03.1628.
4. F. Alinaghi, C. Zachariae, J. P. Thyssen, and J. D. Johansen; Temporal changes in chromium allergy in Denmark between 2002 and 2017, *Contact Dermatitis*, vol. 80, no. 3, pp. 156–161, 2019, doi: 10.1111/cod.13181.
5. K. Ogata, Y. Kumazawa, Y. Koyama, K. Yoshimura, and K. Takahahi; Complete inhibition of hexavalent chromium formation from chrome-tanned leather with combined inhibitors, *Journal of the Society of Leather Technologists and Chemists*, vol. 101, no. 1, pp. 27–32, 2017.
6. N. K. C. Babu, K. Asma, A. Raghupathi, R. Venba, R. Ramesh, and S. Sadulla; Screening of leather auxiliaries for their role in toxic hexavalent chromium formation in leather - Posing potential health hazards to the users, *J Clean Prod*, vol. 13, no. 12, pp. 1189–1195, 2005, doi: 10.1016/j.jclepro.2004.07.003.
7. K. Ogata, Y. Kumazawa, S. Hattori, K. Yoshimura, and K. Takahashi; Self-Conversion of hexavalent chromium formed in chrome-Tanned leather during long-term storage and perfect inhibition with a combination of inhibitors, *JSLTC*, vol. 102, no. 2, pp. 53–58, 2018.
8. J. Font *et al.*; Presence of chromium (VI) in sheepskins. Influence of tannery processes, *JSLTC*, vol. 82, no. 91, 1998.
9. M. A. Torkmahalleh, L. Lin, T. M. Holsen, D. H. Rasmussen, and P. K. Hopke; The impact of deliquescence and pH on Cr speciation in ambient PM samples, *Aerosol Science and Technology*, vol. 46, no. 6, pp. 690–696, 2012, doi: 10.1080/02786826.2011.654285.
10. AFIRM Group, Restricted substances list - AFIRM - Apparel and Footwear International RSL Management Group. p. 40, 2022.
11. C. Hauber;Formation, Prevention & Determination of Cr(VI) in Leather. A short overview of recent publications, UNIDO 2000.
12. J. Font, A. Rius, A. Marsal, C. Hauber, and M. Tommaselli, Prevention of chromium(VI) formation by improving the tannery processes, IULTCS Eurocongress 2006.
13. INDITEX, Health Product Policy. 2022.
14. E. Heidemann, *Fundamentals of leather manufacturing*. 1993.
15. N. J. Cory; A practical discussion session to deal with opportunities for improvement of customer/end user satisfaction, *JALCA* vol. 92, no. 5, pp. 119–125, 1997.
16. U. Sammarco; Formazione di Cr (VI) nelle pelli e possibilità di eliminazione, *Cuoio, Pelli, Materie Concianti*, vol. 74, pp. 83–94, 1998.
17. J. Font, R. M. Cuadros, R. Reyes, J. Costa-López, and A. Marsal; Influence of various factors on chromium (VI) formation by photo-ageing, *JSLTC* vol. 83, no. 6, pp. 300–306, 1999.
18. C. Hauber and H.-P. Germann; Investigations on a possible formation and avoidance of chromate in leather, *Leatherpedia*, 1999. https://www.lederpedia.de/veroeffentlichungen/englisch/investigations_on_a_possible_formation_and_avoidance_of_chromate_in_leather_1999 (accessed Oct. 31, 2022).
19. M. A. Salehi, S. M. Trey, G. Henriksson, and M. Johansson; Effect of model lignin structures on the oxidation of unsaturated fatty acids, *Polymers from Renewable Resources*, vol. 1, no. 2, pp. 69–90, 2010, doi: 10.1177/204124791000100201.
20. U. Mustafidah and R. Laili; Comparison the effect of using different fatliqour to the formation of chromium (Vi) in leather production, *Materials Science Forum*, vol. 948 MSF, no. Iii, pp. 217–220, 2019, doi: 10.4028/www.scientific.net/MSF.948.217.
21. T. Xu, X. Jiang, Y. Tang, Y. Zeng, W. Zhang, and B. Shi; Oxidation of trivalent chromium induced by unsaturated oils: A pathway for hexavalent chromium formation in soil, *J Hazard Mater*, vol. 405, no. 24, p. 124699, 2021, doi: 10.1016/j.jhazmat.2020.124699.
22. Leather Working Group, Guidance for tanners on CrVI prevention, 2018. https://www.leatherworkinggroup.com/news-events/news/new-information-bulletin-released-/ (accessed Oct. 31, 2022).
23. A. Pizzi, C. Simon, B. George, D. Perrin, and M. C. Triboulot; Tannin Antioxidant Characteristics in Leather Versus Leather Light Stability: Models, *J Appl Polym Sci*, vol. 91, no. 2, pp. 1030–1040, 2004, doi: 10.1002/app.13047.
24. B. Zümreoglu-Karan, A. Ay, and C. Unaleroglu; Ascorbic acid as a potential masking agent in the tanning process. Olated chromium complexes involving ligating ascorbate and bridging sulfate groups, *Transition Metal Chemistry*, vol. 27, pp. 437–441, 2002, doi: 10.1023/A:1015029708445.
25. A. Kilikli, F. Izquierdo, and I. Reetz; Comparison of the inhibition efficiency of natural and synthetic phenolic antioxidants on Cr(VI) formation, *JALCA* vol. 112, no. 3, pp. 81–87, 2017.
26. R. Liu and S. A. Mabury; Synthetic Phenolic Antioxidants: A Review of Environmental Occurrence, Fate, Human Exposure, and Toxicity, *Environ Sci Technol*, vol. 54, no. 19, pp. 11706–11719, 2020, doi: 10.1021/acs.est.0c05077.
27. S. Nagarajan *et al.*; Antioxidant activity of synthetic polymers of phenolic compounds, *Polymers (Basel)*, vol. 12, no. 8, pp. 1–27, 2020, doi: 10.3390/POLYM12081646.
28. K. D. Breese, J. F. Lamèthe, and C. DeArmitt; Improving synthetic hindered phenol antioxidants: Learning from vitamin E, *Polym Degrad Stab*, vol. 70, no. 1, pp. 89–96, 2000, doi: 10.1016/S0141-3910(00)00094-X.
29. A. Shrivastava; Environmental Aspects of Plastics, *Introduction to Plastics Engineering*, pp. 207–232, 2018, doi: 10.1016/b978-0-323-39500-7.00007-1.
30. T. J. Henman; Role of packaging additives in yellowing, *Textile Progress*, vol. 15, no. 4, pp. 25–36, 1987.
31. O. D. Bangee, V. H. Wilson, G. C. East, and I. Holme; Antioxidant-induced yellowing of textiles, *Polym Degrad Stab*, vol. 50, no. 3, pp. 313–317, 1995, doi: 10.1016/0141-3910(95)00156-5.

32. I. M. Rizwanul Fattah, M. H. Hassan, M. A. Kalam, A. E. Atabani, and M. J. Abedin; Synthetic phenolic antioxidants to biodiesel: Path toward NOx reduction of an unmodified indirect injection diesel engine, *J Clean Prod*, vol. 79, no. x, pp. 82–90, 2014, doi: 10.1016/j.jclepro.2014.05.071.
33. J. Font, M. Bacardit, N. Pascual, R. Cuadros, and F. Izquierdo; A simple test to determine the propensity of a sample of leather to the formation of chromium(VI), *JALCA* vol. 113, no. 2, pp. 65–71, 2018.
34. I. Hintersteiner, L. Sternbauer, S. Beissmann, W. W. Buchberger, and G. M. Wallner; Determination of stabilisers in polymeric materials used as encapsulants in photovoltaic modules, *Polym Test*, vol. 33, pp. 172–178, 2014, doi: 10.1016/j.polymertesting.2013.12.004.
35. Y. Wu, M. Venier, and R. A. Hites; Identification of Unusual Antioxidants in the Natural and Built Environments, *Environ Sci Technol Lett*, vol. 6, no. 8, pp. 443–447, 2019, doi: 10.1021/acs.estlett.9b00415.
36. O. Okamba-Diogo *et al*., Quantification of hindered phenols in polyamide 11 during thermal aging, *Polym Test*, vol. 52, pp. 63–70, 2016, doi: 10.1016/j.polymertesting.2016.03.023.
37. J. Font Vallès, A. Rius Carrasco, A. Marsal Monge, C. Hauber, and M. Tommaselli; Chrom6less Project 'Prevention of chromium (VI) formation by improving the tannery processes funded by the European Community, Craft Contract no. G1ST-CT-2002-50264. 2006.
38. I. Compte, R. Cuadros, F. Izquierdo, F. Combalia, and A. Bacardit; A Simple Test to Determine the Propensity of a Fatliquor to Trigger the Formation of Chromium (VI) in Leather, *JALCA* vol. 117, no. Vi, pp. 479–487, 2022.
39. M. Fontaine, N. Blanc, J. C. Cannot, and C. Demesmay; Ion chromatography with post column derivatization for the determination of hexavalent chromium in dyed leather. Influence of the preparation method and of the sampling location, *JALCA* vol. 112, no. 10, pp. 319–326, 2017.

LEATHER

AVELLISYNCO

Selected Dyestuffs

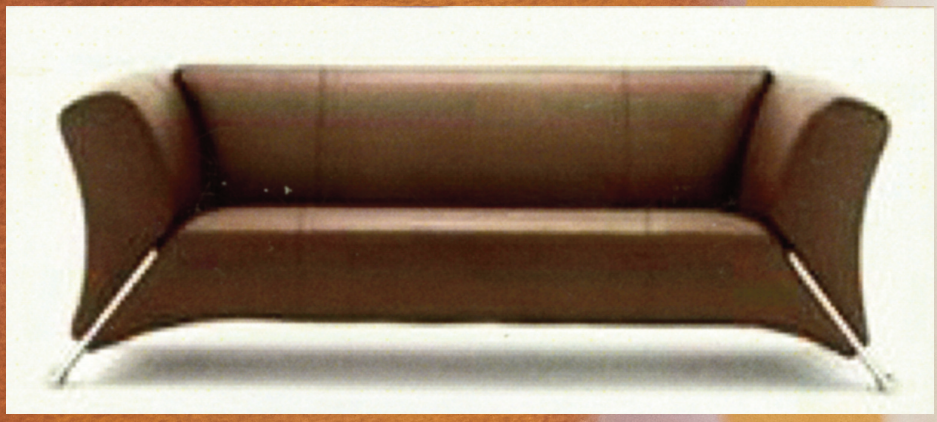

CHEMTAN

17 Noble Farm Drive • Lee, NH 03861 (Office)
57 Hampton Road • Exeter, NH 03833 (Manufacturing)
Tel: (603) 772-3741 • Fax: (603) 772-0796
www.CHEMTAN.com

Lifelines

Ze Liang obtained a Bachelor's Degree in College of Biomass Science and Engineering from Sichuan university (Chengdu, China) in 2020. Since then, he has been studying for a Masters degree under the supervision of Prof. Zhengjun Li with a major in Light Industry Technology and Engineering at Sichuan University (Chengdu, China). His main research interest is in green chrome-free tanning technology.

Zetian Zhang obtained a Masters Degree in College of Biomass Science and Engineering from Sichuan university (Chengdu, China) in 2020. Since then, he is studying for a PhD Degree under the supervision of Prof. Zhengjun Li with a major in Light Industry Technology and Engineering at Sichuan University (Chengdu, China).

Yang Liu obtained a Masters Degree in College of Biomass Science and Engineering from Sichuan university (Chengdu, China) in 2020. Since then, he is studying for a PhD Degree under the supervision of Prof. Zhengjun Li with a major in Light Industry Technology and Engineering at Sichuan University (Chengdu, China).

Zhengjun Li, doctoral supervisor, obtained his PhD degree in 2008, the first trans-century outstanding young talents of Sichuan province, member of the science and technology committee of China leather association, vice President of Sichuan leather association. He is working, as a professor, at the National Engineering Laboratory for Clean Technology of Leather Manufacture, Sichuan University, China. His research interests center on chrome-free tanning leather process and environmentally friendly leather chemicals. Besides, he also focuses on preparation of collagen-based composite functional materials and development of environmentally friendly chrome-free tanning agents.

Min Jiang obtained a Bachelor's Degree in the School of Chemical Engineering at Nanjing University of Science and Technology (Nanjing, China) in 2018. She has been studying for the Masters Degree under the guidance of Professor Wei Lin in the College of Biomass Science and Engineering at Sichuan University (Chengdu, China) since 2020.

Yuanhang Xiao obtained a Bachelors Degree in Light Chemical Engineering from Qilu University of Technology (Jinan, China) in 2017. He obtained a Masters Degree in the College of Biomass Science and Engineering from Sichuan University (Chengdu, China) in 2020. Since then, he has been studying for the Doctoral Degree under the guidance of Professor Wei Lin in the College of Biomass Science and Engineering at Sichuan University (Chengdu, China).

Chunhua Wang received a B.S. in Light Industry Biological Technology (2011), a M.S. in Leather Chemistry and Engineering (2014), and a Ph.D. in Leather Chemistry and Engineering at Sichuan University (2017). Since then, she has been working in Professor Wei Lin's group as a Research Assistant at Sichuan University. Now she is doing Postdoc research at the University of New Brunswick. Her research interests focus on design and developing environmentally friendly coating materials with antibacterial function applied in leather finishing or other fields.

Jun Sang received a B.S. in Polymer Science and Engineering at Yantai University (2007), a M.S. in Leather Chemistry and Engineering at Shanxi University of Science and Technology (2010), and a Ph.D. in Leather Chemistry and Engineering at Sichuan University (2017). Now he is working in China leather and Footwear Research Institute Co. LTD. His research interests focus on leather standardization and leather chemical materials.

Jiajing Zhou obtained his PhD in bioengineering from Nanyang Technological University in 2016, under the supervision of Prof. Hongwei Duan. He worked with Prof. Frank Caruso as a postdoctoral fellow at The University of Melbourne (2018-2020), and then worked with Prof. Jesse V. Jokerst at University of California San Diego (2020-2022). In 2022, he joined Sichuan University, where he established his independent research focusing on the synthesis of functional nanohybrids and 3D printing of biomass materials.

Wei Lin received her Ph.D. in Leather Chemistry and Engineering at Sichuan University (Chengdu) in June 2000. She moved to University of Science and Technology of China (Hefei) in September 2000 as the postdoctoral fellow for two years in Professor Qingshi Zhu and Professor Chi Wu's research groups. After an additional postdoctoral research associate position in Professor Michal Borkovec's group in the Department of Inorganic, Analytical and Applied Chemistry at University of Geneva during April 2003 to August 2005, she returned to the Department of Leather Chemistry and Engineering at Sichuan University and promoted to Full Professor in June 2006. Her research interests center on environmentally friendly leather chemicals and leather-making process. She focuses on studying macromolecular structure and property of collagen and its interactions with tanning substances, as well as collagen-based biomass materials. She also focuses on the design and development of environmentally friendly non-chrome tanning agents, and the risk screening of the chemicals used in leather-making.

Yiwen Zhu is a postgraduate student at Sichuan University, China. Her research work focuses on the development of efficient leather bating technologies. She is under the guidance of Prof. Biyu Peng.

Jinzhi Song see JALCA **118(2)**, 2023

Xu Zhang see *JALCA* **117(10)**, 2022

Mengchu Gao see JALCA **117(10)**, 2022

Biyu Peng see *JALCA* **117(10)**, 2022

Chunxiao Zhang see *JALCA* **114**, 189, 2019

Irene Compte is an Analytical Chemist (Universitat de Barcelona, Spain, 2015) and Leather Engineer (University of Lleida, Spain, 2019). She has been a researcher in A3 Leather Innovation Center (University of Lleida, Spain) and she is currently working as a consultant and and project manager in Technical Advice (Spain). She is involved in consumer and product safety of leather and textiles.

Quim Torras holds a Chemical Engineering degree (Universitat de Lleida, Spain, 2021) and a post-graduate degree in Data analysis (Universitat Oberta de Catalunya, Spain, 2022). He has been a product developer for the leather finishing sector at Cromogenia Units (Spain) and a process engineer in an unhairing and tanning leather factory (Industrial Igualadina SL, Spain).

Francina Izquierdo see JALCA 112, 81 2017

Anna Bacardit see JALCA 101, 284, 2006

Rosa Cuadros see JALCA 108, 420, 2013

Felip Combalia see JALCA 105, 353, 2010

Obituary

Paul B. Flagg
September 4, 1926 – August 22, 2023

Paul Flagg, who built a reputation and business in the U.S. leather tanning industry has died. He was 96.

Tanneries with which Flagg was associated include: Flagg Tanning, Milwaukee, WI; A. K. Salz, Santa Cruz, CA; Wisconsin Leather, Milwaukee, WI and of course, Paul Flagg Leather of Milwaukee and Sheboygan, WI. Flagg continued to consult into the 2000s.

Born Paul Benjamin Flegenheimer in Baiertal, Germany on September 4 1926 to Lion Benjamin and Robertine Bernheim Flegenheimer, Paul with sister Lore, survived three Nazi concentration camps—Lion and Robertine did not.

Paul and Lore were liberated from the third camp, located outside Marseilles, by a Swiss Red Cross nurse who separated the children for medical attention and conveniently never returned them.

Paul then joined the French Resistance. His actions and those of his comrades were recognized with commendations awarded personally by Charles De Gaulle at the end of the war.

Following World War II, Paul returned to Wiesloch, Germany to reclaim what he could of his family's farm which had been confiscated by the Nazis when the Flegenheimer family were deported in 1940. Amid Germany's broken post-war economy, Paul made his living trading in the black market rampant at the time.

In 1949, Paul faced the choice of following friends to Israel or accepting a promise of employment from a distant relative in Milwaukee, WI. He emigrated to America and arrived in Boston aboard the liberty ship General LeRoy Eltinge.

In Milwaukee, Paul began his tenure in leather manufacturing at his relative's tannery, Eagle-Flagg. Here, Richard Flagg initiated Paul by having him unload fresh hides by hand from railcars in the summer heat. At five-foot-six, Paul remembered finding himself draped in the wet skins that his more seasoned fellow workers tossed over him.

Over the next half-century, Paul would go on to build an impressive reputation and business in the U.S. leather tanning industry.

At Eagle-Flagg, Paul met Cornelia Peterson. In time, Eagle-Flagg became Flagg Tanning and by the end of the 1950s, Paul and Connie were officers in the company. Connie would play a significant role in building Paul's tanning business. They married in 1960 and were together until her death in 2018.

In 1960, Paul joined A.K. Salz Company in Santa Cruz, CA. By focusing on logistics, quality, paring costs and modernization—he converted Salz from vegetable tanning to chrome tanning—Paul re-established the one-hundred-year-old tannery's prominence.

Paul returned to Milwaukee in 1970 to run Wisconsin Leather for Spencer Foods. Later, a second Spencer acquisition on the east coast was added to his responsibilities.

By 1974, Paul established Paul Flagg Leather to contract-tan leather in Muscatine, IA and at Reuping in Fond du Lac, WI. The business grew to require its own plant in Milwaukee and later in Sheboygan, WI. Paul Flagg Leather was sold to Marmon Group in 1997. Paul continued to consult into the 2000s.

Paul Flagg died at his home in Mequon, WI just shy of his 97th birthday.

At Paul's request, there will be no memorial.

Contributions are encouraged to the United States Holocaust Memorial Museum, the Milwaukee Symphony Orchestra, or the University of Wisconsin–Madison School of Veterinary Medicine.

CALL FOR PAPERS

FOR THE 118th ANNUAL CONVENTION OF THE AMERICAN LEATHER CHEMISTS ASSOCIATION

Hershey Lodge, Hershey Pennsylvania
May 21–24, 2024

If you have recently completed or will shortly be completing research studies relevant to hide preservation, hide and leather defects, leather manufacturing technology, new product development, tannery equipment development, leather properties and specifications, tannery environmental management, or other related subjects, you are encouraged to present the results of this research at the next annual convention of the Association to be held at the Hershey Lodge, Hershey Pennsylvania, May 21–24, 2024

Abstracts are due by March 1, 2024
Full Presentations are due by May 1, 2024

They are to be submitted by e-mail to the
ALCA Vice-President and Chair of the Technical Program:

John Rodden
Union Specialties, Inc.
3 Malcom Hoyt Dr.
Newburyport, MA 01950
E-mail: johnrodden@unionspecialtiesinc.com

The **Abstract** should begin with the title in capital letters, followed by the authors' names. An asterisk should denote the name of the speaker, and contact information should be provided that includes an e-mail address. The abstract should be no longer than 300 English words, and in the Microsoft Word format.

Full Presentations at the convention will be limited to 25 minutes. In accordance with the Association Bylaws, all presentations are considered for publication by *The Journal of the American Leather Chemists Association*. They are not to be published elsewhere, other than in abstract form, without permission of the *Journal* Editor. For further paper preparation guidelines please refer to the *JALCA* Publication Policy on our website: leatherchemists.org

Full Presentations are to be submitted by e-mail to the *JALCA* editor:

Steven D. Lange, *Journal* Editor
The American Leather Chemists Association
E-mail: jalcaeditor@gmail.com
Mobile Phone (814) 414-5689

When leather feels this good, the boots come off last!

CHEMTAN

Leather chemistry for today.

Tel: (603) 772-3741 • Fax: (603) 772-0796
www.CHEMTAN.com

ISO 9001 Certified